FIELD APPLICATION OF TRANSIENT ANALYSIS METHODS FOR PIPELINE CONDITION ASSESSMENT

By

Jeffrey Tuck

This thesis is submitted for the Degree of Masters of Engineering in Civil Engineering

Department of Civil and Natural Resources Engineering,

University of Canterbury,

Christchurch, New Zealand

December 2016

ABSTRACT

Reliable water supply is an integral component of any functioning society, improving quality of life through health and sanitation and promoting economic growth. Condition assessment of pipelines is central to the management of water systems and reliable water supply. As demands on water systems increase through population growth, suitable methods of condition assessment are required for strategic planning of ongoing maintenance and renewals of aging pipeline infrastructure. A developing pipeline condition assessment approach is fluid transient response analysis. The approach analyses a systems response to specifically generated transients and identifies characteristic behaviour that can determine the state of that system using direct or inverse analysis procedures. For the analysis procedures to be effective the interaction between transients and pipeline features needs to be well understood. Effective analysis is also dependent upon the ability to identify the response caused by a system on a specifically generated transient signal.

The interaction of fluid transients with extended blockages and changes in pipe wall thickness have been investigated by examining numerical and experimental results in time and frequency domains. These features can be caused through deterioration of pipeline condition and it is found that they can significantly alter the fundamental period of a pipelines transient response, maximum and minimum transient pressure heads and the evolution of the transient signal. The ability of existing models to represent extended pipeline faults under transient conditions is evaluated through direct comparisons of numerical transient responses with new experimental results from the laboratory and through inverse analyses. Direct comparisons show that the transient behaviour is modelled with a good level of accuracy over the first few periods of oscillation and that the level of accuracy decays with time. Inverse analyses show that despite reducing model accuracy with time extended period analysis can provide improved results due to the significant changes an extended fault can have on the periodic response. A periodic Fourier analysis of the data demonstrates that the damping rates of the experimental response are higher than the numerical predictions and that the transient signals exhibits larger damping rates in the higher frequency components of the response.

Research has been focussed on procedures using valve closures as the primary method of transient signal generation, which create single step waves of large magnitude. These valve closure signals can be difficult to identify in live water distribution networks due to hydraulic noise, limiting the application of the technology. To improve field application of transient based condition assessment methods a new signal generation system has been developed. The system, referred to as Pipe SONAR (PCT/EP2015/059540) uses a piezoelectric actuator capable of generating customised, small amplitude pressure signals that vary in frequency and magnitude. The signal generation system is suitable for use

on live water distribution networks and has been tested in an international field testing program on 31 sites in New Zealand and China. The field testing program includes tests on steel, cast iron, ductile cast iron, reinforced concrete, asbestos cement, medium/high density polyethylene and polyvinyl chloride pipes with pipe diameters ranging from 100 mm to 600 mm. The Pipe SONAR technology has been assessed through application to two condition assessment techniques; the first is identifying valve condition via a method based on measuring signal transmission through a valve and assesses the ability of the valve to achieve a water tight seal; the second is determining pipeline wave speed for determining pipe wall condition. The technology is found to be practical and functional for application to field use.

ACKNOWLEDGEMENTS

First of all, I would like to acknowledge and thank my supervisor, Dr Pedro Lee for your expertise, time and never ending enthusiasm for the research. I wish to thank my co-supervisors, Dr Mark Davidson for input and suggestions and Dr Robert May for your valuable industry perspective and hours of field testing assistance.

In addition, I would like to thank the laboratory technicians Alan Stokes, Ian Sheppard, Kevin Wines and Michael Weavers who have all made significant contributions to this project from fabricating fittings and building customised testing equipment to constructing entire pipeline systems.

I would like to thank fellow and former students and office mates for ongoing technical discussions, banter and company, Dr Akaya Kashima, Dr Adi Ramakanth, Dr Colin Whittaker, Gareth Morris, Dr Mark Stringer and Audsley Jones.

A big thank you to my parents for your support, enthusiasm and encouragement to keep my head in it.

Most of all, my wife, Anna your assistance, love and support has been crucial to me completing this work and it has been greatly appreciated.

TABLE OF CONTENTS

LIST OF FIGURES

LIST OF TABLES

NOTATIONS

A = Pipe cross-sectional area

a = Wave speed

B = Characteristic impedance

c_1 = Parameter for pipe constraint conditions

C_r = Courant number

C_v = Valve coefficient

D = Pipe diameter

dt = Time step

dx = Space step

e = Pipe wall thickness

E = Young's modulus

E_ω = Spectral energy

f = Darcy-Weishbach friction factor, Frequency

g = Gravity

H = Head

H_D = Downstream head

h_f = Total friction losses

h_{fs} = Steady friction losses

h_{fu} = Unsteady friction losses

H_i^m = Measured head response

H_i^p = Predicted head response

H_J = Joukowsky head rise

H_R = Head of reflected wave

H_T = Head of transmitted wave

H_U = Upstream head

H_W = Head of incident wave

h_ω = Head response for frequency component ω

i = Counting variable

K = Bulk modulus of fluid

k = Local loss coefficient

L = Pipe length

N = Length of sequence

Q = Flow

R = Damping factor

R = Resistance coefficient

Re = Reynolds number

$\hat{R}$ = Cross-correlation function

s = Residual error

T = Period

t' = Dummy time variable

t_{lag} = Signal propagation time

TR = Transmission ratio (peak)

TR' = Transmission ratio (full)

t_v = Valve closure duration

W = Weighting function

x_c = Distance to centroid

y = Input signal

ε = Roughness height

v = Viscosity

ρ = Density

τ = Orifice opening ratio

Common subscripts

0 = Denotes initial conditions or undisturbed value

1 – n = Pipe section number

B = Denote property of a blockage

Est = Estimated variable

Local = Local station variable

Remote = Remote station variable

Common superscripts

* = non-dimensional form

1 INTRODUCTION

Water supply is recognised to be at the core of sustainable development (UN Conference on Sustainable Development) and is essential in providing ongoing sanitation and health (OHCHR 2010). The World Water Council identifies the key benefits of functional water supply systems being: improving the health of a community and quality of life at all ages, respecting human values, and generating significant economic benefits. In developed nations, functional and reliable water supply systems have become an expected and essential service and their associated construction and maintenance expenses are significant. For example, in New Zealand, with a population of 4.4 million, the estimated value of the water infrastructure in urban areas is NZ$11.4 billion, with annual running costs of NZ$605 million. It is expected that an additional NZ$3.9 billion in capital expenditure is also to be spent over the current decade (National Infrastructure Plan 2010). An important component in modern water supply systems is pipelines. Pipelines are the primary method of transport for delivery of water from the source to the end user and it is necessary to ensure that pipelines are maintained to uphold water quality and supply. For efficient asset management, it is beneficial to regularly assess pipeline condition and diagnose faults. This can include identifying pipe wall degradation, blockage formation, leaks and faulty valves. By identifying pipeline deterioration, selective maintenance and renewals can be scheduled before costly emergency repairs are required and water quality and supply are adversely affected (Marlow *et al.* 2007).

Condition assessment is important for water infrastructure operators as it forms the basis for strategic planning of ongoing maintenance, renewals, upgrade schedules and funding. Condition assessment of pipelines can be carried out using a variety of tools and investigation techniques, which result in assessments that can be made with varying degrees of confidence and corresponding levels of

inconvenience and expense to apply. These include broad desktop studies which use empirical evidence based on material type, soil conditions and complaints from users or statistical analysis based on historic failure rates to predict pipe condition without disrupting operation of the pipeline. Alternatively, on-site investigations can include visual inspection or destructive sampling methods which enable specific information to be obtained at a greater expense with increased disruption, often requiring system shutdowns. The expense of site specific investigations generally restricts their application to large, strategically important pipelines while low cost desktop studies are favoured elsewhere.

The aims of condition assessment include the identification of leaks, blockages and structural deterioration of pipes, valves and connections. Of particular interest to water authorities is identification of pipe wall deterioration or thinning which is a common precursor to failure through pipeline bursts or the development of leaks (CEPA 2016, Liu 2003). Repairs of these failures are often expensive, hence form the basis for justifying rehabilitation. This is particularly problematic in larger diameter trunk mains as it can disrupt supply to large areas of a network. Partial or complete blockage of a pipeline can also affect supply. Blockages or tuberculation can form from internal corrosion, biofilm development, sediment deposits or intrusive foreign objects. These blockages can greatly increase pumping costs in a distribution network and reduce pressure to customers. A 20% reduction in pipeline diameter due to biofilm growth can result in a friction loss 200% greater than its original value (Wang *et al.* 2005a). Blockages can also affect water quality by disrupting flow through sections of a distribution network such that water can be left stagnant for long periods of time. This water can then be withdrawn during high demand events, compromising the water quality (Stephens 2008). Pipeline deterioration or blockage formation can also affect the operation of valves within a system by restricting them from closing sufficiently and ensuring a water tight seal. While valves are not used often and typically remain fixed in an open or closed position for extended periods of time, they are an essential component that is required to isolate sections of a network for emergency repairs or maintenance and must be operable when required (Bouchart and Goulter 1991, Jun *et al.* 2007, Walski 1993).

There is a demand in the market for a system that can provide site specific information on a broad scale while also being economically viable and able to be carried out in a non-invasive manner. Transient response analysis is a technology that has the potential to satisfy this demand. Transients are pressure waves that propagate rapidly throughout pipelines due to a change in hydraulic conditions at some point, such as closing a valve or stopping a pump. These pressure waves are often referred to as “surge” or “water hammer” and normally require specific consideration when designing any pipeline system. Transient behaviour can create large pressure forces that may lead to failure of pumps, system fatigue, intrusion of contaminated water and catastrophic pipeline ruptures (Boulos *et al.* 2005). However, when

transients are specifically generated in a safe and controlled manner, the pressure response of the system can be measured and yield useful information on the condition of the pipelines. This information will be more specific than that gained from broad desktop studies and has the potential to be less disruptive and less expensive than other site specific testing technologies.

In general, transient response analysis works by analysing the pressure response from a transient generated with known characteristics to identify behaviour caused by faults and changes in system condition. The propagation of a transient pressure wave can be affected by any physical property of a pipe including wall material, blockages, leaks, junctions, changes in diameter and roughness (Colombo *et al.* 2009). Therefore, if the effect that each physical component has on the pressure wave is understood, a numerical model of a system could be calibrated to match a measured pressure response, thus describe the condition of the corresponding real network. This method is known as inverse transient analysis (ITA). Where less holistic assessments are required, specific properties of the system can be classified through direct analysis of the transient response. The advantage in using the described transient based condition assessment methods is that the condition and physical state of a pipeline or pipeline network can be determined by taking pressure measurements at a select few discrete locations. These pressure measurements can be simply taken at existing fire hydrants or service connections and transients can be generated through opening or closing a valve at any point in a system. This means that the method can be applied quickly and in a non-invasive manner.

There has been significant research devoted towards transient analysis detection of leaks and other discrete faults. The development of ITA procedures presented in the literature and previous research has primarily involved numerical analysis and laboratory experiments. However, prior to this research program there has been little laboratory work identifying the effect that pipeline wall condition and extended blockages have on a transient response. For this reason, the first component of this research will involve a laboratory study of the effects pipeline wall condition and extended blockages have on a transient signal.

For transient analysis based condition assessment to become a viable product it is necessary to take knowledge gained through numerical and laboratory research and trial it in the real-world environment. This sort of practical application of transient response analysis to the field is currently confined to work from a couple of researchers, from which it has been noted that improvement of transient generation techniques and further field studies will be beneficial. As such, the second component of this research is to develop and test a new transient generation system for practical applications in the field.

1.1 Objectives

The broad objective of this research is to advance the understanding of fluid transient behaviour in pipeline systems and apply transient analysis methods to assist in fault detection and pipeline condition assessment. Then, to develop and test new technology that can be used to practically apply these methods in the field. To achieve this, the research can be divided into two main components:

1. Investigate the behaviour of transient signals in pipelines which include changes in diameter, wall thickness and wave speed. This will be achieved by:

    - Conducting laboratory experiments on pipelines with simulated faults, including extended blockages and variations in wall thickness, and identifying important features in the responses.

    - Comparing experimental results with numerically modelled responses and evaluating the performance of the numerical models.

    - Attempting to locate and classify pipeline faults using inverse transient analysis and improve the inverse fitting process by identifying the sensitivity of the analysis to various parameters.

2. Develop a novel system capable of generating and measuring controlled high frequency transient signals and evaluate performance for practical application on real pipelines:

    - Test the system in partnership with an international water management consultancy (Veolia) in New Zealand and China to evaluate its performance on a range of pipeline sizes, types and configurations.

    - Apply the system to the applications of valve condition assessment and pipe wall condition assessment, while evaluating performance against existing methods of transient generation.

1.2 Thesis outline

Chapter 2 contains an outline of pipeline deterioration and commercially available condition assessment methods. An overview of transient analysis methods is given and previous application of transient based condition assessment methods to real pipelines are discussed. The equations and modelling procedures for unsteady fluid flow in pipes are given.

Chapter 3 investigates the effect that extended variations in pipeline condition have on a transient response. Laboratory results are used to identify accuracies and inaccuracies in modelling procedures. The detection of extended faults is investigated through ITA. ITA is also used to investigate signal properties which improve application of fault detection methods.

Chapter 4 presents a novel transient signal generation system. Application of the signal generation system to two condition assessment approaches is trailed in the field. The assessment of in-line valves though analysis of signal transmission is investigated and pipeline condition assessment through wave speed analysis is carried out.

1.3 Publication list

Journal Articles:

Tuck, J., Lee, P. J., Davidson, M. and Ghidaoui, M. S. (2013). Analysis of transient signals in simple pipeline systems with an extended blockage. *Journal of Hydraulic Research,* 51(6), 623-633.

Tuck, J. and Lee, P. (2013). Inverse transient analysis for classification of wall thickness variations in pipelines. *SENSORS,* 13-12, 17057-17066.

Lee, P. J., Duan, H. F., Tuck, J. and Ghidaoui, M. (2015). Numerical and experimental study on the effect of signal bandwidth on pipe assessment using fluid transients. *Journal of Hydraulic Engineering,* 141(2), 04014074.

Conference Paper:

Tuck, J., Lee, P. J., Kashima, A., Davidson, M. and Ghidaoui, M. S. (2012). Transient analysis of extended blockages in pipeline systems. *In BHR Group - 11th International Conferences on Pressure Surges*, Lisbon, Portugal., 2012, 101-112.

2 LITERATURE REVIEW

This literature review covers material relating to the detection of faults in pipelines and carrying out condition assessments of pipelines. Common causes of pipeline failure through deterioration are discussed and existing condition assessment technologies are evaluated with a particular focus on the use of transient analysis based methods. There are an extensive range of pipeline condition assessment methods and technologies available so this review focusses on those that are applicable to water distribution pipelines to suit the focus of this research.

2.1 Pipeline deterioration

As pipelines age, deterioration is inevitable, reducing the ability of the asset to perform as required. The performance of a pipeline can be affected in two ways; the structural integrity of a pipeline can decay, resulting in failure where it cannot resist the stresses imposed by operation of the system, or the internal condition of a pipeline can decay resulting in reduced hydraulic capacity, poor water quality and increased operational expenses. To provide context for the condition assessment methods described in this review and later in the thesis a summary of relevant pipe materials and typical deterioration processes is given in Table 2-1. The three pipe types covered (cast iron pipe (CIP), ductile cast iron pipe (DCIP) and asbestos cement pipe (AC)) represent the most tested materials in this thesis and the majority of aging pipeline infrastructure internationally (AWWA 2012, Liu *et al.* 2012).

Table 2-1: Pipeline deterioration indicators and failure mechanisms.

Pipe Material	Deterioration Indicator	Mechanism/Cause	Consequence
CIP & DCIP	Wall thinning	Casting defects – voids, inclusions, eccentricity. Corrosion – pitting.	Reduction of structural integrity increasing likelihood of failure under stress.
	Pitting	Localised electro-chemical corrosion.	Reduction in effective wall thickness and increased chance of cracking from stress concentration
	Cracking	Radial crack – longitudinal pipe movement, poor bedding, increased load conditions. Longitudinal crack – insufficient hoop resistance for given internal pressure.	Results in leaks when cracks become fully developed.
	Lining spalling	Scouring - sediments and high water velocity. Poor compatibility with water chemistry.	Reduction in resistance to internal corrosion of structural material.
	Tuberculation	Internal corrosion producing a build-up of corrosion products (tubercles).	Constrict effective area of a pipe, increasing friction losses and pumping costs. Causes water discoloration to a red/brown. Affect valve operation when occurring on valves.
AC	Wall thinning	Cement softening on internal and external surfaces – sulphur attack, soft water corrosion	Reduction of structural integrity increasing likelihood of failure under stress.
	Cracking	Radial crack - longitudinal pipe movement, poor bedding, increased load conditions. Longitudinal crack – insufficient hoop resistance for given internal pressure.	Results in leaks when cracks become fully developed.

(Davis *et al.* 2008, NZWWA 2001, Liu *et al.* 2012, Ranjani *et al.* 2006)

From the summary in Table 2-1 it can be seen that an initial catalyst for pipe failure (without considering joints and other components) is a decrease of structural integrity through wall thinning mechanisms. This increases a pipes susceptibility to failure through stress induced mechanisms. Early identification of these processes can help to predict pipeline failures, hence assist in asset management.

2.2 Pipe condition assessment and monitoring

The industry employs a number of different methods to carry out condition assessments and ongoing monitoring of their pipeline systems. When implementing condition assessment methods and

technologies there are a range of factors to consider which are affected by the desired outcome. First is to consider reactive and proactive assessments; reactive assessments are those that look for an existing failure that is having a detrimental impact on the system, and proactive aims to identify the potential for failure so that failures may be mitigated. The second factor is considering the spectrum between specific and broad investigations, where specific testing can give detailed and accurate information at a particular location, and broad investigations can provide a wider indication of a networks condition. Another factor is whether the assessment method requires invasive testing procedures or not. Invasive testing is that which has an impact on the operation of the system or surrounding infrastructure and these impacts can range from requiring temporary shutdowns of a pipe section to destructive testing which excavates and removes a section of pipe.

Commonly used condition assessment methods and technologies in the water supply industry include desk studies, visual, electromagnetic, and acoustic inspections and acoustic analysis. The relative benefits and limitations of these are discussed in the following sections.

2.2.1 Desktop studies

In smaller distribution networks that are not intensively monitored the earliest indications of faults are often provided by its users. Users often alert local utility providers or authorities to problems such as low pressure and poor water quality. These are common indicators of pipeline faults such as leaks or blockages and can be used to dispatch repair crews or target additional investigations. Notifications like these are undesirable from the providers' point of view and may result in utility providers incurring financial penalties. Databases comprising information from user reports and repair histories can be used to estimate pipeline conditions. Data mining methods can also be used to incorporate location specific historical data with statistical information of specific attributes such as pipe material, age and soil conditions. This can then be analysed in broad studies to identify useful trends that improve residual life predictions (Gasmelseid 2010, Savic and Walters 1999).

Steady state flow models are widely used by consulting engineers for determining the condition of a pipe network. Network modelling software such as EPANET or specific user developed models can be used for such purposes. Available system variables such as pipe size and type, pressure heads, flow rates and pump curves can be used to estimate unknown properties such as pipe wall roughness and local losses. High roughness and loss coefficients can indicate the presence of a fault or extended blockage. Scott and Satterwhite (1998) showed that the presence of a blockage can be indicated through steady state modelling of a pipeline where the pressure heads at each end are known. Jiang *et al.* (1996) also showed that this is possible for a network and that the accuracy of these types of models is

dependent on the amount of information available for the pipe system of interest. Prior knowledge of the pipe networks repairs and maintenance and experience with its components and materials also plays a role in the accuracy of the results generated.

These methods are unable to establish the specific locations and severity of faults (Pudar and Liggett 1992), however they are non-invasive and can be carried out proactively. These factors indicate that the discussed condition assessment methods do not provide conclusive results, however they can provide a basis for deciding where further investigations may be warranted.

2.2.2 Visual pipe inspection

Visual pipeline inspection in its most basic form is carried out by viewing the pipeline externally or inspecting internally for very large diameter mains. For a skilled person, it can be a quick way to achieve an objective assessment. It is limited in most cases as pipelines are either buried or too small to enter. Closed circuit television inspection (CCTV) allows for internal assessment across a broad range of pipe sizes and is currently the most widely used means of onsite pipeline condition assessment. Cameras inserted into pipelines are either attached to small electric vehicles or pushed through by a heavy cable (for smaller pipe diameters). Recordings or images are taken from the inside of a pipeline, which are then viewed to identify pipeline faults. CCTV is relatively inexpensive to apply, though it does require pipelines to be shut down and dewatered which can be costly and disruptive. Automated technologies are being developed to assist the assessor in detecting faults (Guo *et al.* 2009), however, for now the assessment of data can be time consuming, hence costly. The inspections are only qualitative and accuracy is subject to the inspector's proficiency. These systems are restricted by the length over which they can operate, with typical systems reaching in the order of 100 metres. Other limitations also include valves, bends, junctions and blockages which obstruct the passage of a camera or robotic vehicle (Liu *et al.* 2012). To assist with visual inspection, laser-based surface profiling can be used to identify pitting corrosion which can be applied on internal and external pipe surfaces. With the exception of allowing automated processing this technology suffers the same limitations as discussed for CCTV inspection.

2.2.3 Electromagnetic inspection

Where direct access to the pipe wall can be gained, either internally or externally, electromagnetic inspection methods can be used. A common approach to this is magnetic flux leakage (MFL) which measures metal loss from corrosion. This is done by inducing a magnetic field around the pipe wall and any anomalies will create a distortion in the field which can be measured. MFL can provide an accurate and specific measurement of pipe wall thickness however only works on clean, unlined pipes. Internal inspection is invasive as it requires de-watering and can only be applied to large ferrous pipes. Remote

field eddy current tests work in a similar manner by using an exciter coil to generate an electromagnetic field which can be measured, then damage to pipe walls can be determined from discontinuities in the signal. This system can provide continuous data along a pipeline and can be used while the pipeline is in operation, provided that suitable entry and exit ports are available (Liu *et al*. 2012). The inspection method can be costly to apply and may be limited by network topology.

2.2.4 Acoustic inspection methods

Acoustic inspection methods rely upon identifying the hydraulic noise created as water is discharged from a pipeline under pressure to locate leaks. There are two methods which directly measure this hydraulic noise and use it to determine a leaks location. The first method (SmartBall®, Sahara®) inserts a listening device into a pipeline, which is moved along with the water flow. It can be tracked as it moves through a system and leaks are identified by assessing the hydraulic noise. Where it is not practical to insert a device into the system or where a fault is expected in a certain pipe section leak correlators can be used. An example of this is the LeakfinderRT™ system which measures the pressure response, which contains traces of the leak noise, at two locations (typically in the order of 100 m apart). A cross-correlation of the two responses can then identify the relative position of the leak provided it is located between the two sensors and the wave speed in the pipe is relatively uniform. These technologies are non-invasive as they are carried out in a fully operational system and can provide a specific fault location, however only a qualitative estimate of the leak size can be determined and they are not always effective for large leaks. These systems are suitable for reactive use as they look for leaks which have already developed.

An extension to this leak finding technology is to use leak noise to determine the wave speed between two measurement locations, which can in turn be used to infer the condition of the pipe (Nestleroth *et al*. 2012, 2013). This is achieved through intentionally generating a noisy leak by throttling a discharge valve and correlating the noise as it passes two measuring points. Where the distance between the two measurement points is known the wave speed of the pipe can be calculated which relates to pipe strength. This method provides a proactive non-invasive assessment method that can be used to give site specific information. A drawback of this method is that it requires fluid to be discharged and wasted during testing. The range and application on various pipe materials is also limited by the transmission characteristics of the noise signal. The detection of these noise signals can also be difficult as they can be confused with, and hidden by, alternative similar sources within the system.

2.3 Transient based fault detection methods

Transient based fault detection aims to detect faults in a pipeline by exploiting various properties of a pressure trace obtained from that pipeline during a transient event. As a pressure wave propagates along a pipeline it will be affected by any physical variation it encounters, therefore a measured transient signal at a discrete point has the potential to provide information on the pipes condition and faults at many points along the pipeline. Furthermore, this method has the potential to be applied without disrupting the function of the system. The literature describes two distinct approaches regarding how a systems pressure trace can be analysed to detect faults. The first of these takes advantage of the oscillatory nature of transients in a pipeline system and analyses the pressure trace in the frequency domain. The second is a more direct method which analyses the pressure response in the time domain.

2.3.1 Frequency domain

2.3.1.1 Frequency response function

The frequency response function (FRF) method for fault detection examines the transient response of a system in the frequency domain. Lee *et al.* (2005) showed that a leak in a pipeline would impose a periodic pattern upon the resonant peaks of the FRF, hence the FRF could be used for the purpose of leak detection. Lee (2005) then modified the FRF method developed for leaks to account for the effects of discrete blockages in a pipeline. Numerical modelling and experimental data showed that a discrete blockage also imposed a pattern upon the peaks of the FRF which enabled the location and severity of the blockage to be determined.

This method is more suitable to large scale systems where a high frequency signal can be injected relative to the frequency of the system. This is confirmed by experimental results which show a low number of peaks in the frequency response, as the system frequency is high relative to that of the injected signal. The number of faults that can be detected is dependent upon the number of observable peaks in the FRF. Problems also arise in determining the location and nature of faults, as a blockage can affect the FRF in the same way as a leak in a mirrored position. The advantage of the FRF method is that a numerical model of the system is not required.

2.3.1.2 Transient damping method

Transient damping refers to the reduction in magnitude of a pressure wave in time and space. Damping of a pressure wave can be caused by many physical properties and components in a pipeline system

including friction, leaks and pipe constrictions. Researchers have attempted to exploit this effect to help determine the location and magnitude of various faults in a pipeline system.

Wang (2002) derived an expression for a dimensionless resistance parameter for a discrete blockage by treating it as an orifice:

$$G = \frac{K_B Q_0}{2aA} = \frac{K_B \frac{Q_0^2}{2gA^2}}{\frac{aQ_0}{gA}} = \frac{\Delta H_B}{H_S} \tag{2-1}$$

Where ΔH_B is the blockage-induced head loss and H_s is the Joukowsky pressure head rise.

A Fourier expansion was applied to an expression for the initial flow condition of a pipe connecting two constant head reservoirs, with the blockage-induced damping of the transient signal given by:

$$R_{nBi} = 2G_i cos^2(n\pi x_{Bi}^*) \tag{2-2}$$

Where G_i is the blockage resistance parameter for the ith blockage at a dimensionless location x_{Bi}^*. Thus an analytical solution was derived for a transient signal in a pipeline containing multiple blockages. When this analytical solution was compared with a method of characteristics model which accounted for non-linear effects, a high degree of accuracy was found.

Blockage-induced damping depends on the position of the blockage and the harmonic component, suggesting that the transient signal is frequency dependent. The ratio of two blockage-induced damping coefficients depends only on the blockage location:

$$\frac{R_{n_2 B}}{R_{n_1 B}} = \frac{cos^2(n_2 \pi x_B^*)}{cos^2(n_{21} \pi x_B^*)} \tag{2-3}$$

Where the friction damping factor R is calculated from steady flow condition and is dependent on an estimated pipe friction factor f.

Wang (2002) concluded that transients could be used in the detection of blockages. It has also been shown by numerical and experimental results that discrete blockages could be detected and located

when the cross-sectional area was greater than 20% of the pipeline. It is suggested that the method of transient damping may not be feasible to apply to complex systems, as a good estimation of the fault free friction dampening is required.

2.3.2 Time domain

2.3.2.1 Time domain reflectometry

Time domain reflectometry (TDR) is a method whereby the system response is analysed in the time domain and a fault can be detected by the signal reflected from it. Adewumi *et al.* (2000) numerically demonstrated that it is possible to locate a discrete or extended blockage in gas pipelines. Adewumi *et al.* (2003) went on to show that multiple blockages could be detected by numerically decomposing the signal.

Lee (2005) identified shortfalls of the conventional TDR technique, noting that the technique relied upon knowing a fault free system response. Also, an accurate estimation of the reflection signal arrival was difficult.

2.3.2.2 Impulse response function

The system response function in the time domain, otherwise known as the impulse response function (IRF), is an improvement upon standard time domain reflectometry (Lee 2005). The IRF is a refinement of the output from a system. Each reflected signal in the output is represented as a spike based upon a unit impulse input. This means that the IRF is independent of the shape of the input or output, such that it is a property of the system (Vítkovský *et al.* 2003a). The IRF is found by a process known as deconvolution, however this is complicated for finding the IRF for the original system output. This can be done alternatively by first finding the FRF and removing the high frequency components which correspond to the system noise. An inverse Fourier transform of the FRF will yield the IRF.

The IRF method overcomes the issues highlighted for TDR as it refines the reflected response from each fault as a single spike, thus overcoming the problem of accurately determining the arrival of a reflection. The IRF is also independent of the shape of the input, thus a fault free benchmark is not required.

2.3.2.3 Experimental testing of extended blockages

Kim (2008) experimentally investigated the effect of extended blockages on a transient signal for the purposes of numerical model development. The experiments investigated the effect of hard and soft blockages by inserting constrictions into the pipeline that were formed from copper and silicon

respectively. The soft blockages demonstrated behaviour comparable to that observed from an air pocket, while the hard blockages generated a high frequency pressure spike in the observed signal. The blockage length was 153 mm (0.4% of the experimental pipelines length) and the internal bore size was varied between 2 and 15 mm while the outer diameter was at a constant 25.4 mm over the length of the pipeline. Blockages with internal roughness were also investigated.

The high frequency of the pressure spike can be attributed to the wall thickness and length of the blockage used in the experimental apparatus. Kim (2008) observed little difference between the results obtained from the blockage with and without internal roughness. This was attributed to the dominant physical phenomenon being eddy inertia of the turbulent jets formed at the constriction and expansion of the blockage, indicating that the diameter to blockage length ratio was large. Also the experimental data was sampled at a rate of 4 kHz indicating that only two pressure measurements could be taken during the time taken for the wave to pass through the blockage. These factors indicate that the length of the blockage limits the ability to show the effect of a blockage with significant axial extension on transient behaviour.

2.3.3 Inverse transient analysis

Inverse transient analysis (ITA) attempts to replicate a transient response by iteratively calibrating a numerical model. Generally networks are evaluated by first knowing demands and system properties (e.g. pipe roughness and local loss coefficients). The network is then solved for flows and pressure heads. Pudar and Liggett (1992) introduced a method for determining the location of leaks and illegal water connections whereby the network state is known (e.g. pressure heads and pipe flow), and the system properties are solved for. A derivative-based Levenberg-Marquardt (LM) method was applied to optimise the least squares difference between calculated and measured pressure heads. The authors recognised that in practice the amount of data available would be less than that required to determine where leaks exist, hence leading to an under-determined problem. It was suggested that without masses of data, inverse analysis would only be suitable as a supplement to conventional leak surveys.

Liggett and Chen (1994) recognised that transient signals can be used to provide continuous information about a pipeline along its length. Hence data from a select few measurement points can provide an infinite number of data points, moving from an under-determined steady analysis as described above to an over-determined transient analysis. This method requires an accurate numerical transient solver to be coupled with an optimisation algorithm to iteratively reduce the error between the measured and calculated transient signals.

The development of more accurate and efficient optimisation techniques has been of significant interest in the development of ITA. The optimisation methods can be broken into two areas. The first of these is the derivative-based LM method as employed by Pudar and Liggett (1992), who showed that fast convergence to a solution can be achieved. It can however become trapped at local minima or maxima, limiting its application to complex systems. The second method employs sample and search routines such as genetic algorithms (GA). GA overcome the risk of unconverted solutions but require significant amounts of computational power.

Vítkovský *et al*. (2002) showed the LM method to be inadequate for the inverse calculation of experimental transient problems. The authors employed a shuffled complex evolution (SCE) algorithm which proved to be accurate, however required significantly longer computational time (approximately 30 times longer). This inefficiency prompted the implementation of a systematic Levenberg-Marquardt (SLM) algorithm. SLM reduces the chance of a less than optimal solution by initially solving for a trial leak at all locations. The most accurate of these trial leaks is then set for further iterations until solution convergence is achieved. Test results showed SLM to be faster and more accurate than SCE (Vítkovský *et al*. 2002).

Kapelan *et al*. (2003) developed a hybrid GA (HGA) which pools the advantages of the LM and GA methods. The HGA-based inverse transient model proved to be more computationally efficient than the GA and more robust than the LM method. A weighted objective function was then introduced to account for prior information of system calibration parameters (Kapelan *et al*. 2004).

2.3.4 Field application

Field applications of transient detection methods reported in the literature are primarly targeted at the improvement and validation of transient based detection models (Stoianov *et al.* 2003, Covas *et al.* 2004 and Stephens *et al.* 2004a). Other field applications of transient analysis have focussed on determining operational characteristics and general performance of water distribution systems (Karney *et al.* 2007 and Karney *et al.* 2008).

Stoianov *et al*. (2003) presented field investigations which sought to detect and locate leaks in a water transmission pipeline. The authors concluded that a leak of 1.8% of the pipelines base flow did not affect the propagation of the transient signal, thus could not be detected. However, the investigation used pump trips to generate the transient signals which generate a long and smooth pressure rise, reducing the resolution of the recorded data. A following experiment showed that pressure signals generated by quickly closing an inline gate valve may be more successful in detecting and locating leaks. Faster valve closures for leakage detection were investigated by Covas *et al.* (2004) who

generated transients through manually closing a fire hydrant valve opened by one turn. Employing inverse transient methods the authors found that the location of a leak in a water transmission pipeline could be found, accurate to 1% of the pipeline length. The accuracy of these results was reduced by the pressure transducers maximum sampling rate of 20 Hz, theoretically limiting the detection accuracy to approximately 50 m. Stephens *et al.* (2004a) carried out similar investigations on a 378 m long ductile iron concrete lined (DICL) water distribution pipeline with a diameter of 100 mm. Transients were generated by a torsional spring operated valve to generate a very quick pressure rise. The valve was mounted on a fire hydrant standpipe and pressure measurements were taken by pressure transducers capable of a 2000 Hz sampling frequency. Inverse transient analysis was shown to accurately detect the location of a 10 mm leak and predicted it to have a size of 8.5 mm. The author also demonstrated that an air pocket of 1.6 L could be accurately located, with a predicted volume of 1.4 L.

Stephens *et al.* (2004a) and Stephens *et al.* (2005b) presented results of transient tests carried out on water distribution systems subject to discrete blockages. The authors determined that like leaks and air pockets a discrete blockage would produce a distinct change in the transient response of a pipeline. Stephens *et al.* (2005a) then considered the situation where a section of pipe is fully blocked in a complex pipeline network, for example where a valve has inadvertently been left closed. The investigation successfully demonstrated that identification of closed valves in a pipeline network using transient analysis is possible where an appropriately calibrated model is implemented. Each of the investigations outlined that for ITA to be successfully applied improvements to the existing transient models were required to account for the practical complexities found in real pipeline systems.

Stephens *et al.* (2005c) sought to determine the relative importance of including unsteady friction models while modelling large scale pipelines. The investigation considered the efficient approximation of unsteady turbulent flow conditions model developed by Vítkovský *et al.* (2004). Numerical results produced with and without the unsteady friction model were compared to transient response measurements taken from a 13.5 km water transmission pipeline. The study demonstrated that for a "fault free" pipeline the inclusion of unsteady friction would increase the observed rate of damping by 9.5%. The increased rate of damping was significant and improved the fit between numerical and experimental results, suggesting that the inclusion of unsteady friction models in transient analysis is warranted.

Stephens *et al.* (2008) investigated the use of transient analysis for the condition assessment of pipeline walls. The investigation was carried out on the 750 mm diameter Morgan Transmission Pipeline (MTP) in South Australia. The authors categorised the condition of the pipe walls into four groups of varying wave speeds based on CCTV footage captured from a 400 metre section of the pipeline. The variations

in pipe condition were included in a numerical transient model. The numerical results were compared to pressure traces obtained through deliberately inducing and measuring a transient signal in the MTP, and the results were found to be comparable. This indicates that transient signals have the potential to be used for the condition assessment of pipe walls.

Karney *et al.* (2007) performed a set of transient field tests on a section of London's water distribution system to improve understanding of the systems operational characteristics. The investigation generated controlled transient events in the water distribution system using a sequence of pump start-ups and shut-downs. The system response was measured by pressure transducers distributed about the network. A numerical transient model of the system was developed and calibrated to match the response from the field tests through an inverse transient procedure, with focus given to frictional effects and distribution demands. The authors concluded that the study had provided fruitful information about the daily operational behaviour of pump start-ups and shut-downs as well as demands and pipe friction factors. Karney *et al.* (2008) sought to determine of performance of water supply transmission mains in the region of Peel, Ontario. Pressure recordings were taken from permanently installed monitoring devices over an extended period of time. The research found that the surge chambers and other transient protection devices installed on the system effectively suppressed the transient shocks caused by pump and valve operations. As for the paper previously described, calibration of a numerical model was carried out to match the test results. The authors' goal was to use the calibrated model to confidently and economically model any potential changes or expansions to the system. Surge protection measures may also be optimised using the calibrated model. The authors concluded that the performance of the analysis was good and that ITA has potential as a low cost and low resource method of system analysis.

Haqshenas (2010) investigated the application of piezoelectric transducers for leak detection in pipelines. Experiments were conducted on a straight section of a water distribution system constructed from 180 PEH (polyethylene high density) pipe. Piezoelectric transducers set to oscillate at frequencies between 340 Hz and 550 Hz were mounted at one end of the pipeline while a discharge valve 86 m from the transducer was used to simulate a leak. Pressure measurements of the system response were made with hydrophones sampling at 24 kHz. The system response was analysed in the frequency domain at each time step and efforts were made to reduce the level of noise contamination in the results. Examination of the frequency response and knowledge of the system boundaries was employed to guess a wave speed for the system. Comparison of the systems wave speed and known leak location determined that the presence of the leak produced a variation of the systems frequency response.

2.3.4.1 Observations and summary of field testing

Much of the field based research presented in the literature identifies transient analysis as a viable method for fault detection or condition assessment of pipelines. The distinct advantages of transient analysis are that a large section of pipeline or network may be assessed cheaply with few resources and personnel when compared with other available technologies. Through observation of the existing research several common limitations to the application of the methods have been identified. The first is the ability of the data acquisition systems and pressure transducers to measure the transient response at a high enough frequency to analyse small features within the system. The second is the inability to generate sharp and distinct transients that can be easily identified from naturally occurring transients from pipeline systems operation. The third is a lack of detailed understanding of transient behaviour where variations in pipeline conditions occur, as well as a lack of computing power to resolve small scale pipeline geometries.

2.4 Governing equations and transient modelling

The simplified equations of mass and linear momentum that govern unsteady one dimensional pipe flow are of the following form (Wylie and Streeter 1993):

$$\frac{gA}{a^2}\frac{\partial H}{\partial t} + \frac{\partial Q}{\partial x} = 0 \qquad (2\text{-}4)$$

$$\frac{1}{gA}\frac{\partial Q}{\partial t} + \frac{\partial H}{\partial x} + \frac{fQ|Q|}{2gDA^2} = 0 \qquad (2\text{-}5)$$

Where H = head in the pipe, Q = pipe discharge, A = cross-sectional area of the pipe, D = pipe diameter, a = wave speed, f = Darcy-Weisbach friction factor, g = acceleration due to gravity, x = distance along the pipe and t = time. These equations assume that the fluid and pipe will deform in a linear elastic manner and that the compressibility of the fluid is low. These two equations form a pair of hyperbolic partial differential equations with two dependent variables, flow and hydraulic grade, and two independent variables, distance and time. Equations (2-4) and (2-5) can seldom be solved analytically (Ghidaoui *et al*. 2005), so their solution must be determined through numerical methods. Methods that have been applied in the literature for this purpose include the method of characteristics (MOC), wave plan, finite difference and finite volume methods. The MOC is the most widely used and accepted of these.

2.4.1 Method of characteristics

A practical solution to Equations (2-4) and (2-5) can be found by solving in the time and space domain using the MOC. MOC transforms the governing equations into four ordinary differential equations. This is done by a linear combination of the two equations using an unknown multiplier λ. The like terms of head and flow are then grouped together as shown in equation (2-6).

$$\frac{1}{gA}\left(\frac{\partial Q}{\partial t} + \lambda gA\frac{\partial Q}{\partial x}\right) + \lambda\frac{gA}{a^2}\left(\frac{\partial H}{\partial t} + \frac{1}{\lambda}\frac{a^2}{gA}\frac{\partial H}{\partial x}\right) + \frac{fQ|Q|}{2gDA^2} = 0 \qquad (2\text{-}6)$$

Now if the independent variable x is considered to be a function of t, the chain rule can be applied.

$$\frac{dH}{dt} = \frac{\partial H}{\partial t} + \frac{\partial H}{\partial x}\frac{dx}{dt} \qquad \frac{dQ}{dt} = \frac{\partial Q}{\partial t} + \frac{\partial Q}{\partial x}\frac{dx}{dt} \qquad (2\text{-}7)$$

Through comparison of equation (2-6) with equations (2-7) the following expression can be found,

$$\frac{dx}{dt} = \lambda gA = \frac{1}{\lambda}\frac{a^2}{gA} \qquad (2\text{-}8)$$

And equation (2-6) can be re-written as an ordinary differential equation.

$$\frac{1}{gA}\frac{dQ}{dt} + \lambda\frac{gA}{a^2}\frac{dH}{dt} + \frac{fQ|Q|}{2gDA^2} = 0 \qquad (2\text{-}9)$$

The solution of equation (2-8) gives two particular values for λ when limitations are imposed on how the distance x varies with time t.

$$\lambda = \pm \frac{a}{gA} \tag{2-10}$$

$$\frac{dx}{dt} = \pm a \tag{2-11}$$

Through substituting the expression for λ into equation (2-9), two equations can be found which are known as the positive and negative characteristic equations, C^+ and C^- respectively. These equations are only valid along a specified line in space and time. This line is known as the characteristic line and is defined by the compatibility equations.

$$C^+ \qquad \frac{1}{gA}\frac{dQ}{dt} + \frac{1}{a}\frac{dH}{dt} + \frac{fQ|Q|}{2gDA^2} = 0 \qquad \frac{dx}{dt} = +a \tag{2-12}$$

$$C^- \qquad \frac{1}{gA}\frac{dQ}{dt} - \frac{1}{a}\frac{dH}{dt} + \frac{fQ|Q|}{2gDA^2} = 0 \qquad \frac{dx}{dt} = -a \tag{2-13}$$

For a pipeline divided into a number of reaches (N) with lengths of Δx equations (2-12) and (2-13) can be integrated along the characteristic line to derive a pair of finite difference equations that are dependent on space and time. If the dependent variables H and Q are known at points A and B as shown in Figure 2-1, the two finite difference equations which follow the positive and negative characteristic lines can be solved at point P for the unknown dependent variables.

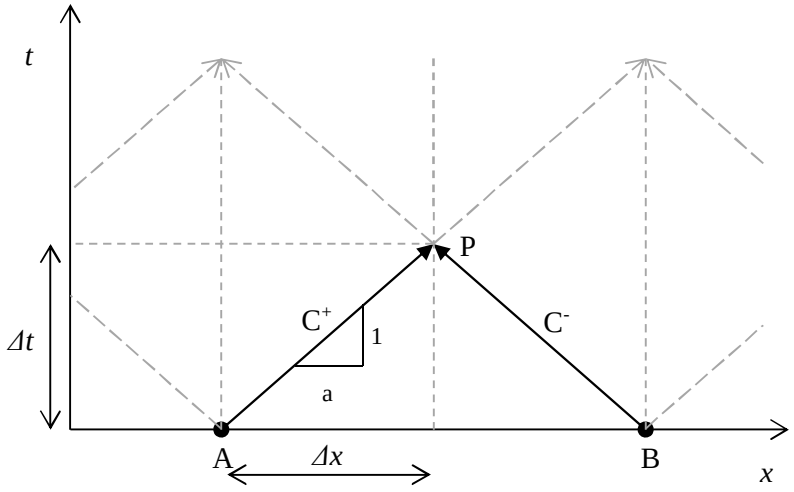

Figure 2-1: Method of characteristics grid

To get the equations into a form suitable for integration they must be first multiplied by $a\,dt/g = dx/g$ as shown for the C^+ equation. Equation (2-12) can then be integrated along the characteristic line AP.

$$\int_{H_A}^{H_P} dH + \frac{a}{gA}\int_{Q_A}^{Q_P} dQ + \frac{f}{2gDA^2}\int_{x_A}^{x_P} Q|Q|dx = 0 \qquad (2\text{-}14)$$

The trapezoidal rule is used to approximate the variation of Q with x as shown in the last term. This maintains the linear form of the integrated equations while achieving second order accuracy. Integration yields the following finite difference equations.

C^+ $$H_P - H_A + B(Q_P - Q_A) + R(Q_P|Q_A|) = 0 \qquad (2\text{-}15)$$

C^- $$H_P - H_B - B(Q_P - Q_B) - R(Q_P|Q_B|) = 0 \qquad (2\text{-}16)$$

Where B is a function of the pipeline and fluid properties. This is often referred to as the pipeline characteristic impedance:

$$B = \frac{a}{gA} \qquad (2\text{-}17)$$

And R can be referred to as the resistance coefficient:

$$R = \frac{f\Delta x}{2gDA^2} \qquad (2\text{-}18)$$

Equations (2-15) and (2-16) can be solved simultaneously to determine H and Q at some point P in a future time step. The initial conditions for an MOC analysis are set at the steady state values, while boundary conditions, such as reservoirs or valves are determined though substituting known variables into the appropriate positive or negative characteristic equation. Transient behaviour can then be added to the system and successively analysed at each specified node in the time and space domain using the MOC.

2.4.1.1 Interpolation methods

The MOC as derived previously is suitable for a system with a single wave speed, hence a uniform grid in space and time can be implemented. Many pipelines will have variations in properties such as wall thickness or diameter, thus leading to a corresponding change in wave speed. The wave speed determines the slope of the characteristic line, so a change in this wave speed will lead to a discontinuity between nodes. This means that an interpolation method is required to determine values for H and Q that can be used in the calculations at the subsequent nodes. Three of these methods and their variations are described here.

2.4.1.2 Space line interpolations

Linear space line interpolation projects the characteristic line back from the unknown node to the previous time step. A linear interpolation can then be made between two known nodes. There are two variations of this interpolation which depend on the size of the grid relative to the wave speed. The first case, where the wave speed is higher than that which the grid was specified for, is shown in Figure 2-2. Values at R and S can be found from interpolating between nodes A and B. In the second case, as shown in Figure 2-3, the wave speed is slower than that which dictated the grid size. Here the characteristic lines are extended some distance greater than Δx, to where they meet the previous time step. This is known as a reachout method, where values at R and S can be found from interpolation along the space lines A-A' and B-B' respectively.

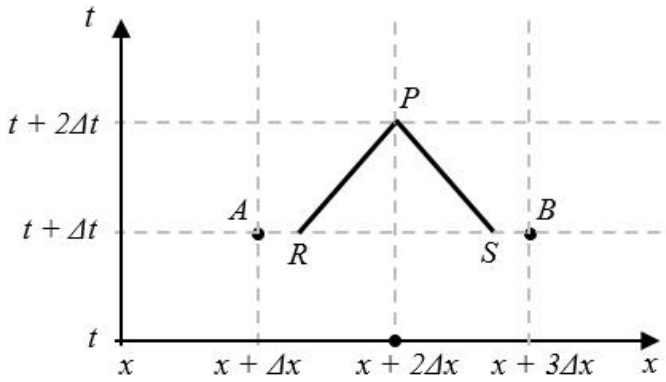

Figure 2-2: Space line interpolation

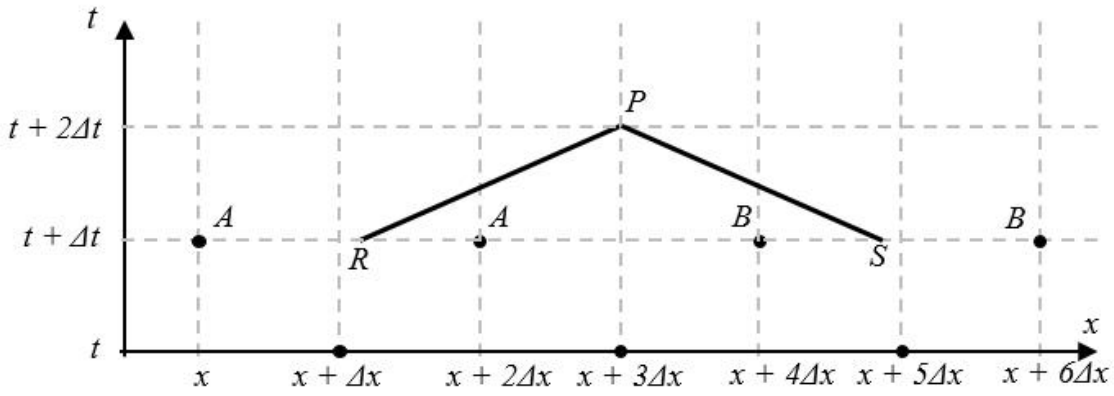

Figure 2-3: Reachout space line interpolation

Sibertheros *et al.* (1991) found that using higher order cubic spline interpolations improved the accuracy of the MOC solution over that achieved using linear interpolations. The cubic spline interpolation however, uses information from multiple nodes along the space line which introduces numerical diffusion by spreading the limits of the interpolation formula (Chen 1995). This method also cannot be efficiently applied to branching and looped pipes, so is not suitable for pipe network calculations.

2.4.1.3 Time line interpolations

Wylie and Streeter (1993) suggest a linear interpolation along the time line as shown in Figure 2-4a. The characteristic lines are projected back from the unknown node P to where they cross the adjacent time line at points R and S. Linear interpolation can then be done along the lines A-D and B-E respectively. Figure 2-4b shows the situation where the wave speed is lower than that which determined the grid. Here an implicit numerical scheme must be solved to determine the unknowns at the next time step. Or to maintain the explicit form, the characteristic lines must be projected backwards in time and over two or more space steps to an intersection with a timeline where the system state is known.

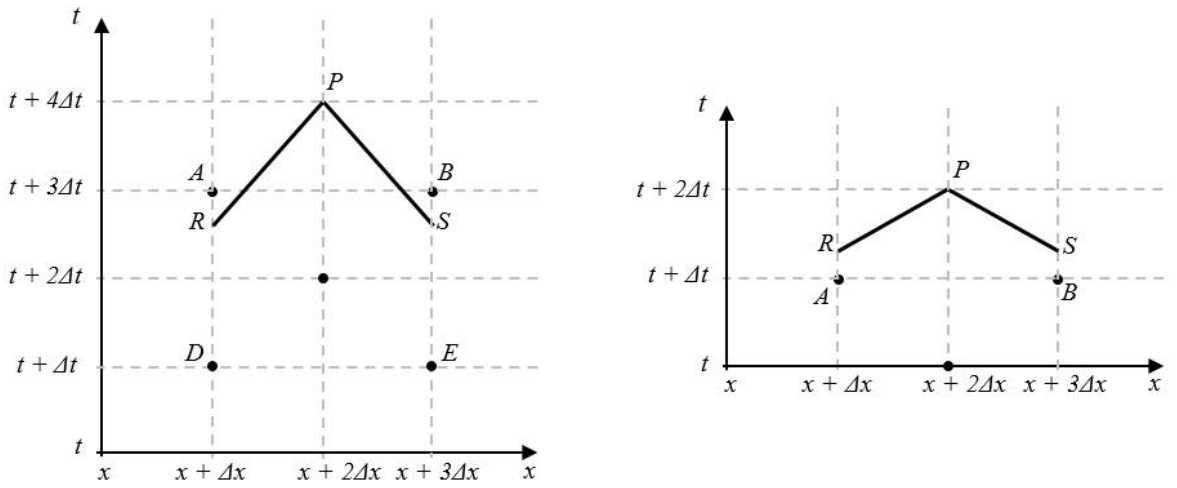

(a) (b)

Figure 2-4: Time line interpolations

As with space line interpolation, higher order schemes can be employed along the time line. These schemes use time derivatives instead of spatial derivatives. Chen (1995) found a cubic interpolation scheme to be the most computationally efficient with regards to solution accuracy, when compared with linear and fifth order schemes. Time line interpolation schemes are well suited towards pipe networks as they do not directly require information from adjacent nodes.

2.4.1.4 Wave speed adjustment method

The simplest method of interpolation described in the literature is the wave speed adjustment method. The method artificially adjusts the wave speed such that the characteristic line aligns with the grid, hence effectively inducing a physical variation from the system that is being modelled. The advantage of the wave speed adjustment method is that it is neither dissipative nor dispersive, so the total energy in the system is conserved (Ghidaoui and Karney 1994).

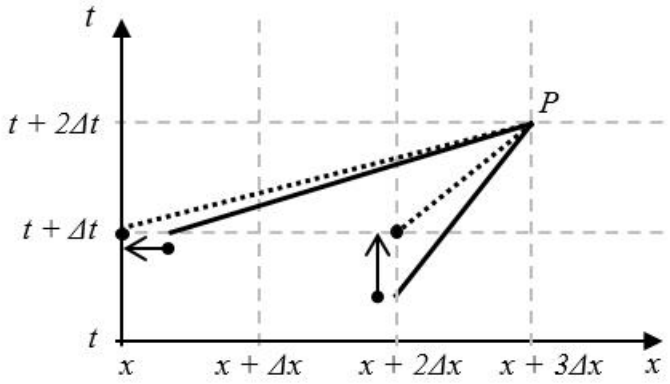

Figure 2-5: Wave speed adjustment method

2.4.1.5 Alternative approach

An alternative approach to the interpolation methods described in the preceding sections is to use a fixed time step grid which allows for variations in the space step based upon the wave speed. This method will introduce an error through shifting the junction between two sections of pipe with different properties to the closest node. The advantage of this method is that the introduced error can then be easily quantified and will have a maximum value of half the discretisation length. The discretisation length can then be set to an appropriate resolution such that the model will account for pipeline variations within an accepted tolerance. The method will also reduce computational requirements as interpolation calculations at each node will not be required.

For the research presented in this thesis the duration over which changes in pressure occur are typically short in comparison to the length of pipeline components. This means that the space step (Δx) required to achieve accurate representation of a wave front will be relatively small, hence errors using this method will be small making it a suitable approach. Where accurate representation of the pressure rise is not required or the wave front is relatively long larger space steps may be feasible to achieve a computationally less expensive model, hence applying a time or space line interpolation scheme may be appropriate.

2.4.2 Unsteady friction modelling

Consideration of frictional head loss (h_f) is important when analysing transient behaviour over a significant period of time or space, as it accounts for much of the damping and attenuation of the

pressure wave. Under steady state conditions frictional head losses (h_{fs}) can be calculated considering the Darcy-Weisbach friction factor (f) by

$$h_{fs} = \frac{fV|V|}{2gD} \tag{2-19}$$

When incorporating frictional head loss into a unsteady flow model it can be determined by making a steady or quasi-steady friction assumption. The steady assumption calculates the Darcy-Weisbach friction factor at steady state and assumes constant for the duration of the unsteady flow analysis, while the quasi-steady assumption calculates the friction factor at each node in space and time to satisfy the immediate flow conditions. These methods can provide a reasonable approximation of the behaviour under some circumstances (Duan *et al.* 2012c, Stephens *et al.* 2005c). In general, however, these methods fail to capture the damping of pressure waves leading to significant discrepancies between numerical and experimental data (Ghidaoui *et al.* 2005). Both of these methods fail to account for the cyclic growth and destruction of boundary layers in the pipeline during transient flow. This cyclic behaviour leads to greater velocity gradients and turbulence, hence greater friction losses. Thus, to accurately model the pressure wave unsteady friction must be accounted for such that the total friction loss per unit length (h_f) is given by

$$h_f(t) = h_{fs}(t) + h_{fu}(t) \tag{2-20}$$

Where h_{fs} gives the quasi-steady component of friction and h_{fu} is the deviation from this due to unsteady flow. Empirical based estimates have been made to determine h_{fu} through determining a coefficient for accelerating and decelerating flow cases (Daily *et al.* 1956). Subsequent experiments found the coefficients to be varied for different flow conditions (Vardy and Brown 1997).

2.4.2.1 Laminar pipe flow

An analytical solution to calculate h_{fu} was first proposed by Zielke (1968) who related the instantaneous velocity to weighted past velocity changes using a constant viscosity assumption. This is achieved through applying the Laplace transform to the axial component of the Navier-Stokes equations to determine wall shear for unsteady laminar pipe flow:

$$h_{fu}(t) = \frac{16\nu}{gD^2}\int_0^t \frac{\partial V}{\partial t}(t')W(t-t')dt' \tag{2-21}$$

where ν is the kinematic viscosity of the fluid, t' is the time as used within the convolution and W is the weighting function, which is found by:

$$W(t) = \begin{cases} e^{-26.3744t^*} + e^{-70.8493t^*} + e^{-135.0198t^*} \\ \quad + e^{-218.9216t^*} + e^{-322.5544t^*} & t^* > 0.02 \\ 0.282095t^{*-1/2} - 1.250000 + 1.057855t^{*1/2} + \\ \quad 0.937500t^* + 0.396696t^{*3/2} - 0.351563t^{*2} & t^* < 0.02 \end{cases} \quad (2\text{-}22)$$

where t^* is a dimensionless time parameter

$$t^* = \frac{4\nu t}{D^2} \quad (2\text{-}23)$$

2.4.2.2 Turbulent pipe flow

Vardy and Brown (2003) followed the method of Zielke (1968) to derive a weighting function for smooth turbulent flow

$$W(t^*) = \frac{A^* e^{-B^* t^*}}{\sqrt{t^*}} \quad (2\text{-}24)$$

where the coefficients are determined through assuming uniform turbulent viscosity and relating wall shear stress to the mean flow (Vardy and Brown 2003).

$$A^* = \frac{1}{2}\sqrt{\frac{\nu_w}{\pi \nu_{lam}}} \quad (2\text{-}25)$$

$$B^* = \frac{\mathrm{R_e}^{\log_{10}(15.29\mathrm{R_e}^{-0.0567})}}{12.86} \quad (2\text{-}26)$$

where ν_w is the kinematic viscosity at the wall, ν_{lam} is the laminar kinematic viscosity and the coefficients are valid for $2000 < \mathrm{R_e} < 10^8$. Vardy and Brown (2004) also developed coefficients for fully rough turbulent pipe flow

$$A^* = 0.0103\sqrt{\mathrm{R_e}}\left(\frac{\varepsilon}{D}\right)^{0.39} \quad (2\text{-}27)$$

$$B^* = 0.352\mathrm{R_e}\left(\frac{\varepsilon}{D}\right)^{0.41} \quad (2\text{-}28)$$

where ε is the roughness height and the coefficients are valid for $10^{-6} < \varepsilon/D < 10^{-2}$

2.4.2.3 Efficient approximation of the weighting functions

To implement Equation (2-21) in a method of characteristics model, numerical integration over the time history at each node in the solution space is required. This is very computationally expensive and

requires a significant amount of memory. To avoid the computationally expensive numerical integration, methods of efficiently approximating the weighting functions have been developed. A number of efficient approximations have been presented for laminar and turbulent flow regimes (Kagawa *et al*. 1983, Ghidaoui and Mansour 2002, Trikha 1975). Vítkovský *et al.* (2004) presented efficient approximations of the weighting functions given in both Vardy and Brown (2003) and Zielke (1968) with a summation of exponential terms, thus avoiding the computationally expensive convolutions. Comparison with experimental results showed that this method was accurate over a number of transient cycles and decayed for long duration transients (Vítkovský *et al.* 2006).

3 ANALYSIS OF EXTENDED FAULTS IN PIPELINES

3.1 Introduction

Deterioration of pipeline infrastructure is a chief concern for managers of water distribution networks. Some of the most concerning and common means of deterioration include reductions in pipe strength through wall thinning or deterioration of mechanical properties and the development of blockages. Depending upon the pipeline material and conditions these variations can occur independently or simultaneously. Pipe strength reduction can occur through poor construction, internal or external corrosion of pipe walls and loss of protective linings, while extended blockages can develop in pipelines via the processes of scaling, bio film growth and sediment deposition or through designed reductions in pipe diameter. Where pipe strength reduction occurs through the process of internal corrosion on metallic pipelines tuberculation can result which results in blockage development. Identification of these faults within pipelines is important as they can be a precursor to more immediate and serious faults such as leaks and bursts or ongoing problems such as poor water quality, decreased pumping efficiency or reduced flow and head to consumers (Stephens *et al.* 2002, 2005b, Baral *et al.* 2006). An emerging area of pipeline fault identification is the analysis of fluid transient behaviour in order to determine the condition of a pipeline. This chapter investigates the effect that extended variations in pipeline conditions have on a transient signal by examining numerical and experimental results in the time and frequency domains. This knowledge is useful for the development of transient analysis based fault detection and condition assessment methods and is also valuable when carrying out transient design of pipeline systems.

3.2 Background

Existing literature has focussed on transient behaviour and transient-based fault detection for discrete faults (defined as faults that can be approximated by a point effect), including Silva *et al.* (1996), Brunone and Ferrante (2001), Ferrante and Brunone (2003), Covas *et al.* (2005), Stephens *et al.* (2005b), Wang *et al.* (2005b), Mohapatra *et al.* (2006b), Lee *et al.* (2008a), Sattar *et al.* (2008), Colombo *et al.* (2009) and Duan *et al.* (2011a). However, real pipelines contain a variety of faults, many of which extend for a significant distance along the pipe and cannot be approximated by a point. These extended faults are looked at in this chapter by considering two significant properties; one is the change in diameter caused by a blockage and the other is the change in wave speed caused by reductions in pipe wall strength.

A discussion by Brunone *et al.* (2008a) numerically demonstrated that a blockage causing a reduction of internal diameter over some length would give rise to significantly different transient behaviour than that from a discrete blockage, while the decay of energy for each case was similar. This chapter follows on from that discussion, focussing on the effect that an extended blockage or constricted pipe section has on a transient signal. The term "extended blockage" in this thesis refers to a reduction in the pipes nominal diameter over some length due to changes in pipeline material and size, tuberculation, scaling, bio film growth or sediment deposition. Adewumi *et al.* (2003) showed numerically that time domain reflectometry could be used to detect extended blockages formed through hydrate deposition in natural gas pipelines. Qunli and Fricke (1991) and De Salis and Oldham (2001) analysed Eigen frequency shifts and resonant frequencies to determine characteristics of blockages in air ducts. Mermelstein (1967) and Schroeder (1967) applied frequency domain analysis of pressure waves to determine the shape of human vocal tracts. Duan *et al.* (2011a) presented a leak detection method for complex series pipelines which consist of pipe sections of multiple diameters. Duan *et al.* (2012a) demonstrated that the formation of an extended blockage would shift the resonant frequencies of a system and a method was developed where the blockage location and size was determined from the systems frequency response function. Duan *et al.* (2012a) also determined that the observed shift in the resonant frequencies is not affected by friction. Meniconi *et al.* (2011a, 2011c) investigated the interaction between transient signals created by a small amplitude pressure wave generator and anomalies which included discrete and extended blockages (of relatively short length) within a viscoelastic pipeline. Further research by Meniconi *et al.* (2012a) focussed on the characteristics and magnitudes of initial reflections from discrete and extended blockages and identified variations in behaviour between the two cases. The authors also evaluated the ability of numerical models including unsteady friction and viscoelasticity components to simulate the observed experimental behaviour.

Pipe wall condition and strength can have a significant effect on wave speed and this property was first investigated by Stephens *et al.* (2008) for the purposes of internal wall condition assessments of pipelines through transient analysis. The authors showed that changes in the condition of wall lining in a 750 mm mild steel cement lined (MSCL) pipeline would create reflections which can be used to characterise wall deterioration. Stephens *et al.* (2008) followed on with this research and presented an inverse transient analysis (ITA) method of condition assessment which divided the pipeline into 15 m long sections, then inversely selected one of five predetermined levels of pipe damage for each section in an attempt to replicate the transient response of the system. The results showed reasonable correlation between the damage predicted by the ITA method and damage determined through the commercially available methods; ultrasonic pipe wall inspections and visual closed circuit television surveys. Hachem and Schleiss (2012) carried out laboratory investigations that aimed to detect deterioration of pipe walls by considering simulated weak sections in a pipeline. The analysis methods used combined fast Fourier transforms and wavelet analysis techniques to locate the weak pipe sections. The weak sections were represented by using different pipe materials over short 0.5 m lengths. The method enabled the location of a single weak section of pipe to be determined along with a fair approximation of the wave speed. Gong *et al.* (2013) presented a time domain reflectometry (TDR) method for the detection of a deteriorated section in a single pipeline. The method calculates the characteristic impedance of a deteriorated section by considering the magnitude of the initial reflection, from which the wave speed and wall thickness of the section can be calculated by considering the equation for wave speed in a fluid filled pipe. The method is shown to produce accurate results for laboratory experiments and is computationally cheap, however it makes a number of assumptions that may limit its application to field based analysis. These assumptions include: that corrosion of the pipe wall only occurs internally and does not affect Young's modulus of the material; that corrosion is uniform in both radial and longitudinal directions; that no corroded material remains attached to the pipe wall and that the time of the induced head perturbation is less than the time it takes for the wave front to travel two lengths of the deteriorated section. Accuracy of the method is also subject to the operator's selection of reference data points.

The literature has highlighted the importance of understanding the time domain and periodic behaviour of transient signals affected by extended changes in pipelines, however only a few comparisons have been made between experimental and numerical data. Specifically lacking is the consideration of cases where the length of variation is significant compared with other pipeline variables such as the diameter and data sets spanning a range within selected variables. In this chapter, the impacts of extended variations on transient responses are determined from numerical and experimental data. The effects of fault length and severity on a transient response are highlighted and comparisons between the numerical

predictions and the experimental results are used to identify behaviour not captured by the current models. ITA is used as a tool to determine the ability of models to accurately predict fault locations in a laboratory system and identify important parameters and transient characteristics.

3.3 Modelling theory

To investigate the effect of extended variations in pipeline condition the method of characteristics (MOC) model is used to solve the governing mass and linear momentum conservation equations for one dimensional unsteady pipe flow (Equations (2-4) and (2-5)). This modelling approach is the most common within the field of transient analysis in pipeline systems (Karney and Ghidaoui 1997, Ghidaoui *et al*. 2005). The MOC solves the governing equations through confining the solution to a grid in the time and space domains by applying the following relationship:

$$C_r \frac{dx}{dt} = \pm a \tag{3-1}$$

where dx is the grid spacing in the along the length of the pipe and dt is the time step for the numerical solution. As the wave speed (a) can vary significantly when considering extended faults, Equation (3-1) shows the grid will not be uniform over an entire solution. To account for this the MOC model is coded in FORTRAN using a constant time step and variable space step discretisation, such that the Courant number (C_r) is always at unity.

This approach allows extended faults to be represented through variations in geometric properties and wave speeds between pipeline reaches, while conserving the total energy in the system. Numerical dissipation and dispersion errors that arise with the use of interpolation methods shown by Ghidaoui *et al*. (1994, 1998) and Chen (1995) are also avoided. While using this grid discretisation approach avoids numerical errors, there can be an error associated with aligning the location of an element (e.g. the start of a blockage) to the nodes on the solution grid. This error is quantifiable and will be less than $dx/2$ or $adt/2$, thus a step size can be chosen to minimise the error to an acceptable value or a larger step size may be chosen which fits the desired solution domain accurately.

Solving the governing equations for one dimensional fluid flow in a pipeline (Equations (2-4) and (2-5)) subject to the condition in Equation (3-1) gives two simultaneous equations which can be used to solve for the head (H_P) and flow (Q_P) at a grid point where the head (H_A, H_B) and flow (Q_A, Q_B) are known values at adjacent nodes in the previous time step (Wylie and Streeter 1993). These equations are referred to as the positive (Equation (3-2)) and negative (Equation (3-3)) characteristic equations.

$$H_P = H_A - B(Q_P - Q_A) - RQ_P|Q_A| \tag{3-2}$$

$$H_P = H_B + B(Q_P - Q_A) + RQ_P|Q_B| \tag{3-3}$$

where B is the characteristic impedance of the pipeline given by

$$B = \frac{a}{gA} \tag{3-4}$$

and R is the pipeline resistance coefficient, which can be calculated by

$$R = \frac{fdx}{2gDA^2} \tag{3-5}$$

where D is the nominal diameter of the pipe section and f is the Darcy-Weisbach friction factor. The additional effects of unsteady friction are accounted for using the smooth turbulent pipe flow friction model (Vardy and Brown 2003).

With the understanding that real blockages can be distributed along the pipe axis, the modelling of a blockage as a length of pipe is a better representation of the physical reality than the point approximations used for discrete blockages in Stephens *et al.* (2005b), Wang *et al.* (2005b), Mohapatra *et al.* (2006b) and Lee *et al.* (2008a). Where a pipe is constricted over some length it is modelled as an extended blockage across one or more spatial reaches and the local loss formula is used to account for losses at the expansion and contraction at each end of the blockage,

$$H_U - H_D = \frac{k|Q|Q}{2gA^2} \tag{3-6}$$

where H_U and H_D represent the head upstream and downstream of the node respectively and k is a steady local loss coefficient for which appropriate values can be determined from Bullen *et al.* (1987). It is assumed that there is no storage at the node, thus

$$Q_U = Q_D \tag{3-7}$$

where Q_U and Q_D represent the flow upstream and downstream of the node respectively. Equations (3-6) and (3-7) can be solved in conjunction with the characteristic equations for positive and negative flow cases to model the transient behaviour at a constriction or expansion with a local loss similar to that done by Wylie and Streeter (1993). This method enables blockage characteristics such as variations in geometrical and physical conditions to be represented in the numerical model.

The discrete blockage model is also shown in chapter to illustrate the differences between a discrete and extended approximation of a blockage and to highlight potential issues with the discrete approximation. The discrete blockage model applies the quasi steady local loss formulation (Equation (3-6)) as described above at a node on the MOC grid and is solved using Equations (3-6) and (3-7). This is shown to suitably represent unsteady behaviour for ratios of constricted flow area to pipeline area greater than 1:32 by Prenner (2000) and 1:62 from Washio *et al.* (1996) when applied to oscillating hydraulic oil flows through an orifice constriction.

The boundary conditions for the series pipeline are set as a constant head reservoir at the upstream boundary and a valve discharging to atmosphere at the downstream boundary. The constant head reservoir is modelled though solving the positive characteristic Equation (3-2) with the condition $H_p = H_R$ where H_R is the head of the reservoir. Local losses at the upstream boundary are accounted for by applying the quasi steady local loss formulation described by Equation (3-6). The downstream valve boundary is modelled through solving the negative characteristic equation (Equation (3-3)) subject to the condition,

$$Q = C_v \tau \sqrt{H_U - H_D} \tag{3-8}$$

where C_v is the valve coefficient and is selected to match the flow conditions though the valve, τ is the ratio which describes the opening position of the valve and is given by A_{Valve}/A_0 and H_D is set to the head at which the valve is discharging to. A value of $\tau = 1$ represents a fully open valve while $\tau = 0$ represents a fully closed valve. Transient flow is generated in the pipeline by defining a valve perturbation such that

$$\tau = \begin{cases} \tau(t) & 0 \leq t < t_v \\ 0 & t \geq t_v \end{cases} \tag{3-9}$$

where t_v is the valve closure duration and $\tau(t)$ is determined by matching experimental transient responses or taken as a step function from 1 to 0 for instantaneous valve closures.

3.4 Numerical analysis

3.4.1 Comparison of discrete and extended blockages

This section compares transient behaviour in single pipelines subject to discrete and extended blockages as depicted in Figure 3-1. The purpose of the comparison is to illustrate the differences between the impact of discrete blockages shown in Stephens *et al.* (2005b), Wang *et al.* (2005b), Mohapatra *et al.*

(2006b) and Lee *et al*. (2008a) and the impact of blockages of extended length on the transient trace. The system is bounded by a constant head reservoir and the pipe discharges into atmospheric pressure at the downstream boundary through a valve. The transient signals are generated by an instantaneous closure of the valve at the downstream boundary. Pressure data of the transient signal is extracted from the model at the downstream valve. For the purpose of describing the pipeline systems presented in this paper L, D and a refer to the length, diameter and wave speed respectively, while the subscript 0 will be used to denote the properties of the original pipeline and 1 to n denote each pipeline section numbered in the direction of steady flow. Assuming a single blockage or fault, the pipeline is represented by three sections and the subscript 2 refers to the properties of the fault as illustrated in Figure 3-1. For the case of a single extended blockage the distance x_c will refer to the midpoint of the blockage, as measured from the reservoir and can be given as the non-dimensional value $x_c^* = x_c/L_0$. The system used for the purpose of numerical illustration has a length, L_0 = 1000 m, wave speed, a_0 = 1000 m/s, diameter, D_0 = 0.3 m and Reynold's number of 1 x 10^5.

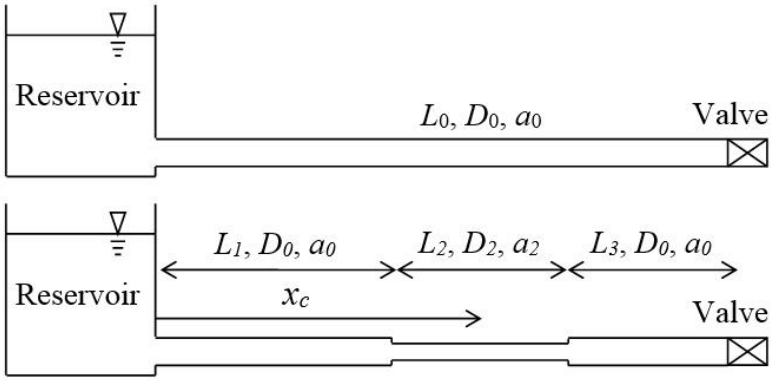

Figure 3-1: Schematic of reservoir, pipe and valve system. Above, uniform, fault free pipeline. Below, pipeline subject to an extended blockage.

Figure 3-2 shows a time domain comparison of the transient response between a uniform pipeline and a pipeline subject to a constriction that is approximated as a discrete blockage. A local head loss element is included in the MOC model to represent the blockage. The steady state flow rates are kept the same in both the uniform and constricted pipe cases. The pressure head responses shown at the downstream valve are presented in the non-dimensional form $H^* = H/H_J$ where H_J is the Joukowsky head rise while the time scale is presented in the non-dimensional form $t^* = 4L_0/a_0$.

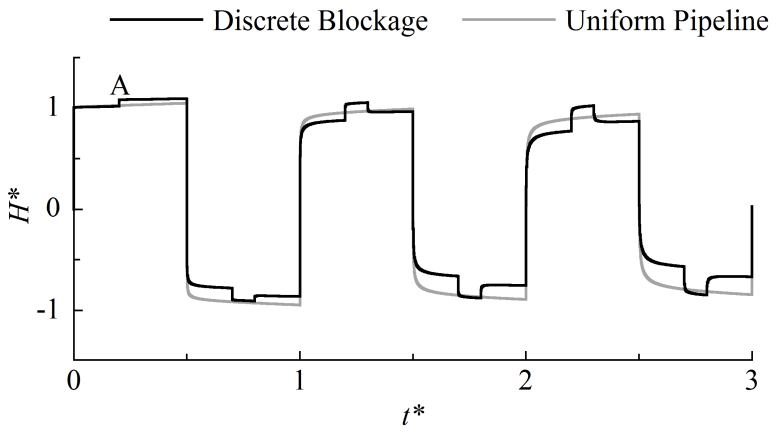

Figure 3-2: Time domain comparison between a uniform pipeline and a pipeline with a discrete blockage at location $x_c^* = 0.6$.

Figure 3-2 shows how the addition of a discrete blockage to the system alters the transient response. The transient response presented is for a discrete blockage located at $x_c^* = 0.6$ with a local loss factor $k = 344$. The response shows an initial positive head rise due to a rapid closure of the downstream valve followed by a reflection from the discrete blockage (point A). The magnitude of this reflection is proportional to the steady state head loss across the discrete blockage (Contractor 1965, Meniconi *et al.* 2011a). This reflection is reinforced with each cycle, as superposition of the pressure waves increases the relative head rise. The discrete blockage imposes a slight increase on the maximum pressure rise at each cycle when compared to the uniform pipeline case and it also increases the damping rate of the signal, however the fundamental period of transient pressure wave propagations remains unchanged. This damping effect is due to the redistribution of the transient energy to the reflected signal and is studied in Duan *et al*. (2011b) with energy losses directly attributed to the local loss coefficient.

As the length of the blockage is increased it is better represented as an extended blockage, which is modelled as a pipe of different properties in the MOC. Figure 3-3 shows a transient pressure response for an extended blockage with a length of $L_2^* = 0.2$ where $L_2^* = L_2/L_0$, constricted nominal diameter of $D_2^* = 0.5$ where $D_2^* = D_2/D_0$ centred at the midpoint of the pipeline ($x_c^* = 0.5$). For a valid comparison between the discrete and extended blockage cases, the local loss factor for the discrete blockage was calculated so that the induced head losses across the blockages are equal for equivalent boundary and flow conditions. It is also assumed that there is no change in the wave speed through the blockage. Variations in wave speed corresponding to the formation of blockages will be investigated later in this chapter. The extended blockage imposes very different changes on the shape of the transient signal when compared to the discrete case.

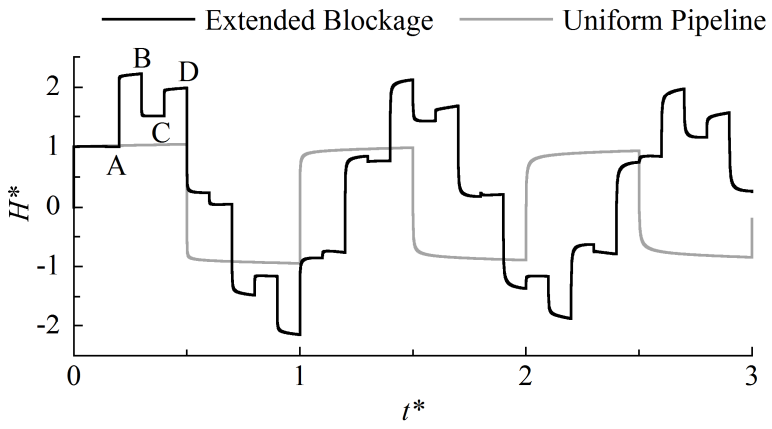

Figure 3-3: Time domain comparison between uniform pipeline and a pipeline with an extended blockage of length $L_2^* = 0.2$.

As the step wave impinges on the blockage, the increase in characteristic impedance means a positive pressure wave is reflected from the blockage interface back towards the valve, which generates the second large pressure rise at point A shown in Figure 3-3. The magnitude of this reflection is larger than that predicted by the discrete blockage model as the extended blockage model accounts for the reduction in nominal diameter where the discrete blockage model does not. Reducing the nominal diameter increases the fluid velocity through the blockage under fixed flow conditions. The higher velocity requires a head rise larger than that generated at the valve to bring the fluid flow to a stop, hence the transient pressure wave is unable to entirely stop the flow though the constriction. This creates a flow imbalance across the interface of the uniform and constricted sections of pipe, which in turn generates the reflection described. This physical process is accounted for in the extended blockage model but not the discrete blockage model leading to the difference in the transient response. Further pressure changes that can be seen over the initial $t^* = 0.5$ time period include; a negative reflection from the rear of the blockage (B), a second positive reflection from the front of the blockage (C), followed by combined negative reflections from the rear of the blockage and the upstream reservoir (D). Comparison of the transient responses for each of the blockage models show that the extended blockage model predicts more extreme pressure heads. This suggests that the method by which a blockage is approximated has significant impacts on the resultant transient response.

It is important to note that due to the superposition of reflected waves and the resistance to wave propagation provided by the impedance of the extended blockage, the pressure at the valve is not fully relieved within the $t^* = 0.5$ time. This gives rise to a unique characteristic that differentiates discrete and extended blockage behaviour. The extended blockage changes the systems fundamental period of

oscillation from the uniform pipeline case, even when there is no change in wave speed in the constricted pipe section. Figure 3-3 shows that the period of the signal has increased from $t^* = 1.0$ to $t^* = 1.2$ for the extended blockage case. The change in the fundamental period of oscillation for the system is unique to extended faults and the relationship between the extended blockage properties and the impact on the oscillation period of the transient response deserves further investigation.

3.4.2 Numerical illustration of pipe wall strength reduction

This section examines the effect that changes in pipeline wall condition have on transient behaviour within a pipeline. Changes in pipe wall conditions can alter three key parameters. The first is the wave speed (a) which can be affected by internal and external corrosion and deterioration of the pipe wall material or delamination of protective linings. The second parameter is a change in the nominal diameter (D), which can increase due to internal corrosion of the pipe wall and delamination of internal protective linings, or decrease where corrosion leads to tuberculation. The delamination and corrosion lead to a reduction in effective wall thickness, while pipe wall deterioration results in a decreased Young's modulus. The third parameter is a change in the friction factor (f) caused by a change in relative roughness. For the purposes of this illustration scale analysis of Equations (3-2) and (3-3) show that the effects of varying the resistance coefficient (Equation (3-5)) are relatively small compared to changes in the characteristic impedance (Equation (3-4)), particularly in the short term transient response. Therefore, changes in the roughness are not focussed on at this point.

To illustrate the effects of pipe wall strength reduction on a transient response we can consider variations in the wave speed. The wave speed for a pipeline can be calculated by the wave speed formula (Parmakian 1955, Wylie and Streeter 1993):

$$a = \sqrt{\frac{K/\rho}{1 + [(K/E)(D/e)]c_1}} \tag{3-10}$$

where the bulk modulus of the fluid (K) is taken as 2.14 GPa, the density of the fluid (ρ) is 999 kg/m^3, e is the effective wall thickness, E is Young's modulus of the pipe wall material and c_1 is a dimensionless parameter which accounts for constraint conditions on the pipeline and is taken as 1 for these examples. For certain pipe materials Young's modulus (E) can decay with time without affecting the diameter or wall thickness. An example of this is asbestos cement (AC) which is common within aging pipeline infrastructure. AC pipes make up 36% of the public water supply pipelines in New Zealand, the majority of which are now more than 35 years old (NZWWA 2001).

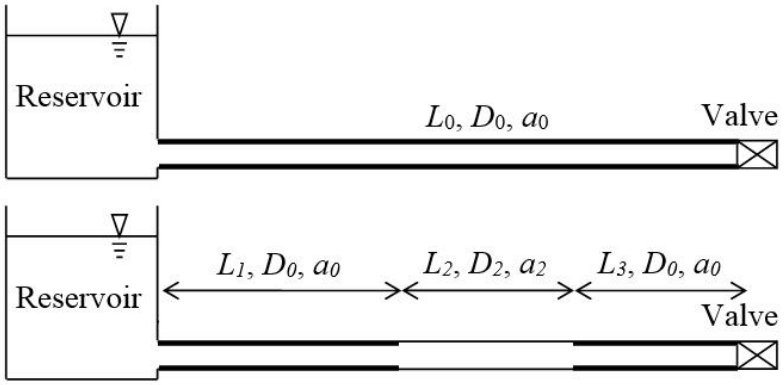

Figure 3-4: Schematic of reservoir, pipe and valve system for, above, an intact, fault free pipeline and below, a pipeline with a section of reduced wall thickness.

Consider an example similar to the previous extended blockage illustration, where an AC pipe suffers an increased rate of deterioration over a length of pipeline ($L_2^* = 0.2$), while the remainder of the pipeline has been well maintained or renewed as illustrated in Figure 3-4. For a pipe with a nominal diameter, D = 300 mm, typical values of e = 22.5 mm and E = 23 GPa can be taken giving a calculated wave speed of 978 m/s. The NZWWA (2001) model for AC pipe deterioration predicts the 75th percentile of pipes will lose effective wall thickness at a rate of 0.2857 mm/year. Thus, considering a 35 year old pipe it is feasible to consider a reduction in wave speed wave speed to 814 m/s over that length.

Figure 3-5 shows a comparison between the unsteady pressure responses for the well-conditioned AC pipeline and that which has a degraded section. Following the initial Joukowsky head rise a reflection is observed from the downstream end of the degraded pipe section which gives a reduction in the pressure head. This reduction is caused by a decrease in characteristic impedance over the degraded section due to a reduction in the wave speed. Following the initial drop in pressure head a reflection is observed from the upstream end of the degraded section which restores the pressure head back towards the observed values for the intact pipeline. Further secondary reflections are then observed before the pressure restoring reflection is observed from the upstream reservoir. The pressure response also shows a phase change, where the period of oscillation is increased for the system due to the decrease in wave speed and hence propagation time over the degraded pipeline section.

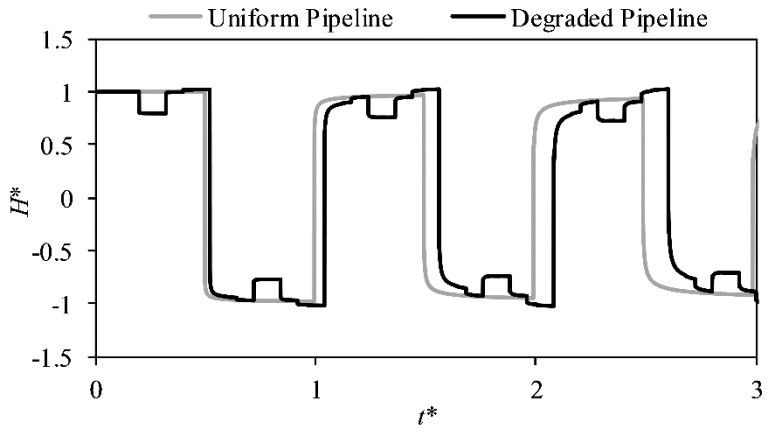

Figure 3-5: Comparison of an intact AC pipeline and a similar pipeline which has a reduction wave speed over a length $L_2^* = 0.2$.

Research presented in Tuck *et al.* (2012 and 2013) (and earlier in this chapter) shows that in addition to a change of wave speed a change in nominal diameter over a section of pipe can generate positive or negative reflections in the pressure response while also changing the fundamental period of oscillation for the system. To further illustrate the combination of these effects, with a focus on the subject of pipe wall condition a numerical case study is used. This example considers a reservoir, pipe and valve system as depicted in Figure 3-4, where a mild steel cement lined (MSCL) pipeline has lost the protective cement lining over a length of $L_2^* = 0.2$ located in the middle of the pipeline. The MSCL pipe considered has a nominal diameter (D) of 300 mm, steel wall thickness (e_S) of 5 mm and cement thickness (e_C) of 10 mm.

To account for the relative strength of the cement lining an equivalent steel thickness can be calculated by the method in Stephens *et al.* (2013) if it is assumed to be fully bonded to the steel:

$$e = e_S + e_C(E_C/E_S) \tag{3-11}$$

where Young's modulus of the pipe wall steel (E_S) is 210 GPa and Young's modulus of the cement lining (E_C) is 25 GPa.

Using Equations (3-10) and (3-11) the wave speed of the intact pipeline is calculated to be 1197 m/s and the wave speed over the section where the cement lining has delaminated is calculated to be 1139 m/s. Figure 3-6 shows a comparison between the unsteady pressure responses from a pipeline with a section of delaminated cement lining and that of an intact pipeline as described above for this numerical case study. Following the initial Joukowsky head rise a reflection is observed from the

downstream end of the degraded pipe section which gives a reduction in the pressure head. This pressure drop is similar to that in the AC pipe example despite the relative reduction in wave speed being close to a quarter of that in the previous example. As for the AC pipe example this reduction is caused by a decrease in characteristic impedance over the degraded section. In this case the increase in flow area due to the loss of internal linings has a dominant impact on the impedance and the effect is approximately 3.6 times larger than that caused by the wave speed. The phase shift observed in this second example is smaller than that for the first as expected with the smaller relative change in wave speed. The additional impact of the change in flow area will be investigated further in the following section.

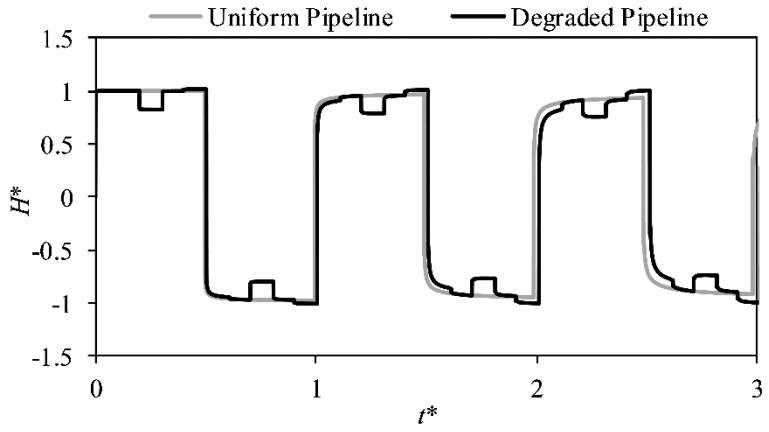

Figure 3-6: Comparison between an intact MSCL pipeline and a pipeline which has lost lining over a length of $L_2^* = 0.2$.

3.4.3 Unique characteristics of extended faults

The imposed changes to the fundamental period of the system and subsequently the magnitudes of the transient response in Figure 3-3 are related to the length and severity of the extended blockage. Figure 3-7 illustrates the transient trace when the length of the extended blockage is increased to $L_B^* = 0.4$. The lengthening of the blockage causes a further increase in the fundamental period of the system, increasing the duration over which fluid or kinetic energy flows into the pipeline, thus allowing more energy to enter the system. Depending upon the location and length of the blockage, the increase in the fundamental period can also lead to an increase in the magnitude of the pressure response as multiple reflected wave fronts are superimposed upon each other as shown in Figure 3-7. Similar effects are observed as the blockage severity is altered, as shown in Figure 3-8 where a change in the nominal diameter of the constricted section is considered. The reduction in the severity of the constriction reduces the change in characteristic impedance at the blockage ends, ultimately reducing the magnitude

of the reflections (Wylie and Streeter 1993). This reduction in reflection magnitude has also reduced the change in oscillating period as the time to full pressure relief in the system is reduced.

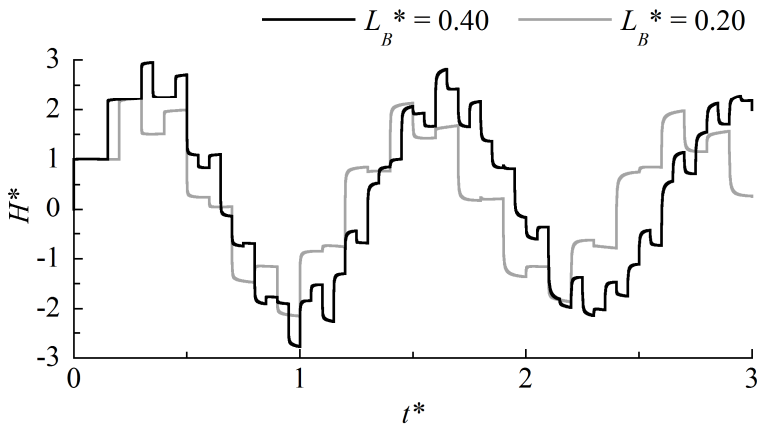

Figure 3-7: Time domain response for an extended blockage of diameter D_B* = 0.5, with varying length.

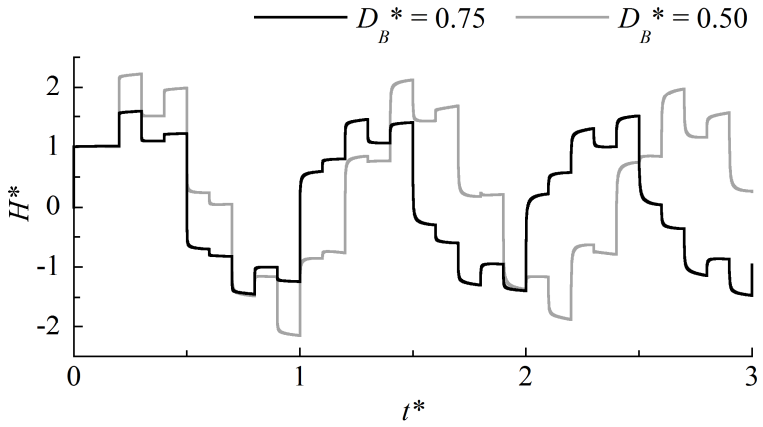

Figure 3-8: Time domain response for an extended blockage of length L_B* = 0.2, with varying severity.

Another common extended fault is pipe wall degradation or thinning, which can lead to a reduction in wave speed without significant variation in the nominal diameter (Stephens *et al.* 2005b). An increase in wave speed may also be observed where a pipeline section is replaced or a pipe with different properties is used. Figure 3-9 compares system responses for both increases and decreases in wave speed through a section of pipe with length L_B* = 0.2 and located at x_c* = 0.5. Note that no change in pipe diameter through the degraded section is assumed for this case. The system responses exhibit similar reflection patterns to the extended blockage as well as a shift in the fundamental period, however

the mechanism causing this shift is primarily the propagation speed of the wave though the system and not the superposition of pressure waves as seen in the blockage case. The findings of Figure 3-7 through to Figure 3-9 illustrate that the shifts in the fundamental period of a system containing an extended fault can be caused through changes in length, diameter or wave speed of that fault.

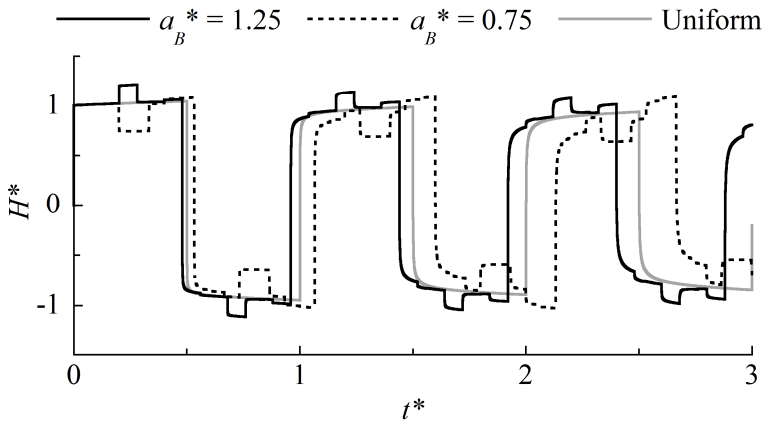

Figure 3-9: Time domain response for a change in wave speed (a) over a section of pipe L_B* = 0.2 in length centred at the midpoint of the pipe.

Figure 3-10 shows how the systems fundamental period varies for different combinations of blockage length and severity, when the wave speed through the blockage is kept the same as the original pipe. The fundamental period T is determined through a spectral analysis and is identified as the dominant oscillating component of the signal and can be normalised as $T^* = T/t^*$ where $t^* = \sum 4L_n/a_n$. As the blockage length tends towards zero, the impact of the extended blockage approaches that of a discrete blockage and the fundamental period of oscillation approaches the uniform pipe case. For the case presented, the change in the fundamental period increases to a maximum when the length of the blockage reaches half the pipe length. After this point the fundamental period starts to approach that of the original pipe again, as the entire system is replaced with a constricted section of the same wave speed. The different blockage constriction severities shown in Figure 3-10 demonstrate that the shift in the fundamental period is proportional to the size of the constriction.

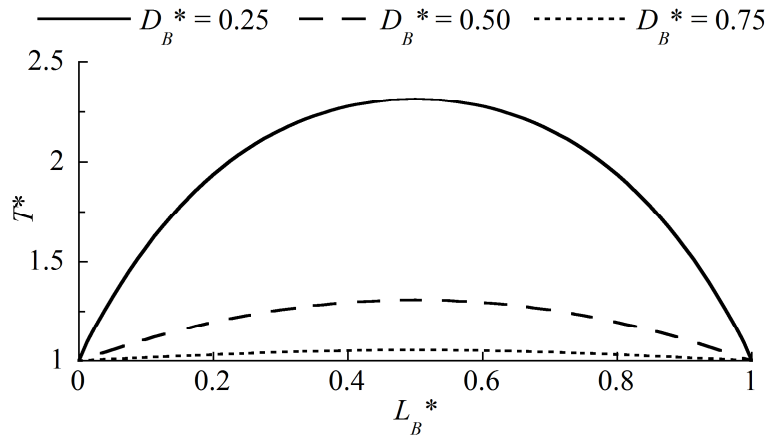

Figure 3-10: The effect of increasing the length and severity of a blockage centred at the midpoint of the pipeline on the fundamental period.

In cases where extended blockages are a by-product of pipeline degradation, both changes in pipe diameter as well as changes in wave speed can occur simultaneously (Stephens *et al.* 2005b). Figure 3-11shows how the combinations of changes in blockage diameter and wave speed can affect the fundamental period. The contour plot shows how the normalised fundamental period T^* varies with the normalised wave speed (a_B*) and diameter constriction ratio (D_B*). The system modelled consisted of a blocked section (L_B* = 0.5) of pipe located at the centre of the pipeline which was the case that resulted in the greatest change in the periodic behaviour from Figure 3-10. Figure 3-11 shows that the fundamental period has a low sensitivity to incremental changes in blockage diameter when the flow area through the blockage is close to the uniform pipeline diameter (D_B* = 1). This effect is shown by the near vertical contour lines close to D_B* = 1. In this region variation in the wave speed has a dominant effect on the periodic response of the system. The sensitivity of the periodic response then grows considerably as the constriction ratio increases to the point where the fundamental period is essentially independent of wave speed at the extreme constrictions (D_B* < 0.4).

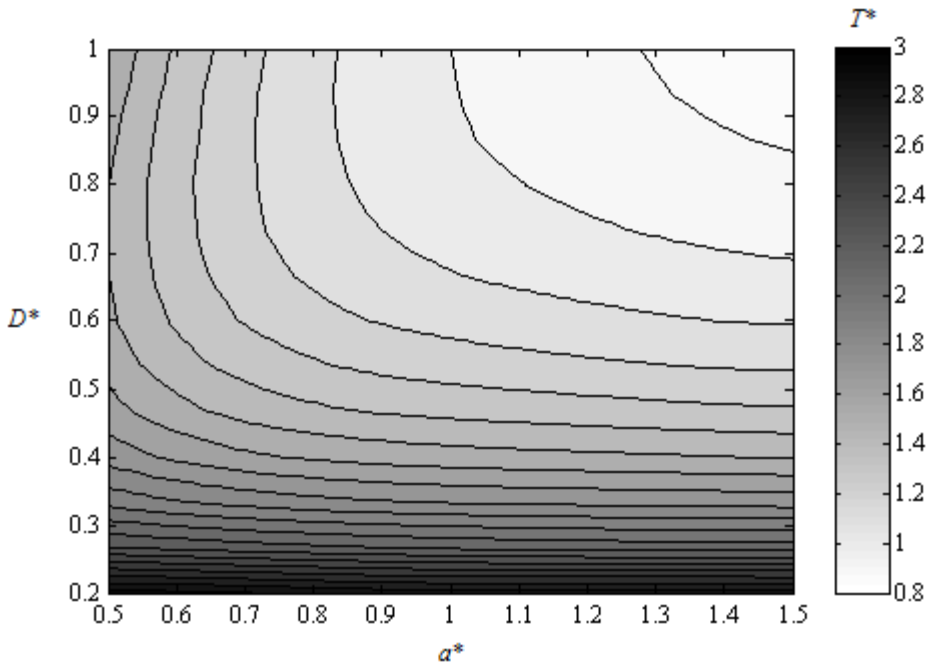

Figure 3-11: Comparison between the effects of diameter change and wave speed change on the fundamental period for a pipeline, where the varied section is L_B* = 0.5 in length and centred at the midpoint of the pipeline.

3.5 Experimental system and procedures

Experimental investigations of extended blockage effects on the transient trace were carried out using the transient pipeline facility at the University of Canterbury. The experimental system consists of a 41.517 m long stainless steel pipeline with a nominal diameter of 72.4 mm and wall thickness of 1.5 mm. This is solidly mounted to a heavy steel beam with rubber clamps at 0.5 m centres to minimise deformation of the pipeline and fluid structure interaction during testing. The pipeline is bounded by two pressure regulated tanks that simulate constant head reservoirs as shown in Figure 3-13 and Figure 3-12. Transient signals are generated through the rapid manual closure of a side discharge valve adjacent to the downstream inline valve, once a desired steady flow is reached. The resulting pressure response is measured at the point of generation at a sampling rate of 5 kHz by high resolution Thermo Fisher Scientific, flush face, dynamic pressure transducers. Extended variations are simulated through the installation of a pipe sections with varying properties. Experimental results presented in this chapter focus on two types of variations which include diameter changes and wall thickness changes. To look at the effect of pipeline constriction two pipe diameters have been investigated; the first constricted section of pipe has a nominal diameter of D_2 = 47.8 mm, while the second has a more severe constricted

diameter of D_2 = 22.2 mm. The average wave speeds of each pipe have been experimentally determined by measuring wave travel times between two points over the pipeline, giving wave speeds of 1180 m/s for the 73.2 mm diameter pipe, 1265 m/s for the 47.8 mm sections and 1370 m/s for the 22.2 mm sections. Each of the pipe sections has been constructed from hygienic grade stainless steel tubing with a nominal wall thickness of 1.5 mm. To look at the effect of changes in pipe wall thickness a section of pipe with a nominal diameter of D_2 = 68.8 mm and wall thickness of 3.7 mm is used. The pipe dimensions are selected such that the external diameter matches the existing pipeline. A larger wall thickness is used as safety and manufacturing practicalities restrict using a thinner walled pipe and it was not feasible to replace the whole pipeline. The experimentally determined wave speed of this pipe is 1315 m/s.

Figure 3-12: Top-left: Diameter change connection. Top-right: Flanged pipe connection with mounting brackets. Bottom-left: Upstream pressurised reservoir. Bottom-right: Downstream pressurised reservoir.

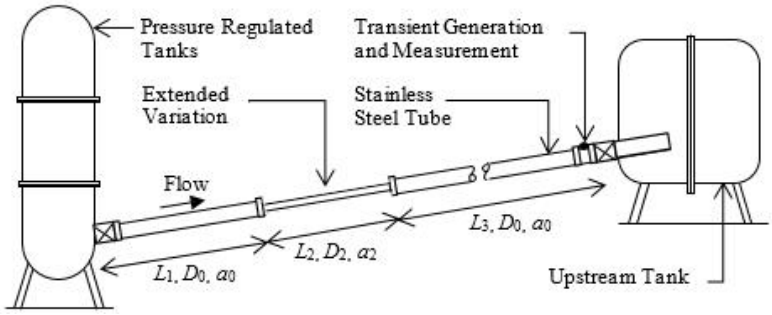

Figure 3-13: Schematic of experimental reservoir, pipe and valve system subject to an extended blockage.

3.6 Experimental analysis of periodic behaviour

Pressure traces are presented for seven different extended blockage cases as summarised in Table 3-1 and these test cases are used to further investigate the differences between the described numerical model and experimental results. Figures 3-14 to 3-17 show the experimental transient responses in the time domain for a representative selection of the cases outlined. Comparisons have been made to these experimental responses using the MOC model with the inclusion of unsteady friction and local losses at the blockage junctions. The experimental results presented were carried out in the turbulent flow regime, where Reynold's numbers ranged from 2.2×10^3 to 1.5×10^4 in the uniform and blocked pipe sections. Thus, to account for unsteady friction effects, an unsteady turbulent friction model for smooth pipe flow has been employed (Vardy and Brown 2003).

Table 3-1: Experimental system geometry

Case	Geometrical Information				D_2 (mm)/ a_2(m/s)	D_0 (mm)/ a_0(m/s)
	L_1 (m)	L_2 (m)	L_3 (m)	L_2/L_0		
1	9.027	11.882	20.612	0.286	47.80/ 1265	73.20/ 1180
2	12.034	8.875	20.612	0.214		
3	15.036	5.873	20.612	0.141		
4	18.043	2.866	20.612	0.069		
5	8.837	12.068	20.612	0.291	22.20/ 1370	
6	11.844	9.061	20.612	0.218		
7	14.846	6.059	20.612	0.146		

The resulting transient response follows a similar pattern of reflections to that shown in Figure 3-3. There is a large initial positive reflection from the fault due to the compounding effect of wave speed and diameter changes on the characteristic impedance. Visual examination of the seven cases indicates

that the fundamental period is increasing as the blockage length and severity increase, which agrees with the findings shown in Figure 3-10. Comparison between experimental and numerical responses for each of the first four cases shows good agreement for both reflection magnitudes and occurrence times over the first few periods. Likewise, cases five to seven show good agreement initially, however the accuracy of the numerical solution visibly decays after the first period of oscillation.

For each case the agreement between reflection times and fundamental period continues over subsequent periods of oscillation. Table 3-2 presents the values of the fundamental period determined from experimental and numerical data for each case and the associated error. The fundamental period calculated by the numerical model agrees reasonably well with that from the experimental data. The errors range between 0.6% and 1.4% of the experimentally determined fundamental period. The fundamental periods follow a similar pattern to that previously discussed with reference to Figure 3-10 and Figure 3-11 when considering changes in length, diameter and wave speed.

The numerical response for all cases shows a discrepancy in the reflection size developing with each cycle (shown most clearly in Figure 3-16), which indicates a difference in the magnitudes of the signals reflected and transmitted by the blockage. The modelling error is more pronounced for severe pipe constrictions. Further analysis showed that for cases five to seven increasing the nominal diameter of the constriction represented in the numerical model from 22.2 mm to 22.8 mm significantly improved the fit with experimental results. While this change in diameter is small, it is still greater than the manufacturing tolerance for the given pipe. This indicates that the observed discrepancy is not caused by experimental error and can therefore be attributed to the numerical modelling method. Also, changes to the wave speed inputs within the range of experimental accuracy were proven to have little effect on improving the fit when compared to changes in the diameter. The results show that inaccuracies in the numerical model grow with time, reducing the ability of the model to accurately represent the physical system in extended simulations. This behaviour has also been observed by researchers in the field, where matches between measured and modelled responses are only achieved within the initial stages of the transient (Karney and Radulj 2009, Stephens 2008).

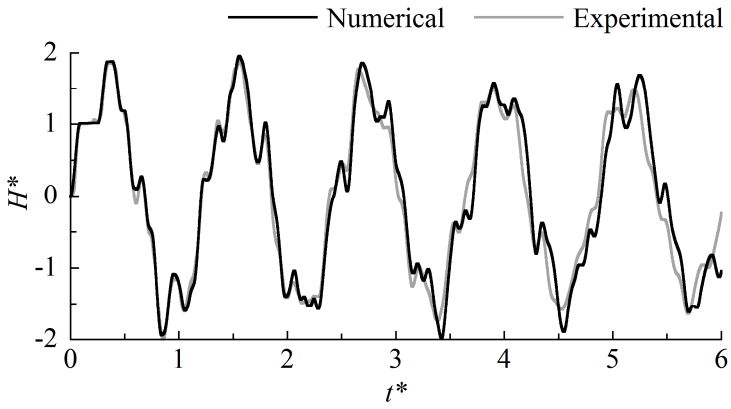

Figure 3-14: Comparison between numerical and experimental data for a blockage of diameter D_2^* = 0.65 and length L_2^* = 0.286, case 1.

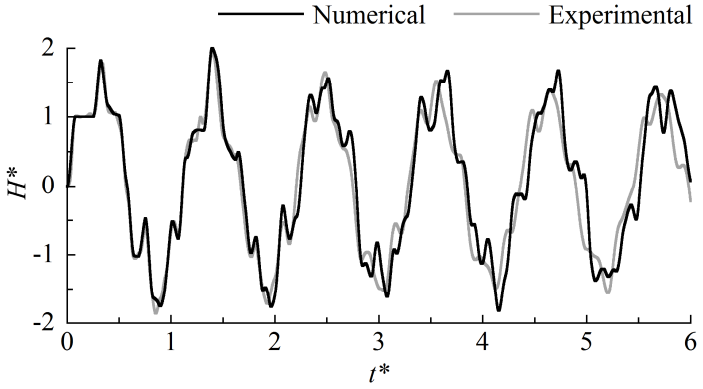

Figure 3-15: Comparison between numerical and experimental data for a blockage of diameter D_2^* = 0.65 and length L_2^* = 0.141, case 3.

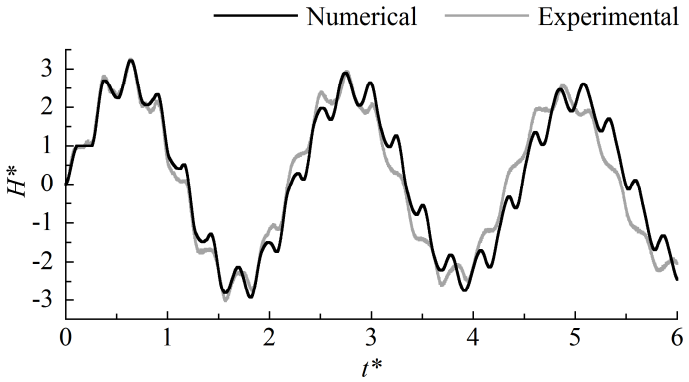

Figure 3-16: Comparison between numerical and experimental data for a blockage of diameter D_2^* = 0.30 and length L_2^* = 0.291, case 5.

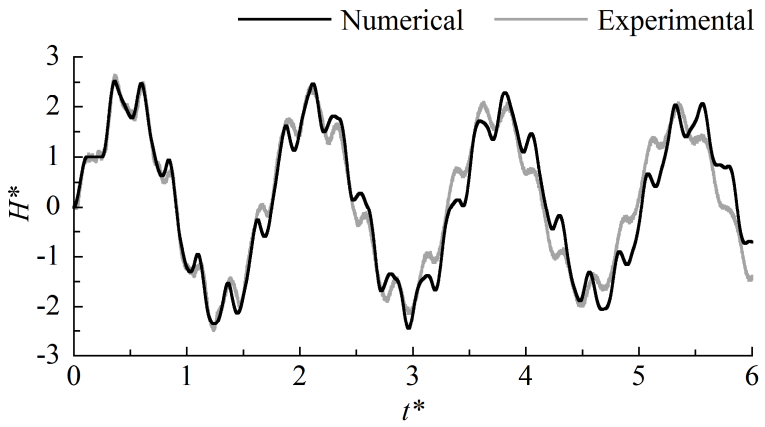

Figure 3-17: Comparison between numerical and experimental data for a blockage of diameter $D_2^* = 0.30$ and length $L_2^* = 0.146$, case 7.

Table 3-2: Comparison of experimentally and numerically determined fundamental periods of oscillation.

Case	Fundamental Period, T^*		Error (%)
	Experimental	Numerical	
1	1.19	1.20	0.67
2	1.13	1.15	1.26
3	1.08	1.09	1.29
4	1.04	1.06	1.22
5	2.15	2.18	1.40
6	1.91	1.93	0.99
7	1.63	1.65	1.26

The discrepancy between the predicted and observed wave transmission and reflection behaviour at the blockage boundaries changes the way the transient energy is redistributed through wave scattering, ultimately leading to differences in transient damping rates (Duan *et al.* 2011b). Observing the transient response after an extended period of time in case five, as depicted in Figure 3-18, shows a difference in the way the experimental and numerical pressure responses attenuate with time, with the numerical model under-predicting the rate of decay. The experimental response is smoother than the numerical prediction, indicating there is a difference with how energy in the higher frequency components of the signal is damping.

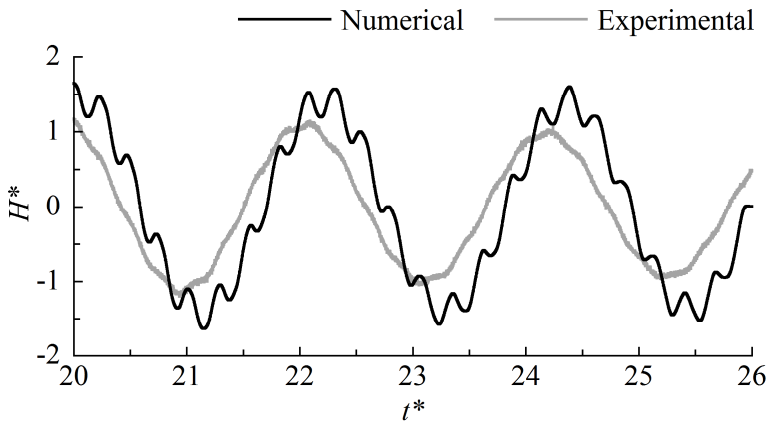

Figure 3-18: Extended time domain comparison between experimental and numerical responses for case 5.

The damping rate of the transient response is found through an analysis of how the magnitude of each frequency component is attenuating in time. Fourier components of transient responses have been shown to damp at an exponential rate (Wang *et al.* 2002) and the magnitudes of head response for each particular frequency component, h_ω, within subsequent periods are expected to follow a function of the form

$$h_\omega = E_{\omega,(T^*=1)} e^{-Rt^*} \tag{3-12}$$

in a linear pipeline system, where $E_{\omega,(T^*=1)}$ is the integrated frequency domain head response of the first transient cycle, R is a damping factor and t^* is the dimensionless time. It is recognised that Equation (3-12) is developed for a linear system and the system considered contains non-linear components, thus it is not used to define the damping rate and the form is only applied as a means to determine comparative damping rates between experimental and numerical data. The accuracy of this form of the equation when fitted to experimental and numerical data can be seen in Figure 3-19 and Figure 3-20 respectively. For the purpose of this analysis a Fourier transform has been performed individually on each of the first ten transient cycles for each data set. Examples of these spectral responses are shown for experimental data in Figure 3-19 and numerical data in Figure 3-20 for selected cycles from case five. The figures show that the magnitude of the Fourier transform is decaying with time and the rate of decay is higher in the experimental data.

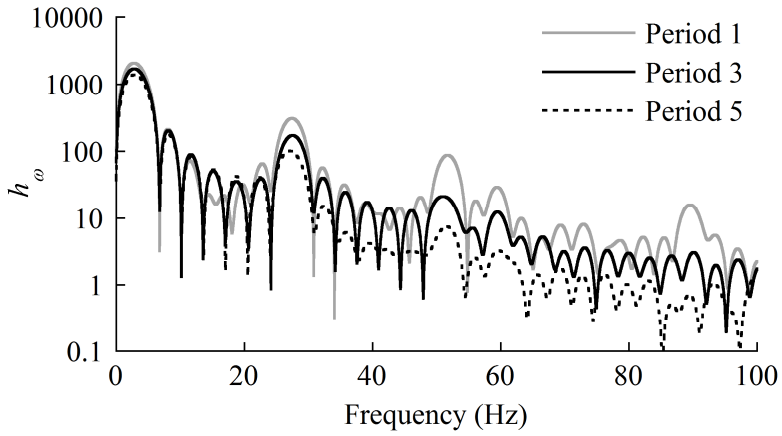

Figure 3-19: Spectral response of selected transient cycles from case 5 for experimental data.

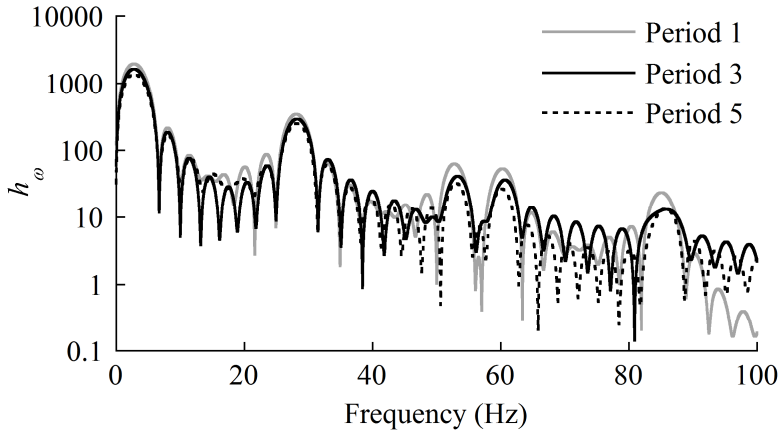

Figure 3-20: Spectral response of selected transient cycles from case 5 for numerical data.

To analyse the rate of decay, the frequency spectra for each transient cycle are integrated over intervals of 20 Hz providing the energy content within of the frequency range of $E_\omega = \int h_\omega df$. The energy over each period of the transient response for a particular frequency range is normalised by the energy observed in the first period of the response, $E_\omega^* = E_\omega / E_{\omega,T^*=1}$. The energy of a particular band of frequency is then plotted against the time (t^*) corresponding to each transient cycle, to show the attenuation of each frequency component with time. The normalised values of the signal energy have been shown for bandwidths between 0 and 60 Hz of case five in Figures 3-21 and 3-22**.** An exponential damping factor (R) for each frequency range has been determined through fitting a line to the discrete data points using a least squares optimisation routine.

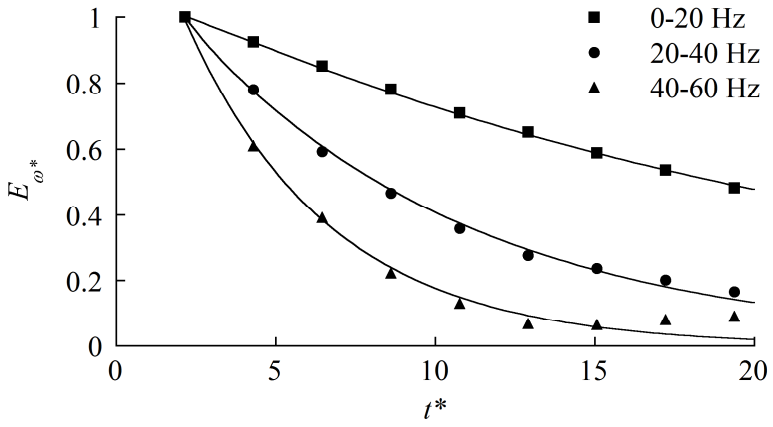

Figure 3-21: Integrated Fourier components over the first 10 transient cycles for experimental data.

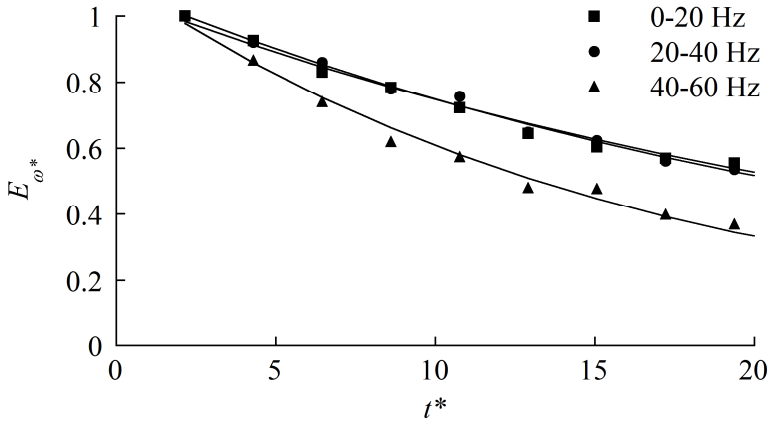

Figure 3-22: Integrated Fourier components over the first 10 transient cycles for numerical data.

Figures 3-23 and 3-24 show the damping factors (R) for each of the seven experimental and numerical cases plotted against the frequency intervals up to 100 Hz. Comparing Figures 3-23 and 3-24 shows that for the low frequency component the rate of damping increases with the blockage severity, with an average damping factor of R = 0.031 for the D_2* = 0.65 blockages and R = 0.045 for the D_2* = 0.30 blockages. The systems fundamental frequency for each of the seven cases ranges between 3.4 and 6.8 Hz, and the results show that the damping rates within this range of frequencies (0 – 20 Hz) are the lowest. Within this frequency band the damping factors predicted from the numerical model are most similar to the experimental behaviour, with an average across all cases of R = 0.027 for the numerical model and R = 0.037 for the experimental data. The accuracy of the predicted damping behaviour within this fundamental frequency range provides the reasonable fit observed on the global scale in Figure 3-18. In comparison, noticeable discrepancies between the experimental and the numerical predictions

are shown for the damping rates for the higher frequency bands. The experimental results show the damping rates to significantly increase with frequency (on average from R = 0.037 to R = 0.243 for 0 - 20 to 80 - 100 Hz ranges), while the numerical model does not exhibit this behaviour with significantly less variation in the damping rates (from R = 0.027 to R = 0.052 for 0 - 20 to 80 - 100 Hz ranges). These higher damping rates at the higher frequencies translate to a loss of signal detail and have a smoothing effect on the transient signal. This behaviour is poorly captured by the numerical model. The inability of the model to capture these effects has implications on the accuracy of long duration transient modelling as well as on the application of transient models to inversely analyse complex pipelines.

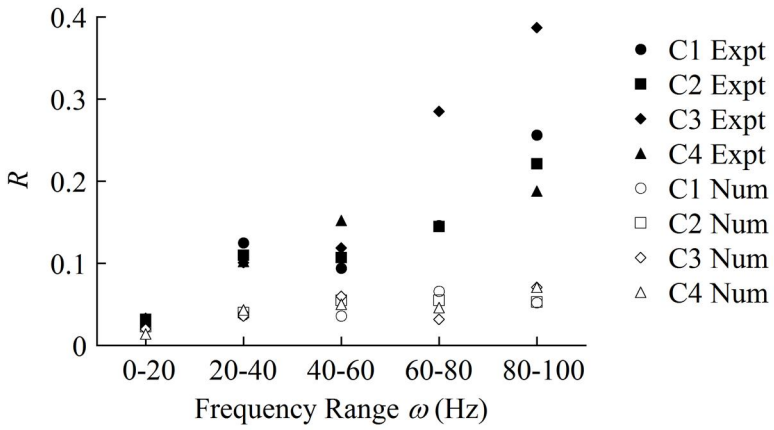

Figure 3-23: Comparison of experimental and numerical damping rates by frequency, for D_2*= 0.65 cases.

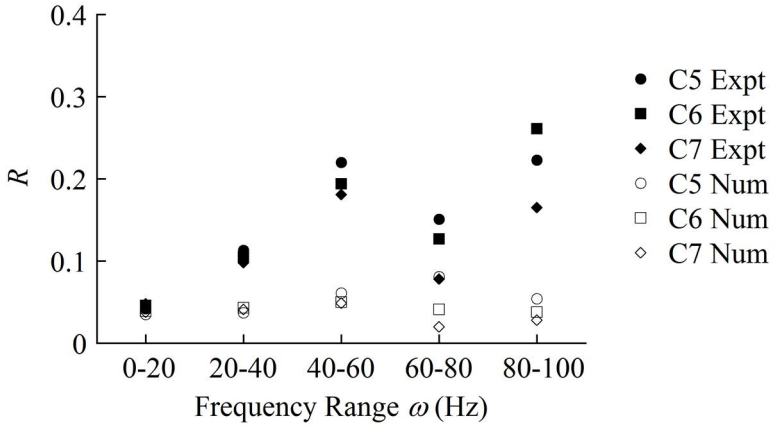

Figure 3-24: Comparison of experimental and numerical damping rates by frequency, for D_2*= 0.30 cases.

One potential source of damping unaccounted for in the current model is the eddy inertial effect shown by Washio *et al.* (1982) for highly constricted unsteady orifice flows. The effect of eddy inertia may be an important physical phenomenon at the sudden contractions and expansions at each end of the blockage and deserves further investigation. While this analysis has offered insight to the difference between the experimental results and numerical model predictions, it is important to note that the presented damping factors are specific to the system investigated, as they will vary with geometry and flow conditions. It is also worth noting that while the laboratory system has been custom made to minimise non-uniformities, small mechanical damping from non-pipe components and air within the system may have a minor contribution to the observed damping rates.

3.7 Inverse transient analysis of extended faults

Inverse transient analysis (ITA) can be used to detect and classify faults within a pipeline system. It can also be useful in determining how well a numerical model can represent real measurements and identify signal properties that can improve application of the technique. One version of ITA takes transient pressure measurements from strategically placed pressure sensors in a pipeline system. Then, the transient pressure response can be used to determine the condition and physical state of a pipeline through inversely calibrating a numerical model to match the response in the time domain, hence theoretically replicating the pipeline. Alternative variations of this approach are discussed in the literature, though this direct time domain approach as first proposed by Pudar and Liggett (1992) will be applied here. For ITA to be successfully carried out a good understanding of the unsteady fluid behaviour in complex systems is required. It is also beneficial to have an understanding of the critical parameters in order to achieve an accurate solution; some of these are tested in the following analysis.

This section considers the problem where the variables which define the "faulty" pipe section are unknown. To determine the unknown parameters the method of ITA can be used. This method aims to determine the value of the unknown variables which achieve the best fit between predicted and measured pressure responses using the least squares analysis:

$$s = \sum_{i=1}^{N} (H_i^m - H_i^p)^2 \tag{3-13}$$

where s is the residual error, N is the number of data points, H_i^m is the measured pressure response and H_i^p is the predicted pressure response. Equation (3-13) can be minimised using a genetic algorithm (GA) optimisation routine, where the GA used for this research is MATLAB's inbuilt "ga" function. The GA optimisation routine is one of the more computationally expensive algorithms that has been applied to

ITA, with researchers previously using the gradient based Lavenberg-Marquardt algorithm (Pudar and Liggett 1992, Nash and Karney 1999) and various variations of this (Vítkovský *et al.* 2002). These methods can be efficient, though are more susceptible to finding a false minima and missing the globally optimal solution. As computing power is increasing the benefits of these algorithms are reduced and the robustness of evolutionary algorithms, such as particle swarm optimisation (PSO), shuffled complex evolution (SCE) and genetic algorithm (GA), have become desirable (Vítkovský *et al.* 2002, Jung and Karney 2004, Stephens *et al.* 2013). The most common of these is the GA so it is applied in this thesis. In this analysis the inverse analysis is carried out considering only data from a single measurement location, however it has been shown that further measurement locations can improve the results of the inverse analysis (Vítkovský *et al.* 2003b).

To compare results in the following sections a fitness parameter (s^*) is defined as a normalised sum of the residual square and is given by,

$$s^* = \frac{s}{NH_f^2} \tag{3-14}$$

Normalising by the length and magnitude of the response enables a reasonable comparison between responses of varying duration and size.

3.7.1 Inverse transient analysis for changes in wall thickness

It has been shown in Figure 3-25 that a MOC model can produce an accurate representation of transient flow behaviour where variations in pipe wall thickness occur and the measured parameters are defined. Variations in pipe wall thickness were investigated using the system as described in Section 3.5. The length of the thick-walled section (L_2) is 10.407 m and it is located at a distance (L_3) of 16.550 m from the downstream valve. The wave speed of the standard pipeline (a_0) is experimentally determined as 1180 m/s and the wave speed of the thick-walled section (a_2) is 1315 m/s.

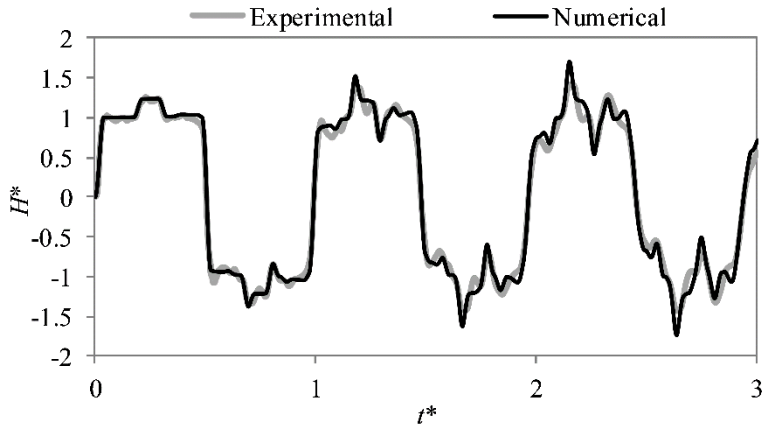

Figure 3-25: Comparison between numerical and experimental pressure responses for a pipeline with a thick-walled section.

Figure 3-25 shows a comparison between the experimental pressure response and the MOC model over the first 3 periods of oscillation using the numerical model described in Section 3.3. The time step for the numerical model is taken as 0.0001 s to match the resolution of the experimental data which is sampled at a rate of 10 kHz. The comparison shows that the MOC model can provide a reasonable prediction of the transient behaviour and captures the complex reflection patterns induced by the thick-walled pipe section. For this case the initial reflection observed from the thick-walled section is positive as the nominal diameter is decreased and the wave speed is increased which increases the impedance of the section, giving the opposite effect to that observed in the numerical case studies. The differences observed between the numerical and experimental results can be attributed to differences in physical behaviour and in the experimental system which are not accounted for by the one-dimensional model. These differences include fluid structure interaction, assumptions of fluid properties, non-uniformities in the pipe materials due to manufacturing tolerances and additional damping from non-pipe elements such as the air bleed valves located on the experimental pipeline.

For this inverse problem the variables that are said to define the faulty section are its wave speed (a_2), diameter (D_2), distance from the downstream valve to the fault (L_3) and length of the faulty section (L_2). The variables are assigned the following bounds; 800 m/s < a_2 < 1440 m/s, 0 m < D_2 < 0.0762 m, 0 m < L_1 < L_0 and 0 m < L_2 < L_0 which are determined by allowing a lenient range of feasible values. To ensure that all solutions fall within the known pipeline geometry the following condition must also be met: $L_1 + L_2 \leq L_0$. Through selection of these variables and bounds the following assumptions are made; at most there is a single section of faulty pipeline, and the relative roughness does not increase significantly over the faulty section. To solve the inverse problem for four variables the GA

optimization uses a population size of 60, a cross over factor of 0.8, and 102 generations are required to identify the optimal solution for each case.

To improve the potential accuracy of the inverse analysis problem it is first necessary to determine an appropriate closure profile for the valve such that the head perturbation for the numerical response is similar to that of the experimental data. This step enables significantly more accurate results to be taken from the analysis and theoretically overcomes the problem discussed in Gong *et al*. (2013), where discrepancies in the magnitude of a reflection can occur if the operation time of the transient generation device is greater than that required for a pressure wave to travel two lengths of a pipe section causing an overlapping of the reflections. Where the profile of the generated head perturbation is appropriately matched the overlap of reflections from the front and rear of one or multiple sections can be accounted for in the simulations. Figure 3-26 shows a typical match between an experimental response and the numerically simulated response. Accurate matches are achieved for $\tau(t)$ through applying a cubic reduction with time multiplied by a linear regression. A closer fit of the initial pressure rise could be achieved through inversely calibrating τ with a discrete valve for each time step through the entire perturbation, however no benefit was observed using this more detailed approach.

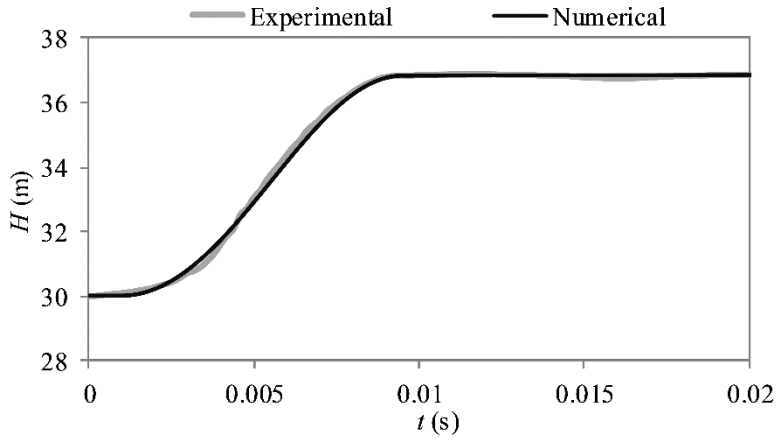

Figure 3-26: Valve closure profile fitted to match numerical simulation with experimental response.

Table 3-3 shows the results for seven ITAs, the first five of which investigate the effect that simulation time has on the accuracy of the results. In the first case the simulation time is taken as just less than the time for the pressure restoring wave to return to the downstream valve, $t < \Sigma 2\, L_n/a_n$. Here the accuracy of the predicted values are poor, where the error is calculated as (| Measured Value – Predicted Value | /Measured Value)×100%. The accuracy is poor as no reflection from the end of the system is observed for the wave speed to be scaled against, so the fundamental period of the system is not matched. In this case the optimisation does not have a feature within the time domain pressure response

which defines the total length of the pipeline that is determined by the variables $\sum(L_n/a_n)$ and t. Thus, it can select a combination of values for a_2, D_2, and L_2 to accurately match the positive and negative reflections from the test section that provide an optimal but not an accurate solution. This is indicated by the relatively low fitness parameter (s*) which shows a close match between the model and experimental measurements. The magnitude of the reflection is determined by the characteristic impedance which is a function of a_2 and D_2 while the time lag between the pressure rise and subsequent reduction from the end of the test section is a function of a_2 and L_2. Without a following reflection from a known point the inverse problem is under defined and these two properties have no relation binding them allowing multiple solutions. From the second case, which is simulated over a whole transient cycle, to the fifth case, which is simulated over four transient cycles, there is an observable trend towards increasing accuracy. This trend has also been noted for leak detection application by Vítkovský *et al.* (2000). It can also be noted that this increase in accuracy is achieved despite a trend of declining fit between the predicted and measured response; it is expected that this is due to variations in damping rates as found in Section 3.6 and minor pipeline features not incorporated into the model. Case 5 shows that a solution to the inverse problem can be determined to a high level of accuracy with relative errors of between 0.3% and 0.8 % for each parameter. Two factors contribute towards the improved accuracy where the inverse analysis is simulated over a longer period of time. The first is that a larger number of transient cycles will lead to a greater importance being placed upon matching the fundamental period of oscillation for the system which is affected by extended variations in pipelines (Tuck *et al.* 2013). The second is that the extended variations create the same change in each period of the signal and this is progressively reinforced with each cycle. It should also be noted that confining the numerical solution domain to a grid in space and time limits the theoretical accuracy of the ITA to $dx/2$, where dx is the space step used in the numerical model as determined by Equation (3-1). For the fixed time step discretisation method adopted in this analysis and a specified time step of 0.0001 s, the resolution of the MOC grid could account for an error of up to 0.36% for values of L_1 and 0.63% for values of L_2.

Table 3-3: Inverse transient analysis results for changes in wall thickness.

Case	ITA Duration, T (s)	a_2 (m/s)		D_2 (m)		L_1 (m)		L_2 (m)		s^*
		Result (m/s)	Error %	Result (m)	Error %	Result (m)	Error %	Result (m)	Error %	
	Measured Values	1315	-	0.0688	-	16.550	-	10.407	-	
1	t < 2L/a	1054	19.8%	0.0623	-9.4%	19.422	17.4%	7.945	23.7%	0.0015
2	t = 4L/a	1336	1.6%	0.0706	2.6%	15.814	-4.4%	12.211	17.3%	0.0036
3	t = 8L/a	1360	3.4%	0.0717	4.2%	15.826	-4.4%	12.568	20.8%	0.0041
4	t = 12L/a	1339	1.8%	0.0704	2.3%	16.777	1.4%	10.457	0.5%	0.0412
5	t = 16L/a	1326	0.8%	0.0683	-0.7%	16.426	-0.7%	10.442	0.3%	0.0112
6	t = 16L/a, fixed $D_2 = D_0$	1320	0.4%	0.0732	-	17.543	6.0%	10.215	-1.8%	0.0256
7	t = 16L/a, fixed $a_2 = a_0$	1180	-	0.0590	-14.2%	18.997	14.8%	12.325	18.4%	0.1650

In an attempt to reduce the size of solution domain, cases 6 and 7 involved runs where changes in either the diameter or the wave speed were excluded from the inverse calibration. An approximation such as this could prove useful where multiple faulty pipe sections are considered and can reduce the number of variables in the solution domain. This approximation is valid where the relative effect of one variable is much less than the others. The relative effects of diameter and wave speed can first be considered by looking at the magnitude of the initial reflection from a fault. Scale analysis of Equation (3-4), which represents the pipeline impedance, indicates that for a general case the effect of a change in diameter is more important than that of a relative change in the wave speed because the pipe area changes proportionally to the square of the diameter. For this specific set of experiments the percentage change in wave speed is 11.44% while the change in area is similar at 11.66%. However, the results presented in cases 6 and 7 indicate that for an ITA carried out over four periods ($16L/a$) the wave speed variable becomes significantly more important in achieving accurate detection. This can be explained by considering the phase change exhibited in the system response. The phase shift in the system response is shown to be most affected by the relative change in wave speed by Tuck *et al.* (2013) for the given range. Cases 6 and 7 show that the solution domain can be simplified by excluding variations in the diameter or wave speed from the ITA, though considering both variables separately significantly improves results as shown by comparison with case 5.

3.7.2 Inverse transient analysis for extended blockages

The ITA method presented for variations in wall thickness in Section 3.7.1 is repeated here for the extended blockage data set described in Section 3.6. Table 3-4 presents analysis results covering each of the seven cases for durations of T = 0.5 to T = 4 s. The normalised sum of residual squares (s*) is calculated for each of the analyses, including for the numerical response modelled from the measured system parameters. An error between the predicted and measured values is given as a percentage of the intact pipeline parameters to allow comparison between cases of differing blockage length, wave speed and severity.

Suitability of the ITA method coupled with a GA optimisation routine can be determined by comparing the fit of the optimal solution and the model response based on measured results. In six from seven cases ITA found a solution with a closer fit to the experimental data than achieved through direct numerical simulation. This indicates that the optimisation routine is not the limiting factor in this inverse calibration approach and a more accurate model could improve the results.

The inverse analysis consistently predicted a lower wave speed and larger diameter than expected across all test cases. Both these variations contributed to a reduced characteristic impedance, while having opposite effects on the phase. The lower wave speed extends the phase and the larger predicted diameters balance this by reducing the phase. The result of this effect is shown in Figure 3-27 where ITA does not accurately represent the full magnitude of the initial reflection from the blockage and places a greater emphasis on matching the secondary oscillations and phase of the whole signal. This supports the results found in Section 3.6 that show the numerical model does not capture the magnitude of damping in the measured response, particularly in the higher frequency ranges.

Based on the observations from this data set there is the potential for more accurate solutions to be determined by improved modelling sources of transient damping. Causes of this could include irregularities in the pipeline, pipe fixtures or small quantities of free air within the system. An alternative approach could be to apply a weighting function (W) across the sum of least squares to heighten the importance of the initial features in the signal while still accounting for the phase represented by the longer signal. One form of this weighting function could take the form of the non-dimensionalised system response ($H^*(t)$) multiplied by an inverse exponential function such that $W = H^*(t)e^{-x}$.

Table 3-4: Inverse transient analysis results for extended blockages

Case	ITA Duration, T (s)	a (m/s)		D (m)		L_1 (m)		L_2 (m)		s^*
		Result (m/s)	**Error %**	**Result (m)**	**Error %**	**Result (m)**	**Error %**	**Result (m)**	**Error %**	
1	Measured	1265	-	0.0478	-	9.027	-	11.882	-	0.013
	0.5	1235	-2.58%	0.0486	1.13%	9.083	0.14%	11.894	0.03%	0.002
	1	1259	-0.50%	0.0492	1.91%	8.700	-0.79%	12.547	1.60%	0.006
	2	1233	-2.69%	0.0487	1.29%	8.650	-0.91%	12.659	1.87%	0.009
	4	1227	-3.25%	0.0482	0.52%	9.046	0.05%	12.154	0.65%	0.013
2	Measured	1265	-	0.0478	-	12.034	-	8.875	-	0.040
	0.5	1226	-3.32%	0.0484	0.78%	12.382	0.84%	8.402	-1.14%	0.003
	1	1219	-3.91%	0.0486	1.07%	11.901	-0.32%	9.366	1.18%	0.012
	2	1242	-1.94%	0.0488	1.35%	11.535	-1.20%	9.445	1.37%	0.020
	4	1120	-12.30%	0.0466	-1.65%	13.692	3.99%	8.301	-1.38%	0.049
3	Measured	1265	-	0.0478	-	15.036	-	5.873	-	0.041
	0.5	1209	-4.74%	0.0495	2.32%	14.962	-0.18%	5.918	0.11%	0.003
	1	1187	-6.60%	0.0490	1.62%	15.194	0.38%	5.719	-0.37%	0.007
	2	1151	-9.69%	0.0499	2.87%	14.425	-1.47%	6.720	2.04%	0.020
	4	1221	-3.73%	0.0442	-4.91%	16.343	3.15%	4.514	-3.27%	0.029
4	Measured	1265	-	0.0478	-	18.043	-	2.866	-	0.063
	0.5	1249	-1.38%	0.0546	9.27%	16.908	-2.73%	4.350	3.57%	0.002
	1	1153	-9.51%	0.0556	10.67%	16.448	-3.84%	5.112	5.41%	0.009
	2	1122	-12.10%	0.0596	16.18%	14.595	-8.31%	8.817	14.33%	0.028
	4	1069	-16.61%	0.0618	19.14%	14.537	-8.45%	8.418	13.37%	0.033
5	Measured	1370	-	0.0222	-	8.837	-	12.068	-	0.309
	0.5	1198	-14.61%	0.0212	-1.35%	9.775	2.26%	10.880	-2.86%	0.040
	1	1183	-15.82%	0.0218	-0.60%	9.658	1.98%	11.180	-2.14%	0.087
	2	1145	-19.05%	0.0248	3.51%	6.507	-5.61%	14.566	6.02%	0.087
	4	1035	-28.38%	0.0243	2.93%	7.256	-3.81%	14.702	6.34%	0.055
6	Measured	1370	-	0.0222	-	11.844	-	9.061	-	0.186
	0.5	1192	-15.09%	0.0233	1.53%	11.009	-2.01%	9.474	0.99%	0.007
	1	1128	-20.53%	0.0230	1.11%	11.465	-0.91%	8.919	-0.34%	0.011
	2	1261	-9.23%	0.0232	1.32%	11.036	-1.95%	9.079	0.04%	0.050
	4	1285	-7.19%	0.0288	9.07%	5.582	-15.08%	16.374	17.61%	0.056
7	Measured	1370	-	0.0222	-	14.846	-	6.059	-	0.192
	0.5	1198	-14.61%	0.0256	4.62%	12.033	-6.77%	8.911	6.87%	0.003
	1	1068	-25.60%	0.0251	4.00%	13.136	-4.12%	7.413	3.26%	0.008
	2	1186	-15.56%	0.0264	5.69%	11.977	-6.91%	8.283	5.36%	0.016
	4	1154	-18.32%	0.0261	5.29%	12.220	-6.33%	8.083	4.88%	0.016

Note: s^* calculated for the numerically modelled response based on measured parameters is for an analysis period of $T = 4$.

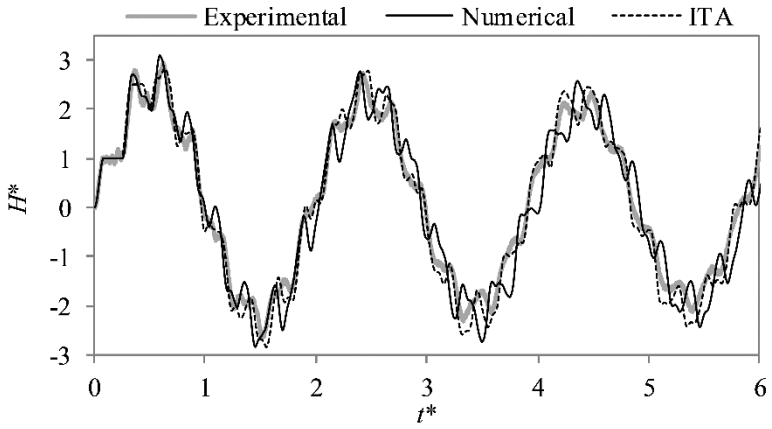

Figure 3-27: Case 6, Illustration of fit between experimental, numerical and ITA responses.

3.7.3 Signal properties affecting detection accuracy

Researchers investigating methods of transient analysis in laboratories and the field have mentioned a desire to achieve quick valve manoeuvres such that a transient response closely matches the "ideal" response generated by numerical models (Stephens 2008, Stoianov *et al.* 2003). However, little analysis demonstrating the expected advantages of faster valve closures has been presented in the literature. Lee (2005) showed how a faster perturbation would increase the frequency content of an input signal and hence increase the bandwidth. The bandwidth defines the frequency range over which the signal energy is concentrated. This section demonstrates how increasing this bandwidth can be beneficial for transient based fault detection by using ITA.

To investigate the effect of signal bandwidth laboratory experiments were conducted on a system with an extended blockage. The system is set up as depicted in Figure 3-13 with an extended blockage represented by a constriction in the pipeline flow diameter. The location and severity of this extended blockage are determined using transient fault detection methods for signals of different bandwidth. The steady state flow through the system is 0.24 L/s giving a Reynolds number of 4200 through the pipeline. Table 3-5 summarises the important dimensions and wave speeds specific to this experimental layout. To alter the bandwidth of the input transient signal, the closure speed of the valve at the downstream end of the pipeline (t_v^*) was varied from 0.025 to 0.497 over six different tests. The normalised valve closure duration is defined as $t_v^* = t_v/\sum(4L_0/a_0)$, where t_v is the closure duration in seconds. Figure 3-28 shows the pressure traces measured at the downstream valve for three of the experimental signals along with the numerical response from the numerical MOC model for an instantaneous valve closure. The line corresponding to the numerical data in Figure 3-28 demonstrates the expected behaviour of the system for a very fast closure, and hence a very high bandwidth signal. For this high bandwidth signal,

the positive reflection caused by the junction between pipes 2 and 3 is clearly defined at $t^* = 0.258$ and is seen as a near vertical change in pressure head. The negative reflection from the other end of the blockage (junction between pipes 1 and 2) is also well defined at $t^* = 0.392$. The experimental responses show that as the closure duration is progressively increased, the reflections become less distinct, especially the reflections that have a small magnitude or where the arrival time between two separate reflections is short. This is evident in Figure 3-28 for the experimental result $t^* = 0.266$, where the magnitude of the first reflection (at $t^* = 0.258$) is reduced as it overlaps with the reflection from the end of the blockage. This superposition means that the impedance of the blockage cannot be determined from the rise height of the initial reflection, and identification of the beginning and end points of the signal (for blockage location) is challenging. The lowest bandwidth experimental signal presented ($t^* = 0.497$) demonstrates that the reflections within the system can be completely masked, resulting in a pressure trace oscillating smoothly at the fundamental frequency of the system.

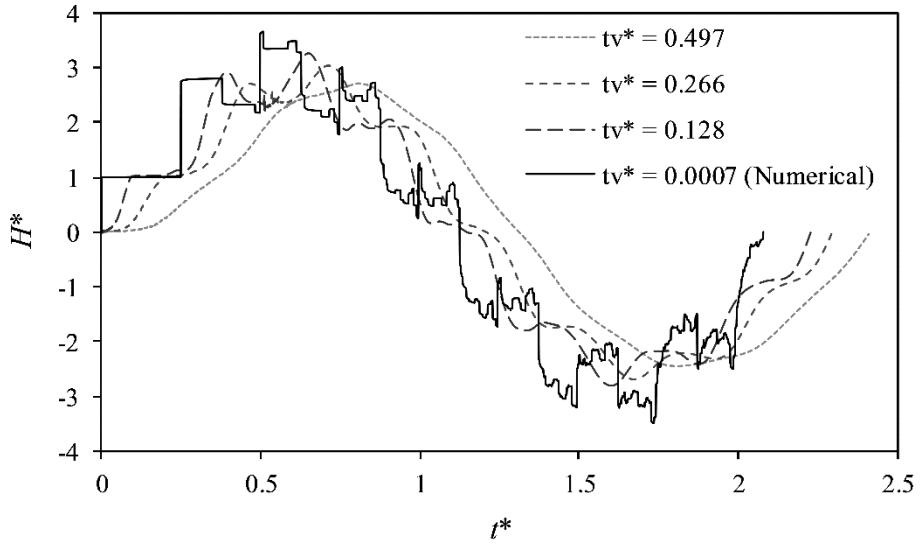

Figure 3-28: Comparison of numerical and experimental transient responses with different valve closure speeds.

To demonstrate the effect signal bandwidth has on the accuracy of transient fault detection, ITA is performed. The GA is used to determine the location, length and severity of the blockage constriction by fitting the outputs from the MOC model to the experimental pressure traces using the blockage properties as the fitting parameters. The unknown variables considered are: the length of the blockage (L_2), the distance between the downstream valve and the blockage (L_3), the severity of the blockage constriction (D_2), and the wave speed through the blockage (a_2). The ITA has been carried out for $t^* = 0$ to $2L/a$ to focus on the initial sequence of reflections. Table 3-5 presents the results of the inverse

transient analysis for experimental signals of different valve closure speeds. The predicted values of each parameter, along with the percentage error from the true value are presented for each signal. The prediction error of each parameter from the GA inverse analysis for different signal bandwidths is plotted in Figure 3-29. The *x* axis of Figure 3-29 is the dimensionless valve closure time, t_v^*. Note that the signal with the longest closure time has the lowest bandwidth. Each point on Figure 3-29 corresponds to the prediction error of a parameter using the GA inverse calibration on a particular signal trace. Linear regression lines for each variable in Figure 3-29 demonstrate that there is a strong correlation between the prediction error and the closure duration (bandwidth) of the signal. The higher bandwidth signals (faster valve closure) produce the most accurate determination of the blockage characteristics by the inverse analysis. The results have demonstrated that a high bandwidth signal is capable of distinguishing closely spaced objects in the pipeline and allows faults to be detected and identified with greater accuracy. This is further investigated in the following chapter with the development of a new transient generation system. Further detailed numerical illustration and discussion of signal bandwidth is given in Lee *et al.* (2015).

Table 3-5: Summary of blockage location and length prediction.

Closure Time (tc*)	a_2		D_2		L_2		L_3	
	Result (m/s)	Error %	Result (m)	Error %	Result (m)	Error %	Result (m)	Error %
Actual	1350	-	0.0222	-	12.248	-	20.612	-
0.025	1214	-10.1%	0.0221	-0.2%	10.75	-12.2%	20.85	1.2%
0.128	1110	-17.7%	0.0219	-1.2%	11.488	-6.2%	21.034	2.0%
0.212	888	-34.2%	0.0292	31.4%	14.996	22.4%	19.969	-3.1%
0.266	890	-34.1%	0.0286	29.0%	15.281	24.8%	20.308	-1.5%
0.341	987	-26.9%	0.0319	43.5%	15.456	26.2%	18.467	-10.4%
0.497	1007	-25.4%	0.0326	46.8%	16.434	34.2%	19.235	-6.7%

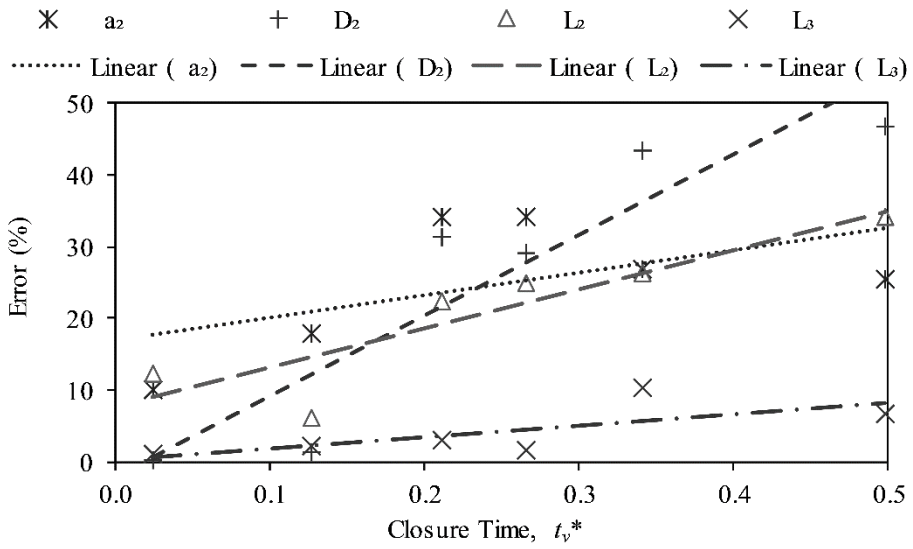

Figure 3-29: Blockage classification errors as determined through ITA, the linear fit lines show trends of increasing error with reducing bandwidth (longer valve closure duration) for all parameters.

3.8 Summary

This chapter has demonstrated that the fundamental period of a system is altered when variations in the pipe diameter and wave speed occur over a significant distance in the form of an extended fault. It has been shown that a blockage can produce reflections that significantly increase the pressure fluctuations in a pipeline during a transient event. These pressure fluctuations are not as severe when the blockage has been numerically approximated as a point. Where an extended blockage model is applied superposition of the reflections from a blockage can also alter the fundamental period of a system. Both of these observations are important when designing pipeline systems against pressure surges, suggesting that careful consideration should be given when employing discrete and extended blockage models. The study shows that where pipe diameters reduce through aging processes, the maximum transient response may increase, compounding the vulnerability of pipeline systems to failure. Thus transient analysis could be improved by considering the effect of gradual pipe deterioration and how this may affect the magnitude of pressure responses and resonant frequencies observed in a system. Analysis of the experimental data has found that the rate of damping significantly increases in the higher frequency components of the pressure response. Comparison of experimental and numerical data has shown that frequency dependent damping is under-predicted by the numerical model and this discrepancy is most noticeable in the high frequency components. This increased damping rate of the higher frequency ranges has a smoothing effect on the transient response.

It has been illustrated that deterioration to pipeline walls can produce a reduction in wave speed and result in changes to the nominal diameter, enabling transient analysis to be used to detect and classify degraded sections of a pipe. Comparison between experimental and numerical blockage affected transient responses shows comparable time domain results over the initial few periods of oscillation. An inverse transient analysis method of fault detection has been implemented and shown to successfully determine the properties and location of "faulty" pipe sections. It has been demonstrated that the method can independently resolve changes in wave speed and diameter over a wide solution space. This enables the method to be applied where prior information about a pipeline condition is minimal. This may be advantageous in the field application of transient based condition assessment methods. The presented method has been evaluated using laboratory data which exhibit strong periodic behaviour. It is found that this periodic behaviour can be beneficial for fault detection and classification accuracy. Where this periodic nature is not so strongly present, such as in large water distribution networks, improvements in accuracy could be achieved through a greater number of measurement points instead of increasing the duration of signal as considered here. Improvements in accuracy are also potentially achieved through increasing the sampling frequency and decreasing the modelled time step of the system response.

The investigation showed that decreasing the closure duration of a valve and increasing the bandwidth of the input signal is advantageous for transient based fault detection. This was demonstrated through performing ITA on a pipeline with an extended blockage, with trends showing an improvement in the accuracy of four variables as closure durations decreased.

4 FIELD APPLICATION OF TRANSIENT ANALYSIS

4.1 Introduction

Pipeline system management efficiency can be improved by identifying asset deterioration early. With this knowledge selective maintenance and renewals can be scheduled before costly emergency repairs are required or water supply and quality are adversely affected. This chapter investigates existing pipeline condition assessment technologies, then develops transient analysis based condition assessment methods and equipment and applies them to practical uses in the field for improved pipeline management.

4.2 Background

Assessment of pipeline infrastructure can be achieved through applying assessment techniques such as coupon sampling or ultrasound and electromagnetic methods (Liu *et al.* 2012, Stephens 2008) which examine a discrete location on a pipeline. These methods can be disruptive when carried out in busy areas such as under roadways as pipe excavation can be required and water distribution cut which is not desirable to users and providers. Moreover the methods only provide discrete samples of a pipeline for analysis which could misrepresent the average condition. A range of commercially available tools exist to conduct inspections over a length of a pipeline, in some cases without excavation and on live pipelines (Rizzo 2010). One common example of this is CCTV inspection. Other inspection technologies focus on listening to the acoustic response inside a pipeline while in operation. Anomalies

such as leaks within a pipeline can create acoustic noise which can be detected with listening devices. More advanced hybrid systems have been developed which combine CCTV for visual inspection with acoustic sensors for leak location and electromagnetic sensors for identifying anomalies in pipe wall condition. One example of this is Sahara®, a tethered system which can be drawn through pipelines greater than 150 mm in diameter using a drag chute and the fluid flow (Liu *et al.* 2012, Nestleroth *et al.* 2012, 2013). The same developer also offers free swimming solutions (SmartBall® and PipeDiver®) for pipes larger than 150 mm which can be propelled with the water. These methods have proved to be largely successful, however do have a limited scope of application. The hybrid systems cannot be used on pipelines smaller than 150 mm and require a connection of at least 100 mm to be inserted. Other than when assessments are made using visual data, wall condition monitoring is restricted to metallic pipelines or pipelines with metallic banding. Free swimming devices require appropriate flow conditions and valve closures are necessary for the units to be directed through a network. There is also a risk of losing devices in complex networks or while trying to navigate pipeline obstructions.

The majority of current leak detection and pipeline condition assessment technologies work by detecting acoustic noise generated by a leak as turbulent water is expelled from a pipe under pressure. Another approach of generating acoustic noise is to repeatedly tap directly on the pipe wall inducing pressure fluctuations through mechanical transfer of vibration. From these noise sources pressure wave velocity between two locations can be measured and related to pipeline strength (Liu et al. 2012, Nestleroth et al. 2012, 2013). The detection of these signals in the presence of background noise is problematic as the signal characteristics are unknown and can vary significantly between tests, and the method of generating these signals is very similar to ambient noise from other sources and is therefore easily masked. Consequently, these technologies are best conducted under controlled traffic and water flow conditions (Liu et al. 2012, Nestleroth et al. 2012, 2013).

An alternative to using the sound generated through the pipeline operation or through continuous discharge of water is to specifically generate a pressure wave in the system for analysis. A common approach is to rapidly close a valve that was steadily discharging water from a system which generates a signal in the form of a step wave. Pressure responses from valve closures have been used for detection of leaks (Colombo *et al.* 2009, Covas *et al.* 2005, Duan *et al.* 2012b, Ferrante *et al.* 2009, Lee *et al.* 2007), blockages (Duan *et al.* 2012a, 2013, Meniconi *et al.* 2012b, Tuck *et al.* 2012, 2013) and wall condition (Gong *et al.* 2013, Hachem and Schleiss 2012, Tuck and Lee 2013) in laboratory pipelines to name a few. Step signals generated through valve closures have been used in the field for a range of condition assessment applications (Stephens *et al.* 2008). Another approach presented in the literature has been to use solenoid valves which allow the generation of a pressure pulse to be electronically

triggered and have been used for leak and blockage detection in laboratory systems (Kashima *et al.* 2013 and Wang *et al.* 2002). Taking advantage of the solenoid valves ability to be controlled electronically allows multiple signal generations to be used for noise suppression and signal magnitude reduction (Lee *et al.* 2005). Lee *et al.* (2008b) modified a solenoid valve to produce a pseudo random binary sequence (PBRS) of pulses which can be used to estimate the system response function.

The use of these valve closure methods for signal generation is simple to apply, inexpensive and has been successfully applied in laboratory settings, however, researchers have found challenges when applying the method in the field. The signal generator (or valve is these cases) relies upon the systems back pressure to generate a flow, so the resulting magnitude and profile can vary significantly between test locations. In this case it is difficult to produce repeatable signals which can be used to reduce signal to noise ratios through signal processing methods such as stacking (Vaseghi 1996). Therefore, signals must be large in magnitude to be distinct and identifiable from background noise. Another practical issue is that to generate these large magnitude signals significant quantities of water must be discharged from the valve to obtain a steady flow before the closure. The discharge of water during testing is undesirable when the aim is to improve distribution systems' efficiency and reduce water losses, particularly in areas where water is considered a scarce and valuable resource. To avoid discharging water Brunone *et al.* (2008b) developed a portable pressure wave maker (PPWM) system which could generate a step wave of finite duration. The PPWM requires a vessel which would contain pressurised air and water; this is connected to a pipeline and an isolation valve opened between the vessel and pipe to cause a positive pressure wave to be generated. While the device eliminates water losses by injecting water back into the pipeline it requires a large pressure vessel to be transported and pressurised for each use. These mechanically operated devices will produce additional mechanical noise that is picked up by pressure transducers and can distort the input signal measurements.

This chapter introduces a new approach to transient signal generation using piezoelectric actuators. Piezoelectric actuators are devices that can convert an applied electrical charge to a precise volume change by distorting a suitable piezoelectric material. This property enables such a device to be used to generate repeatable and controlled acoustic signals within a fluid volume without discharging water. Piezoelectric actuators have been used across a wide variety of fields beginning with their development by Ernest Rutherford and Paul Langevin for SONAR systems to detect submarines in 1917 (Katzir 2012). Further applications have included fine control on lenses and optics, use in biomedical engineering to generate and detect ultrasonic waves for medical imaging (Manbachi and Cobbold 2011, Genovese 2016), use in structural health monitoring (Niezrecki *et al.* 2001, Chopra 2002 and Park *et al.* 2003) and use in acoustical oceanography (Medwin and Clay 1998). Significant research is available

on piezoelectric signal generation and propagation in open water scenarios with focus on SONAR systems and acoustic telemetry (Kilfoyle and Baggeroer 2000). It is identified that where solid boundaries exist, such as in shallow water, the detection of objects or identification of transmitted signals becomes more difficult due to multi path propagation, signal fading and bandwidth limitations (Liu *et al.* 2008, Proakis *et al.* 2001 and Akyildiz *et al.* 2005). To address some of these problems, complex signal designs and signal transmitter and receiver arrays can be implemented to improve signal identification and object detection (Fishler *et al.* 2004, Heutschi and Rosenheck 1997, Klauder *et al.* 1960, Lee *et al.* 2005, Paulo *et al.* 2009, Richards 2014). As signal complexity and length are increased high signal energy and good signal to noise ratio (SNR) can be achieved with smaller magnitude signals.

The use of piezoelectric actuators for acoustic signal generation in pipelines is limited to a few numerical and experimental studies. The most significant is a thesis by Kokossalakis (2006) that investigated the use of a pipeline as a wireless communication network. The thesis presents a range of data coding and analysis methods to transmit data through a short 9 m pipeline and demonstrates propagation characteristics of acoustic signals in pipelines. Expansion of piezoelectric actuators to pipeline condition assessment is, to the author's knowledge, limited to an experiment by Haqshenas (2010) who attempted to use the pulse echo method for leak detection in the field. The experiment was unsuccessful and transmission was not achieved.

This thesis presents an acoustic signal generation device and measurement system for pipeline condition assessment that implements a piezoelectric actuator. The device is tested in international field trials and offers a significant progression in the area of research which has relied on mechanically generated signals with limited published field applications. The system is trialled in the laboratory and field with focus on two pipeline condition assessment applications including the assessment of valve status and pipe wall condition. For each of the applications existing numerical knowledge is developed further to suit application of the technology and methods to the field, and analysis of field data is presented.

4.3 Pipe SONAR system

Active pipeline condition monitoring using fluid transients require the generation of highly controlled pressure signals in the field, often against significant system back pressure and a confusing array of background traffic and fluid turbulence noise. Since most water pipelines run alongside traffic routes, the generation of the signal should be carried out quickly, non-intrusively and with a minimal loss of water. This combination of requirements poses significant challenges for researchers in the field and transient tests were often carried out in the middle of the night where the background noise and traffic volume are low (Stephens *et al.* 2005a, Stephens 2008).

This section applies the existing transient fault diagnostics techniques on signals generated by a piezoelectric actuator. This generator, referred to as Pipe SONAR (PCT/EP2015/059540) can create small pressure fluctuations in the order of 0.1 m in typical water distribution pipelines. Field-testing of the Pipe SONAR technology was undertaken on 31 sites across four operational water networks in China and New Zealand. The networks included the on-campus water network at the University of Canterbury, Christchurch (NZ) and three large-scale municipal water networks; one in New Zealand (servicing a population of 400,000) and 2 in China (servicing populations of 3 to 4 million each); which are operated and managed by Veolia. Field-testing on these different water networks allowed for evaluation of the Pipe SONAR condition assessment applications under live operational conditions on a wide range of infrastructure, in terms of size, material, age, network configuration, and operating conditions.

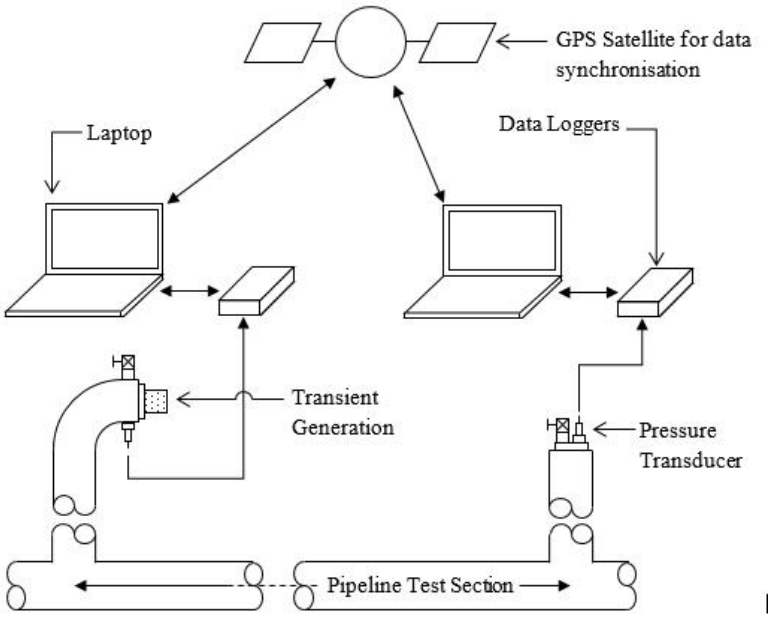

Figure 4-1: Schematic of test system in typical test arrangement.

The measured responses to the generated signals are analysed with signal processing methods proposed in Lee *et al.* (2005) and have been detected suitably for practical use at a range of up to 265 m in a 300 mm diameter pipeline which includes multiple service connections and junctions. This is achieved despite the signal magnitude being much smaller than the noise band within the system. Pressure signals are generated by a custom built piezoelectric actuator (Figure 4-2a) and control system. The piezoelectric actuator is driven by a linear power amplifier and an impedance matching unit. The generator has an operational frequency range of between 40 and 8000 Hz and the signal from the generator is captured using high-speed, dynamic piezoelectric transducers (PCB ICP©) with a response

frequency of 200,000 Hz. The generator and the data recording are controlled using customised software developed at the University of Canterbury using LabVIEW™. One pressure sensor is located at the generator (known as the "local" station) and another is attached to another hydrant upstream or downstream (known as the "remote" station) (Figure 4-1). The data recording is GPS synchronised between pressure sensors and data is recorded onto a laptop computer via a 400 kS/s National Instrument data logger at each station. The data acquisition system is capable of a sampling rate greater than 100 kHz for long durations. Each station is powered by a portable power supply consisting of an inverter and rechargeable lithium ion batteries. The system is compact and is able to be transported and set up by one or two people (see Figure 4-2b).

(a)  (b) 

Figure 4-2: (a) Piezoelectric actuator in mounting flange with air bleed valve. (b) Portable equipment needed for the operation of the Pipe SONAR.

The Pipe SONAR system is attached to existing hydrants through flange connections. Fire hydrants provide the ideal connection points for the assessment of potable water supply networks as they are spaced within 150 metres in urban areas and the fittings are standardised across administrative regions (Stephens *et al*. 2008, NZS 4404:2010). The Pipe SONAR system has been tested on two types of fire hydrants: below-ground hydrants typical in the United Kingdom, Australia and New Zealand (see Figure 4-3); and above-ground hydrants typical in America, China and mainland Europe (see Figure 4-4). For the below-ground hydrants, a stand pipe is used to mount the equipment above the manhole to avoid submergence. Bleeding air from the above-ground hydrants is more difficult than the below-ground systems as a large air pocket can be lodged above the connection ports in the hydrant body. A specially designed air bleeding system was applied to these hydrants to allow the bleeding of this air-pocket (see Figure 4-5). As a comparison to the piezoelectric signal, a 25 mm ball valve was also used at each site to create manual valve closure signals.

(a)  (b) 

Figure 4-3: Below ground fire hydrants fittings for Pipe SONAR testing. (a) Local station (b) Remote station.

(a)  (b) 

Figure 4-4: Above ground fire hydrants fittings for Pipe SONAR testing. (a) Local station (b) Remote station.

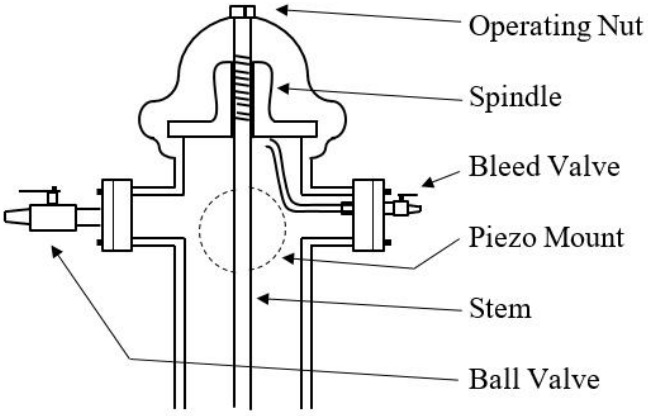

Figure 4-5: Hydrant fittings and bleed system for above ground fire hydrants.

4.3.1 Signal development and processing

The generator is capable of generating customised signals and Figure 4-6 shows an example of one of the signals that has been used in this field trial. The signal shown is the input signal to the generator with the y-axis of the plot indicating the normalised electrical input. The signal is repeated constantly to provide a sequence of evenly spaced, identical chirps with a frequency sweep from 100 to 300 Hz. Chirp sequences such as these are commonly used in SONAR systems as they are broadband and yet temporally compact, and able to contain a wide range of frequencies within a short signal duration. A second signal type was implemented in the second stage of field testing which took advantage of pulse compression techniques to allow improved signal identification. This signal swept logarithmically between randomly selected frequencies over random time intervals within a defined bandwidth for a sequence duration of 10 s, where mean time intervals were defined to optimise the signal response. A segment of this is given in Figure 4-7. A full and detailed investigation of signal development and processing was outside of the scope of this thesis, however the signals and processing methods implemented here were selected to test the equipment and enable further development to take place.

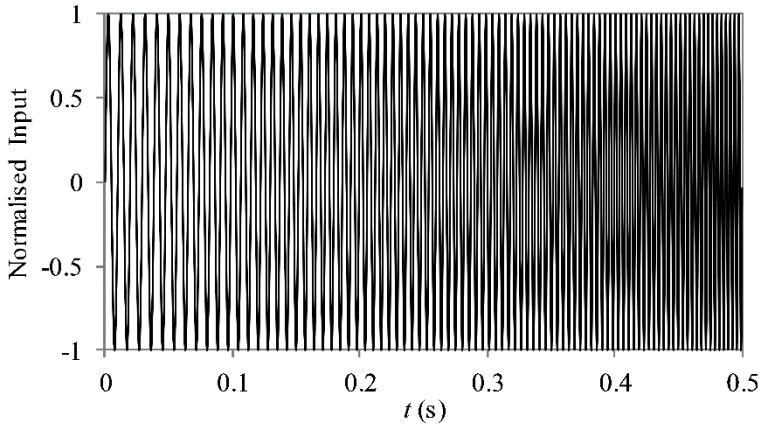

Figure 4-6: Example of simple Pipe SONAR signal consisting of 100-300 Hz logarithmic chirp function with duration of 0.5 s.

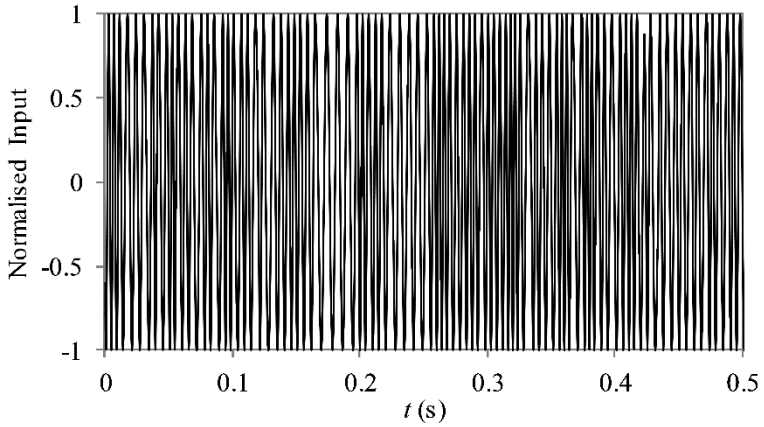

Figure 4-7: Segment of Pipe SONAR signal consisting of randomised logarithmic chirps in time and frequency within a bandwidth of 100-300 Hz.

One significant advantage of the piezoelectric generator is that the signal can be adjusted to suit the field conditions. Figure 4-8 shows the average background pressure noise spectrum taken from 25 different live water networks in the testing program. The noise spectrum is determined from 100 seconds of pressure data sampled at 20 kHz or greater at each site. The noises observed in these measurements are typical of water supply networks and originate from pump operations, changes in demand, flow turbulence and external sources such as traffic vibrations and construction work. Figure 4-8 shows that this background noise is concentrated at the low frequencies with much of the energy below 50 Hz. Field application of fluid transients for condition diagnostics requires the injection of a pressure signal that can be distinguished from this background noise.

Previous publications have shown that the energy of manual valve closures signals are concentrated below 60 Hz, and the signals overlap directly with the background noise band (Lee *et al.* 2004). Band-pass frequency filtering to remove the background noise will also lead to the distortion of the received signal and the positive identification of a valve closure signal in the field requires a signal that is significantly larger than the noise band. Such signals may need to be as large as 30 m head in some systems, with a potential risk of damaging the pipeline.

Alternatively, the Pipe SONAR system can create customised pressure signals that have most of their energy targeted outside the background noise spectrum. Figure 4-9 shows the spectrum for the Pipe SONAR chirp signal shown in Figure 4-6. Most of the signal energy lies above 100 Hz and there is little overlap between the signal and the spectrum of the typical high background noise band, maximizing the potential SNR of the measured responses. The increase in signal frequency and bandwidth is also shown to improve system diagnostic abilities (Lee *et al.* 2015). A simple linear phase delay filter can be applied to the measured signal to remove dominant components of the background noise without affecting the accuracy of the subsequent pipe condition assessment. The Pipe SONAR system can create highly controlled signals of different frequency bands to avoid specific noise sources on each site and this presents a powerful advantage over the manual or mechanical means of signal generation. Due to the clear separation between the generated signal and noise bands, the analysis can be carried out using signals that are as small as 0.1 m in head; this signal can be detected hundreds of metres away from the generator. The signal bandwidth selected for these field trials was chosen so that for the range of pipes being tested the signal would remain within plane wave frequency range while avoiding the spectrum over which the noise is significant. Thus signal dispersion associated with higher order propagating modes is avoided.

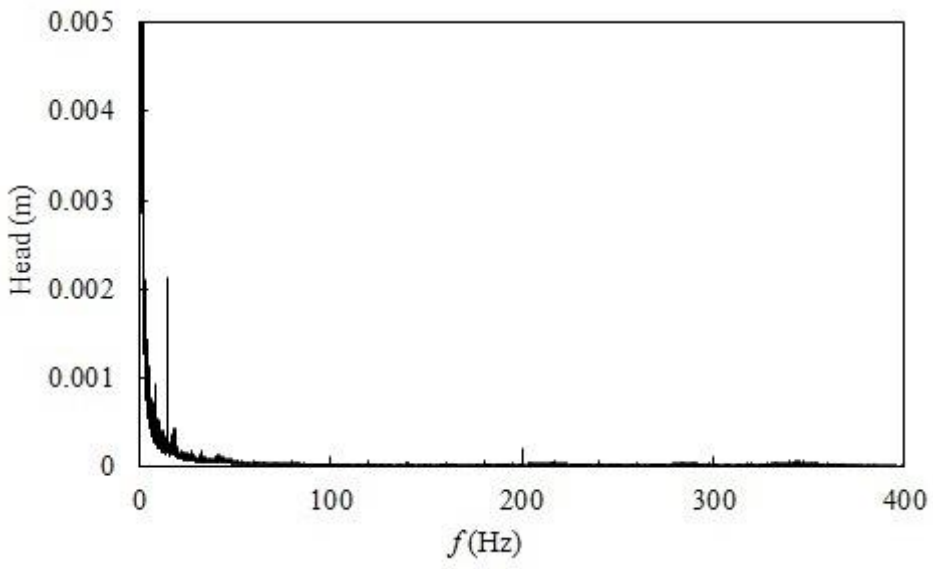

Figure 4-8: Background noise spectrum collected from 25 different sites in live water supply networks.

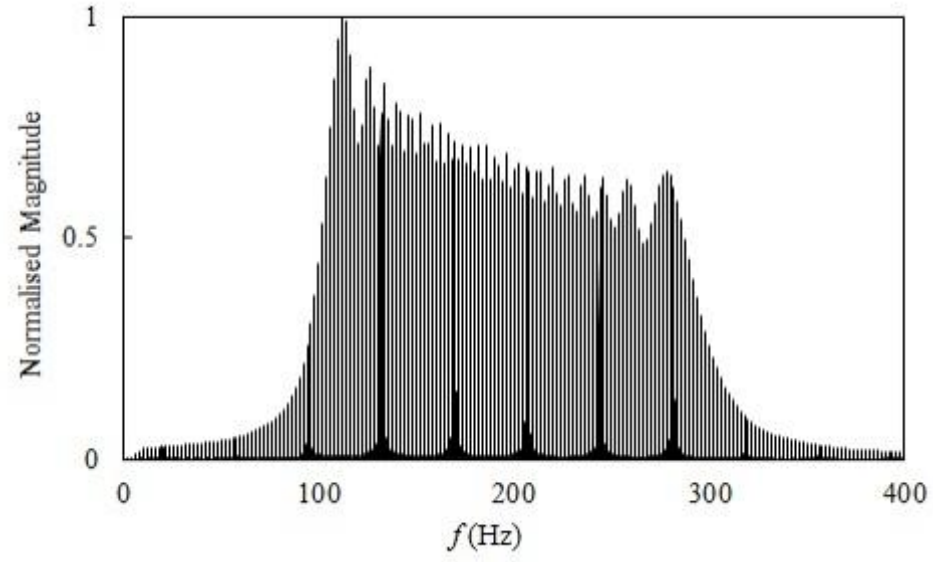

Figure 4-9: Power spectrum of a typical chirp signal from the Pipe SONAR system.

Signal processing and identification was carried out using the cross-correlation method

$$\hat{R}_{Hy}(m) = \sum_{n=0}^{N-m-1} H_{n+m} y_n^* \qquad (4\text{-}1)$$

where *m* is the signal lag, *N* is the vector length, *H* is the measured system response and *y* is the input signal. An unbiased estimate of the response can be found by:

$$\hat{R}_{Hy,u}(m) = \frac{\hat{R}_{Hy}(m)}{N - |m|} \quad (4\text{-}2)$$

4.4 Assessment of valves

An important component of pipeline networks are valves, which are used to restrict or stop flow through a system. Isolation valves are critical for the protection of pipeline networks and can minimise damage in the event of a major burst or disruption to users during system maintenance (Bouchart and Goulter 1991, Jun *et al.* 2007, Stephens *et al.* 2005a, Walski 1993). These valves are often left untested throughout a lifetime spent buried underground, such that the sealing capabilities of these valves are often unknown; but can be negatively affected by sedimentation, tuberculation or corrosion. This section focusses on a method for determining the condition of a valve by assessing the ability for the valve to restrict and stop water flow when closed. In water distribution systems valves are particularly important for isolating sections of a system for routine or emergency maintenance and repairs, however valves are prone to deterioration such that they may not operate suitably when required. Failure of a valve can be due to leaking o-rings and packing, corrosion of the valve body, wear on the valve disk and seating or aggradation of sediment within the valve seating (FCM 2003).

Isolation valves are very common components on a pipeline network. Typically, isolation valves are sited so that they may isolate distribution pipes from mains, or small reticulation mains from larger reticulation mains. They are also typically placed between planning zone boundaries (such as between industrial and residential zones), either side of major transport corridors, between pressure boundaries, or otherwise sited to minimise the effects of shutdowns on the customers (NZS4404:2010, 6.3.14). In addition to this, NZS4404:2010 Section 6.3.14.3.1 specifies that the maximum spacing between isolation valves is to be 300 m for pipe diameters less than 150 mm with the nominal number of service connections being 40, increasing to 1,000 m for pipe diameters greater than 375 mm with a nominal number of connections being 150. BS EN 805:2000 Appendix 19 specifies a maximum spacing of 500 m in urban distribution mains, 2,000 m in principal mains and 5,000 m in trunk mains. Both codes require consideration to be given to the population density, as well as important amenities such as hospitals, where additional isolation valves may be required.

The purposes of these valves mean that they will often be fixed in open or closed positions for long periods of time, however they must be known to be in an operable condition when an emergency requires. Checking of valve condition is most commonly carried out with an isolation test whereby a section of a network can be closed off using valves as required, then the pressure or flow from this section of the network can be monitored to ensure the valve is appropriately stopping any flow. The drawback of this method is that it requires water supply to be temporarily cut to a section of the network which is undesirable. In water system design looped networks with high redundancy are preferred to minimise dead ends which can result in deteriorated water quality, thus using this method generally requires two or more valves to be closed to isolate a specific section. If one of those is found to be faulty, adjacent sections need to be shut off in a trial and error approach to identify which is the faulty valve. Currently there are no commercially applied method to quantitatively assess a valve condition without valve excavation and/or system shutdown (Marlow *et al.* 2007).

An alternative method of determining the condition of an isolation valve in a water supply network is to measure pressure signal transmission through a valve. A poorly sealed isolation valve will behave as a high impedance component in a pipeline, thus will reduce the magnitude of a pressure signal transmitting through it while reflecting the balance of the signal energy. On the other hand, an open valve will have a relatively low impedance and will have little effect on signal propagation, and a well-sealed valve will provide no hydraulic mechanism for water or pressure signal to pass and the signal transmission through the valve will be minimal (Wylie and Streeter 1993). This method can be illustrated through considering a simple pipeline with an in line valve set in three different positions; open, partially open and closed. Figures 4-10 to 4-12 show the response of the system following a small positive pressure pulse (H_W) generated at a time t_0 and the subsequent pressure state at time t_1 after the pressure pulse has propagated past the valve. The open valve case (Figure 4-10) allows close to full transmission of the pressure pulse (H_T) as there is little impedance change from the rest of the pipeline. A partially open valve (Figure 4-11) can result in notable transmitted and reflected (H_R) pressure pulses, while a fully closed valve (Figure 4-12) produces full reflection of the pressure wave and subsequently indicates a valve that can seal completely. The physical behaviour of pressure wave transmission through high impedance elements means that the transmission of a pressure pulse through a valve shows little sensitivity to the valve position when the flow area through the valve is significant, and a high sensitivity to changes in valve position when flow areas through the valve are very small.

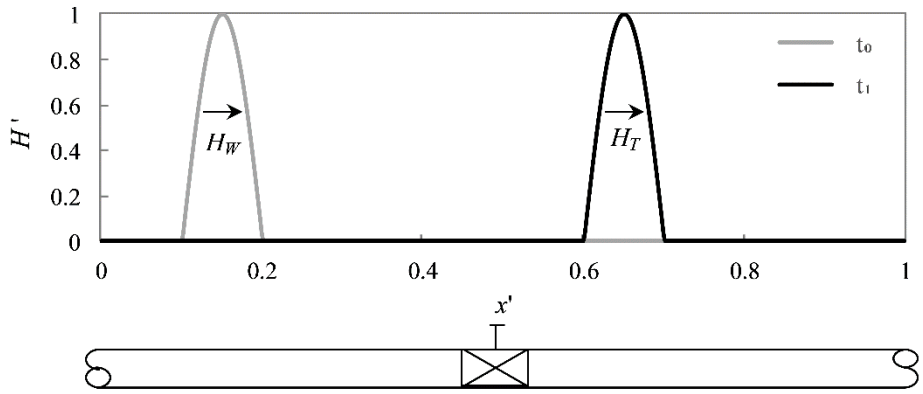

Figure 4-10: Open in line valve with full pressure wave transmission.

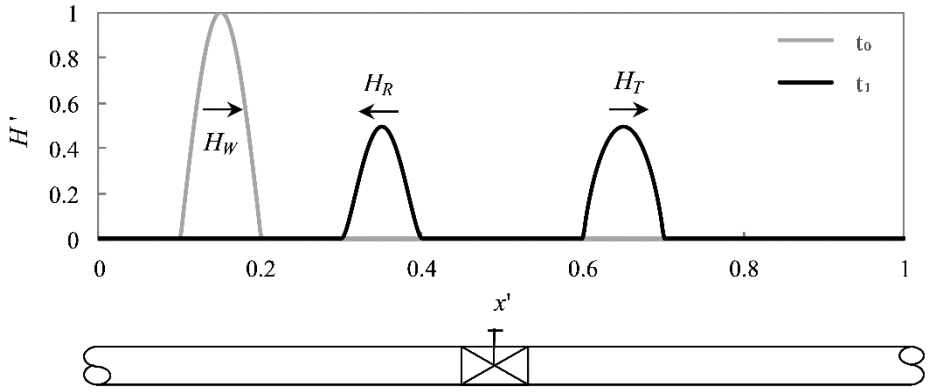

Figure 4-11: Partially open in line valve with 50% pressure wave transmission.

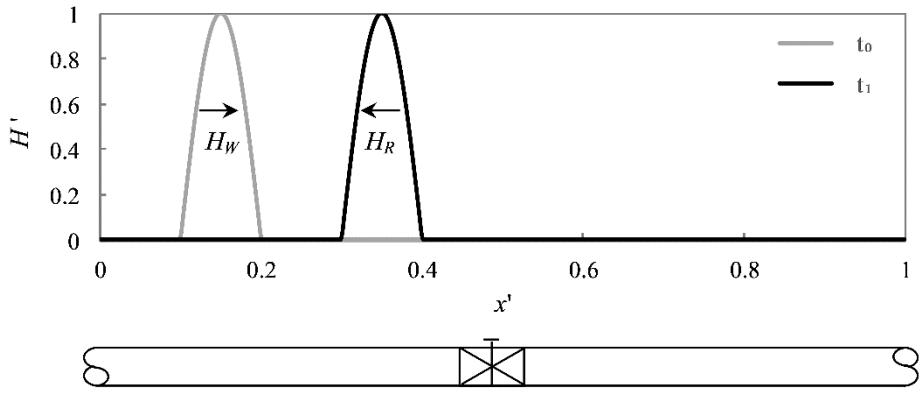

Figure 4-12: Closed in line valve with no pressure wave transmission.

Meniconi *et al*. (2011) investigated the reflection characteristics of step waves from valves and orifices in the laboratory. The research investigated valve openings of 5% and larger and found that the valve

position could be accurately determined using steady state loss assumptions for the unsteady flow behaviour. Misiunas *et al.* (2005) aimed to determine valve condition through measuring the relative size of reflected step waves from nominally closed valves on a transmission main. The results were used to estimate the openings of a valve by assuming a discharge coefficient. These authors showed that analysis of reflections from valves can provide useful information about that valves condition or status. However, the methods used by these researchers could be difficult to apply in many field scenarios. Three practical aspects are of particular importance: 1) To accurately determine the height of the reflection relative to the incident wave, all sources of reflection within range of the valve and measurement point must be quantified and accounted for; 2) The damping characteristics of the wave in the given pipe must be known and field studies carried out as part of this research and others have shown that the damping can be considerable and variable; 3) The reflection from the valve needs to be clearly identifiable and this is difficult where systems create highly periodic responses close to the source, masking the reflection, which is typical of above ground hydrant configurations. In the following section these practical problems are addressed using the Pipe SONAR system and focussing on the wave transmitted through the valve instead of the one reflected from it.

4.4.1 Valve assessment theory

Under steady state flow conditions, a partially open valve will cause a head loss based upon the steady flow rate (Q_0), valve position (τ) and valve coefficient (C_v) and can be determined by the equation:

$$Q_0 = C_v(\tau)\sqrt{H_U - H_D} \qquad (4\text{-}3)$$

Where the head loss is determined by the difference between the head upstream (H_U) and downstream (H_D) of the valve. The valve coefficient is a function of the valve position which is determined by the ratio of open valve area to total valve area. For the case of a closed valve with a good seal the valve position, $\tau \rightarrow 0$ and consequently $C_v \rightarrow 0$, thus for any given head difference the flow will tend towards zero. The valve coefficient is useful in hydraulic modelling as it allows for easy variations in valve position within simulations, however $C_v(\tau)$ is valve specific and an empirically determined relationships are typically reported only for $\tau > 0.1$, which is of little interest for assessing valves in a nominally closed position. In this chapter, specific values for C_v and τ are not required to determine relationships between head and flow for a valve in a fixed position, therefore $C_v(\tau)$ will be substituted with a lumped valve coefficient $C_v\tau$.

Equation (3-6) is considered valid under transient flow conditions if it is assumed that there is no capacity for a change in fluid mass within the valve and that the inertial effects of accelerating and

decelerating waves are ignored (Wylie and Streeter 1993). By solving Equation (3-6) with the positive and negative characteristic equations (Equations (4-4) and (4-5)) across a valve node, a formula can be found for the instantaneous flow through a valve in terms of steady flow, valve position, valve coefficient and the signal magnitude (H_W). This formulation is similar to one presented by Wylie and Streeter (1993), however it is expressed in terms of the valve position and valve coefficient, not the steady state head loss across the valve which is not of primary interest for this application. The derivation assumes steady flow conditions at time t_0 with an incident pressure wave on the characteristic line as depicted in Figure 4-13. The equations are solved at time $t_0 + \Delta t$ to consider the split of the incident wave (H_W) into transmitted (H_T) and reflected components (H_R).

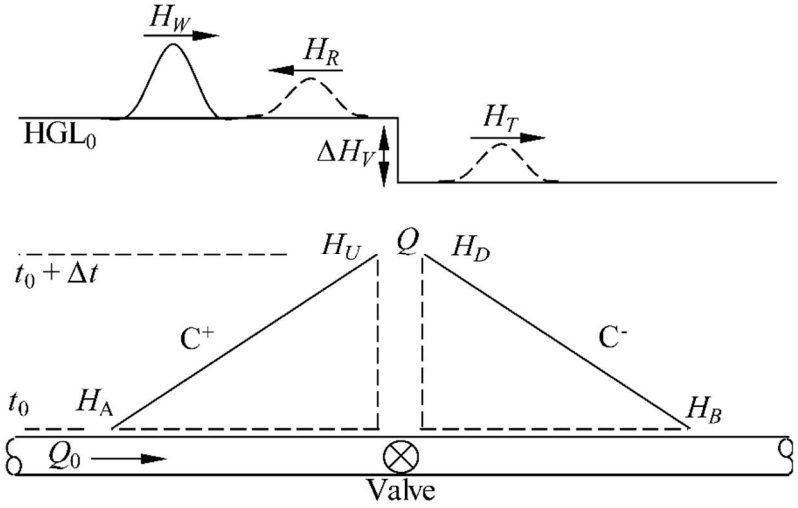

Figure 4-13: Illustration of wave behaviour at a valve and characteristic interpretation.

The characteristic equations are given by

$$C^+: \quad H_U = H_A - B(Q - Q_A) - RQ|Q_A| \tag{4-4}$$

$$C^-: \quad H_D = H_B + B(Q - Q_B) + RQ|Q_B| \tag{4-5}$$

where B is the characteristic impedance,

$$B = \frac{a}{gA} \tag{4-6}$$

and R is the resistance coefficient,

$$R = \frac{f\Delta x}{2gDA^2} \tag{4-7}$$

As the focus is on the behaviour attributed to the valve only, the space step in the characteristic equations, $\Delta x \rightarrow 0$, therefore the resistance coefficient, $R \rightarrow 0$ and can be ignored (Equation (4-7)). By taking the datum to be the hydraulic grade line downstream of the valve the head on the negative characteristic (H_B) is

$$H_B = 0 \tag{4-8}$$

While the head on the positive characteristic (H_A) is given by the sum of the steady state head loss across the valve and the magnitude of the incident wave, such that

$$H_A = \Delta H + H_W = (Q_0/C_v\tau)^2 + H_W \tag{4-9}$$

The flow on the positive characteristic (Q_A) considers the change in steady flow induced by the incident wave, such that

$$Q_A = Q_0 + H_W/B \tag{4-10}$$

And the flow on the negative characteristic (Q_B) is given by the steady flow velocity

$$Q_B = Q_0 \tag{4-11}$$

Solving equation this system of equations gives the flow through the valve (Q) given an incident wave of magnitude H_W.

$$Q = \frac{2BQ_0 + 2H_W + {Q_0}^2/(C_v\tau)^2}{B + \sqrt{B^2 + \left(2BQ_0 + 2H_W + {Q_0}^2/(C_v\tau)^2\right)/(C_v\tau)^2}} \tag{4-12}$$

Derivation of Equation (4-12) is achieved using an alternative to the quadratic equation presented in Forsythe (1970) which is shown to avoid numerical errors caused by computational limitations in this application (Bergant and Simpson 1991).

Wylie and Streeter (1993) define a useful parameter that is determined by the ratio of the transmitted wave size to the incident wave size (H_T/H_W) which gives the transmission ratio (TR) of a signal through a valve. This can be calculated by

$$TR = \frac{H_T}{H_W} = \frac{B(Q - Q_0)}{H_W} \tag{4-13}$$

Substituting Equation (4-12) into Equation (4-13) gives the full equation for TR as

$$TR = \frac{H_T}{H_W} = \frac{B}{H_W}\left(\frac{2BQ_0 + 2H_W + {Q_0}^2/(C_v\tau)^2}{B + \sqrt{B^2 + \left(2BQ_0 + 2H_W + {Q_0}^2/(C_v\tau)^2\right)/(C_v\tau)^2}} - Q_0\right) \tag{4-14}$$

Under typical operating conditions the influence of a valve, or partially closed valve, on unsteady hydraulic behaviour will be small and very high base flows (Q_0) are required for TR to reduce notably from unity (Stephens 2008, Wylie and Streeter 1993). However, this application is focussed on valves that are set to a nominally closed position where any increase in $C_v\tau$ from zero is due to deterioration of valve seals and other mechanisms. Hence $C_v\tau$ is expected to be very small and so variations in TR can be significant and measurable without significant base flows or incident wave magnitude. A useful simplification can be made where the base flow is zero,

$$TR = \frac{2}{1 + \sqrt{1 + 2H_W/(C_v\tau B)^2}} \tag{4-15}$$

Equations (4-14) and (4-15) show that TR is dependent on the magnitude of the incident wave, H_W where all other variables are held constant. This is easily accounted for when considering transmission of step waves as measurements taken from a discrete data point on the signal plateau following the step rise. However, where oscillatory signals are used this results in a change in shape of the transmitted wave form. This physical behaviour becomes important as the transmission of signal magnitude and energy will be different for the same signal. Consideration must be given to this when using cross-correlation functions to analyse signal transmission, as the entire wave form is considered in the calculations. A method to account for this is given in the following section and an illustrated description of the transmission behaviour can be found in Appendix A.

4.4.1.1 Extension of transmission theory to measured signals

To determine the TR for a complex signal measured some distance from the valve it is necessary to compare the transmitted signal strength for open and closed valve cases. The signal transmission strength for an open valve can be taken as the value of $R_{Open}(t = t_{lag})$, where t_{lag} is the time taken for the signal to propagate between the generation point at the local station and the measurement point at the remote station. R_{Open} is given by the cross-correlation of the input signal (y) and the measured head response for the open valve case ($H_{Remote}(t)$), as calculated by Equation (4-2). Similarly the transmission

strength for a closed valve is given by $R_{Closed}(t = t_{lag})$ which considers the measured response for the closed valve case. The transmission ratio is then calculated by,

$$TR' = \frac{R_{Closed}(t = t_{lag})}{R_{Open}(t = t_{lag})} \tag{4-16}$$

where TR' indicates the transmission ratio determined by signal energy transmission as opposed to TR which is determined by peak head transmission. This calculation assumes that the damping rate of the signal is consistent between the two runs and that any difference in signal magnitude at the remote station can be attributed to losses imposed by the valve.

To estimate the lumped valve coefficient ($C_v\tau$) for a valve in a given position it is necessary to relate the experimentally determined value TR' with a theoretical value. The theoretical relationship between signal transmission and the lumped valve coefficient can be calculated by

$$TR'_{Num}(C_v\tau) = \frac{\sum_{t=0}^{t} TR(H_{W,Est}(t))H_{W,Est}(t)^2}{\sum_{t=0}^{t} H_{W,Est}(t)^2} \tag{4-17}$$

where TR is calculated by Equation (4-14) and $H_{W,Est}(t)$ is the estimated pressure response at the local station side of the valve for the open valve case. This is required as TR is dependent on the magnitude of the signal.

To determine the magnitude of the signal as it propagates along the pipeline it is necessary to know the signal magnitude at the remote station (H_{Remote}) and where this is obscured by signal noise its mean value can be determined by

$$H_{Remote} = \frac{R_{Open,Remote}(t = t_{lag})}{R_{Open,Local}(t = 0)} H_{Local} \tag{4-18}$$

As the magnitude of the pressure head generated at the local station can vary with the generators frequency dependent output and signal type, it is convenient to consider the RMS of the generated signal. Making the assumption that the SNR is high at the signal generation location and that the signal is continuous, the signal magnitude can be determined by

$$H_{Remote} = \sqrt{2}\frac{R_{Open,Remote}(t = t_{lag})}{R_{Open,Local}(t = 0)} RMS(H_{Local}(t)) \tag{4-19}$$

And the mean magnitude of signal oscillation at the generator is determined as

$$H_{Local} = \sqrt{2}RMS(H_{Local}(t)) \quad (4\text{-}20)$$

When applying this method a band pass filter should be applied to $H_{Local}(t)$ to remove background noise outside of the signal bandwidth.

The pressure response at the valve can then be estimated by

$$H_{W,Est}(t) = y(t) \times c \quad (4\text{-}21)$$

where $y(t)$ is the input signal used in the analysis. For a typical oscillating signal $y(t)$ can be taken as a quarter period of a sinusoidal wave for computational efficiency, provided it is divided into a suitable number of time steps to ensure the modified wave form is represented. The multiplication factor, c estimates the signal magnitude at the valve located a known distance between the two measurement stations. This is estimated by considering a constant rate of signal damping along the pipeline and fractional magnitude reductions at known pipe junctions (if applicable).

4.4.1.2 Numerical illustration of transmission ratio

To illustrate the usefulness of the transmission ratio for valve condition diagnosis, Equations (3-6) and (4-14) can be used to compare unsteady hydraulic pressure transmission through a valve at varying degrees of closure with the corresponding expected discharge from the valve. Figure 4-14 demonstrates the transmission behaviour for an incident wave of magnitude, H_W = 1.0 m (corresponding to the peak amplitude of a sinusoidal pulse) through a valve in a pipeline with a nominal diameter, D = 0.1 m under no base flow conditions. For a quantitative comparison, a discharge curve shown in Figure 4-14 assumes that a pressure drop across the valve of ΔH = 10 m is applied. This could represent a situation where the valve is required to shut off a section of pipe for maintenance or repair and a system back pressure of 10 m head exists. The scale given on the plot ranges from a flow of 10 L/s, which corresponds to a typical operation flow velocity of 1.27 m/s, down to full curtailment of the flow. The valve coefficient is shown on a logarithmic scale to demonstrate that the transmission ratio becomes very sensitive to valve position as the expected discharge becomes small. This makes it a suitable parameter to evaluate valve condition where degradation allows for small flow areas through a valve assumed to be fully closed.

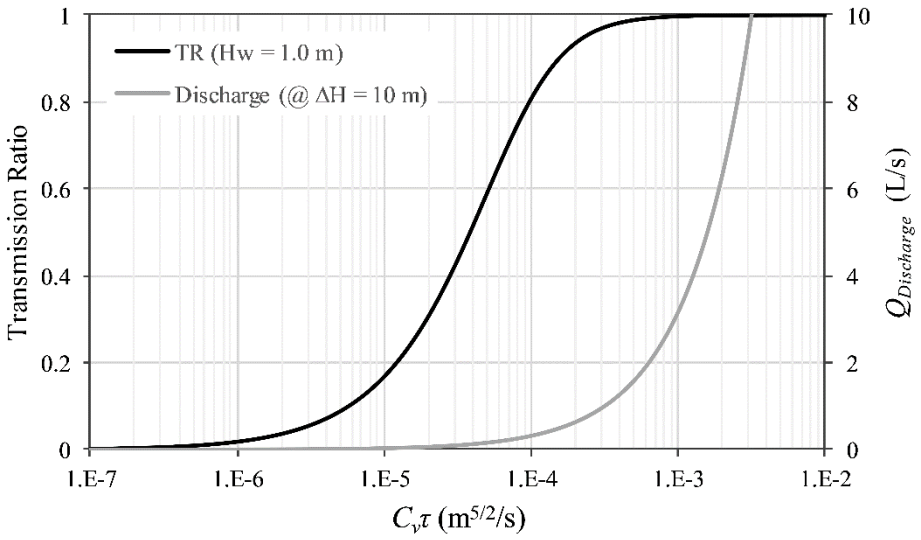

Figure 4-14: Comparison of unsteady hydraulic pressure transmission and steady flow velocity through a pipeline with variable control position.

The transmission curve shown in Figure 4-14 is dependent upon the magnitude of the incident signal. Increases or reductions in the signal magnitude will shift the curve right or left respectively, which indicates that smaller signals will be more sensitive to relative changes in valve position when the opening is very small. This offers a significant advantage to the Pipe SONAR system which can operate with very small and variable magnitude signals while being measureable due to long duration signals.

Figure 4-15 demonstrates the behaviour for the same system described above and considers the effects of variations in signal magnitude and base flow. The curve corresponding to 50% signal transmission is given for signals from 0.001 m to 100 m head and the steady state head loss induced by the base flow is overlaid. The figure shows that where the signal magnitude is approximately one order of magnitude larger than the steady flow, losses across the valve or changes in base flow have little effect on the signal transmission ratio. This is a useful observation when applying the method to looped networks which can be pressurised from both sides of the valve allowing a no flow assumption to be made. However, where there is a forced base flow across a valve knowing its value is useful in determining the valve coefficient accurately. Making the assumption of zero base flow, when it may be greater, will result in an upper bound condition assessment of the valve, such that a valve can confidently be assessed to be in poor condition (i.e. requiring replacement) based on this numerical analysis.

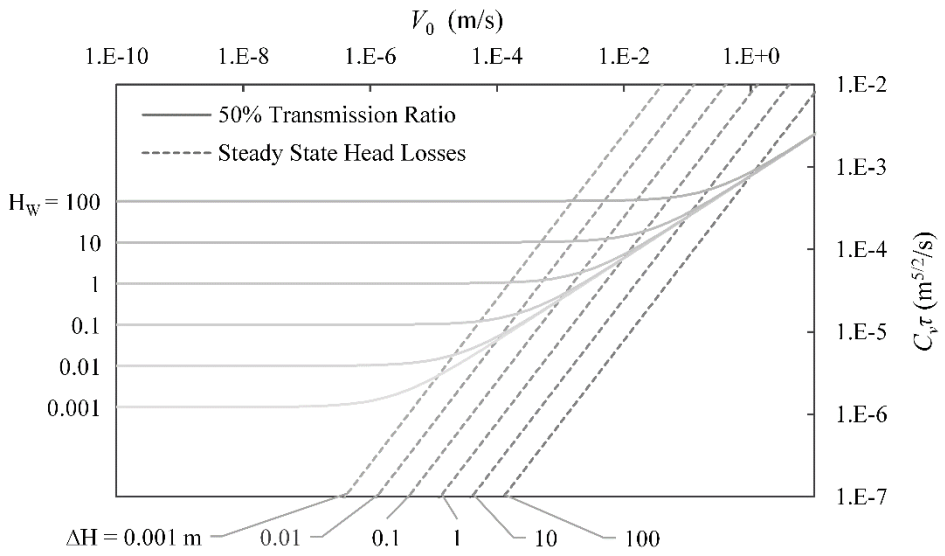

Figure 4-15: Transmission of incident waves at varying magnitudes with consideration to steady state head losses.

4.4.2 Laboratory analysis and verification

Verification of the described valve condition assessment method has been undertaken in the laboratory, with the aim of comparing valve coefficients determined through steady state flow analysis and hydraulic transient analysis. The laboratory experiments are conducted with both Pipe SONAR and valve closure signal generation methods. The laboratory experiments were carried out using the transient pipeline facility at the University of Canterbury as described in Section 3.5. An 80 mm VAAS gate valve has been fitted to the pipeline and modified to include air bleed valves to ensure that the system is free from air which could affect results (Figure 4-17). Steady state flow tests have been conducted on the valve to determine the lumped valve coefficient as a function of valve position. Further details of this are given in Appendix B. The experimental system is setup as shown in Figure 4-16, with pressure transducers located 100 mm either side of the valve and further pressure transducers located installed as listed in Table 4-1. The test system is bounded by a constant head reservoir at the upstream end of the pipe and is closed off at the downstream end. Unlike the test cases in the previous chapter, the signal generators are located upstream of the test section, or gate valve in this case. This is required so that the base flow required to generate a step wave via the valve closure method is not affected by variations in the gate valve position. This requirement may be restrictive when using the valve closure method in the field, however, the Pipe SONAR generator does not suffer these limitations and could be used at any location on the pipeline. For this experiment the two generators are located at the same

position to enable valid comparison of results. With this experimental setup there is no base flow through the valve such that $Q_0 = 0$.

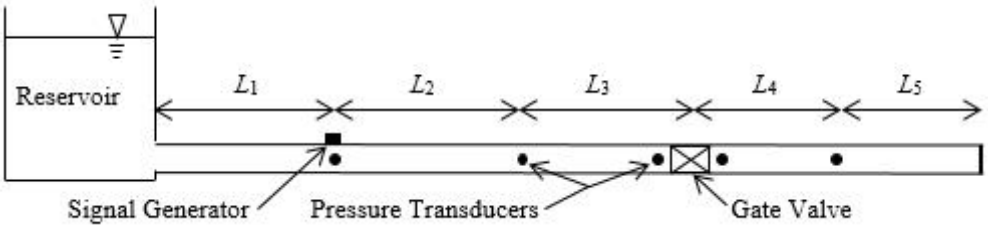

Figure 4-16: Experimental setup for laboratory based transmission tests through a gate valve.

Table 4-1: Experimental system geometry for laboratory based valve transmission tests.

Pipe Section	Length (m)
L_1	14.748
L_2	6.244
L_3	6.241
L_4	6.130
L_5	8.150

Figure 4-17: Vaas gate valve.

Figure 4-18 and Figure 4-19 show the experimental results for signal transmission through the gate valve at varying degrees of closure. To provide a reference point on the figures it can be noted that for the given valve, a valve coefficient of, $C_v\tau$ = 1E-4 corresponds to a flow area reduced to 1% of the pipe area. Figure 4-18 shows the transmission ratios (TR) measured for step signals with an incident wave magnitude, H_W of 1.6 m. The step waves are generated via the valve closure method using a drop weight

mechanism to ensure consistent wave magnitude and closure profile across the data set. Each data point given is calculated from an average of five tests at a given valve position, plotted against the lumped valve coefficient determined from steady state flow analysis. The scatter of the results is very small and follows a well-defined curve. When compared with the numerically determined transmission curve calculated by Equation (4-15), the figure shows that for a step wave signal the transmission is initially affected less by valve position and is more sensitive at smaller openings.

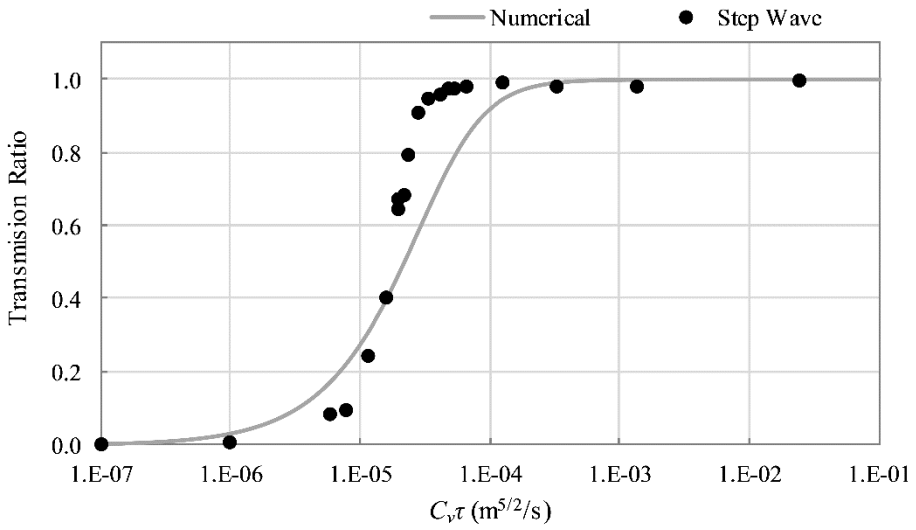

Figure 4-18: Comparison of numerical and experimental transmission ratios (TR) for 1.6 m step waves.

Figure 4-19 shows the transmission ratios (TR') determined from signals generated by the Pipe SONAR system with an average incident wave magnitude, H_W of 0.131 m. The tests implement a large bandwidth randomised time and frequency signal between 100 and 1500 Hz as described in Section 4.3.1. A complementing numerically determined transmission curve is calculated by Equation (4-15) and corrected using Equation (4-17) to account for the transmission analysis being based on analysis of the full wave form. At larger values of TR' the experimentally determined transmission curve over-predicts the lumped valve coefficient which is in contrast to that observed by the larger magnitude step signal. This indicates that the unsteady hydraulic transmission may be less affected by flow changes through the valve than indicated by the steady state flow assumption given by Equation (3-6). Further data sets would be required to definitively determine the cause of the inconsistencies. There is a greater scatter in the results determined from the Pipe SONAR signals than observed in the valve closure signals. This is attributed to the use of a continuous signal in a highly periodic laboratory system, where multiple wave reflections exist causing constructive and destructive interference at measurement

locations. This is somewhat improved by using a wide bandwidth, however is of less concern in field systems where testing distances and signal damping rates are often larger, meaning that interfering reflected signals have a relatively smaller effect. Higher frequency signals were investigated but found to yield erratic results, caused by increasing wave propagation time as the signal frequency is increased.

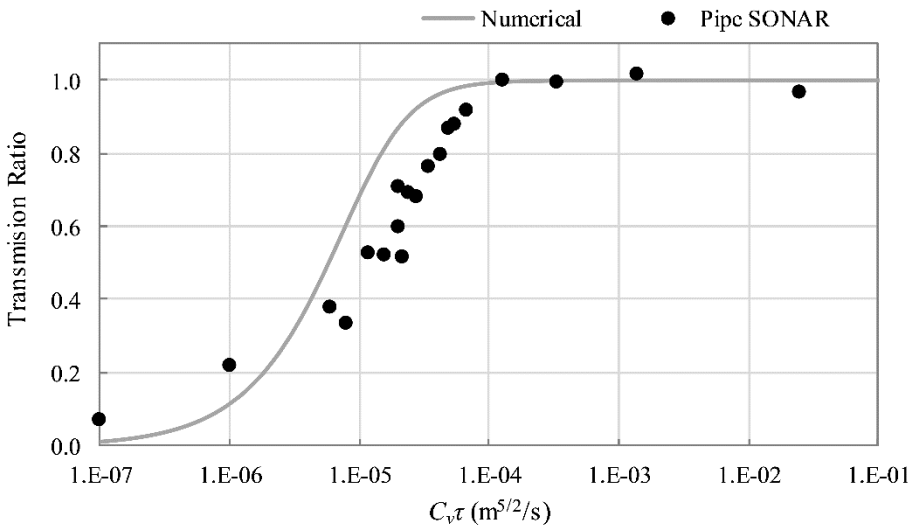

Figure 4-19: Comparison of numerical and experimental transmission ratios (TR') for Pipe SONAR signals between 100 and 1500 Hz .

Based on these two data sets and complementing numerical predictions it is reasonable to assume that the lumped valve coefficient can be determined accurately within an order of magnitude and further validation may improve this.

4.4.3 Field application of valve assessment

The main aim of this field testing program is to test the capability of the Pipe SONAR system to identify poorly-sealed isolating valves. A previous field study has attempted to identify the location of unknown closed valves or valves which have been un-intentionally left closed using transient analysis (Stephens *et al.* 2005a). The results presented here go a step further and target specific valves with a secondary aim of quantifying the valve condition by estimating a lumped valve coefficient and determining the potential for the valve to leak while closed. A total of 800 individual tests were conducted on 13 different valves, spanning six material types and pipe sizes of 100 to 500 mm. The valves were predominantly gate valve types with two butterfly valves on the larger 400 and 500 mm pipes. A selection of the results is discussed in detail in the following section and a full summary of the test sites and the condition of the valves is shown in Table 4-2.

4.4.3.1 Field testing results and verification

To assess the condition of an isolation valve the assessment method described in Section 4.4.1 requires a connection point either side of the valve. The Pipe SONAR equipment is designed to fit serviceable fire hydrants such that the local (signal generating) station is at a hydrant on one side of the valve and the remote station is at another hydrant on the other side of the valve. A Pipe SONAR signal is generated at the local station and measured at the remote station for the valve in a fully open position and set at various degrees of closure. Based on the procedures outlined in Section 4.4.1 the transmission ratios of the hydraulic signals are determined for each of the test sites. For the calculated transmission ratios an estimated lumped loss coefficient is calculated and presented in Table 4-2. A higher lumped loss coefficient indicates a poorly conditioned valve and this can be quantified by determining the expected flow through the valve at a given pressure differential. This can indicate how the valve may behave in situations such as isolating a pipe section for maintenance or repair. To illustrate this an estimated discharge is calculated using Equation (3-6) assuming that each valve is subject to a pressure differential of ΔH = 10 m. Based upon discussions with pipeline system operators a valve assessment is given based on the level of valve sealing that would be sufficient for practical purposes. The given valve assessment may vary given the specific role it plays within a system, though for discussion purposes here a poor condition valve is considered to allow an estimated flow rate in the order of magnitude of 0.01 L/s with an allowance given for large diameter pipelines.

Sites D, G, T, A and E are analysed using the repeating logarithmic chirp signal described in Section 4.3.1 while sites U, R, M and V are analysed with the randomised time and frequency signal. The exceptions to this are sites T and A which consist of PVC pipe which has high signal damping properties and requires a larger piezoelectric actuator than the one currently used in the Pipe SONAR system and site V for which signal transmission was small but measurable for the open valve case, however, signal transmission for the closed valve was inconclusive. For each of these sites, signals generated by rapid valve closure were used.

The poor condition assessment determined for site V was supported by network operators who identified the pipeline as suffering significant degradation. The assessments given for the remaining sites correspond well to the age of the valves with the poor condition valves ranging between 28 and 52 years old. Sites D2 and G are discussed in further detail below.

Table 4-2: Valve assessment summary.

Site Ref.	Material	Pipe Dia. (m)	Valve Type	Install Date	Test Range (m)	TR	$H_{W,Est}$ (m)	$C_v\tau$ ($m^{5/2}/s$)	$Q_{Est}(H=10)$ (L/s)	Valve Assessment
D2	AC	100	Gate	1963	77.5	99%	0.047	1.2E-04	0.369	û
G	CI	100	Gate	1956	68.3	5.6%	0.110	9.7E-07	0.003	ü
T	PVC	100	Gate	2003	80.86	<1%	7.0	<3.4E-06	<0.011	ü*
A2	PVC	100	Gate	2008	105.3	<1%	3.0	<2.5E-06	<0.008	ü*
A1a	PVC	100	Gate	2008	39.7	<1%	3.0	<2.5E-06	<0.008	ü*
A1b	PVC	100	Gate	2008	39.7	<1%	3.0	<2.5E-06	<0.008	ü*
E2a	AC, HDPE	150	Gate	1960s	67.0	33%	0.040	9.9E-06	0.031	û
E2b	AC, HDPE	150	Gate	1960s	67.0	61%	0.018	1.6E-05	0.051	û
E1	AC	150	Gate	1960s	114.0	63%	0.008	1.1E-05	0.036	û
U	S, CIP	200	Gate	1987	81.74	38%	0.003	4.6E-06	0.015	û
R	S	400	Gate	2000	128.53	13%	0.0004	1.9E-06	0.006	ü
M2	DCIP	500	Butterfly	1999	110.88	17%	0.001	5.2E-06	0.016	ü
V	CIP	400	Butterfly	1995	285.71	82%	0.8	1.3E-03	4.038	û*

*Valve assessment result supplemented by low frequency transient signal

4.4.3.2 Example of well-conditioned isolation valve (Site G)

Site G consists of a 100 mm CI pipeline with a gate valve located between two hydrants. This section of pipeline was installed in 1956 and its condition was unknown prior to testing. The distance between the hydrants is 68.3 m and the valve is located 16.4 m from the Pipe SONAR generator. The generated signal repeats every 0.5 seconds and transmission of the signal can be clearly identified by the presence of this pattern in the response function. The amplitude of the repeating pattern provides the strength of the transmitted signal and the severity of the valve leakage.

Figure 4-20 (a, c, e, g) shows the impulse response measured at the remote station when the isolation valve was set to different degrees of closure; from fully open in Figure 4-20(a) through to fully closed in Figure 4-20(g). A dimensionless parameter τ^* indicates the valve position based upon the ratio of number of turns of the valve key open to the number of turns to fully open. The y-axis is the dimensionless impulse response as calculated by Equation (4-1) with the magnitude normalised by the response when the valve was fully open. The strength of the transmitted signal is shown to decrease with the valve closure, and at the fully closed valve position the signal has decreased to 5.6% of the observed transmission strength as when the valve was fully open. Through comparison with the outputs from a method of characteristics model, a lumped loss coefficient is estimated as $C_v\tau$ = 9.7E-7 $m^{5/2}/s$. Based on steady flow considerations a leakage of 3 mL/s could be expected under a pressure head of 10 m, indicating that the valve is well sealed for practical purposes.

To confirm the Pipe SONAR results, low frequency pressure waves are also generated through the closure of a 25 mm ball valve at the local station. The valve closure results are shown in Figure 4-20 (b, d, f, h). The pressure trace at the remote station shows the arrival of the signal at 0.066 s after the creation of the signal at the generator, which corresponds well with the travel time lag observed using the PIPE SONAR system. The closure of the valve resulted in a significant reduction in the size of the wave detected at the remote station, confirming that the valve is well sealed.

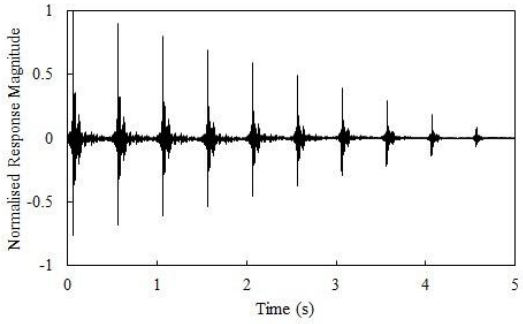

(a)

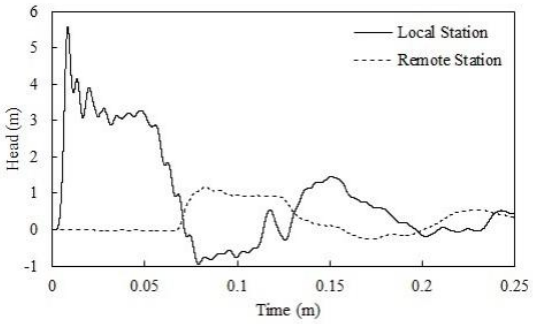

(b)

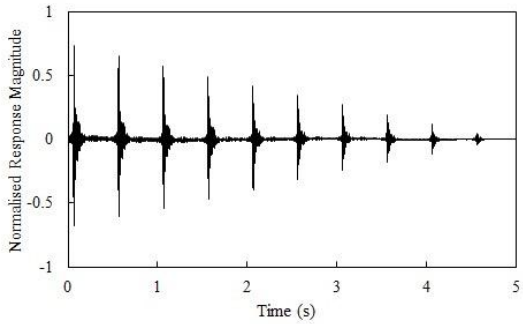

(c)

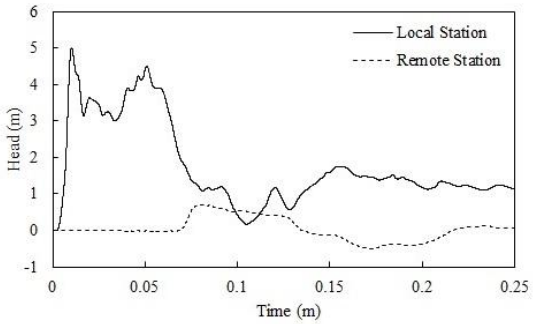

(d)

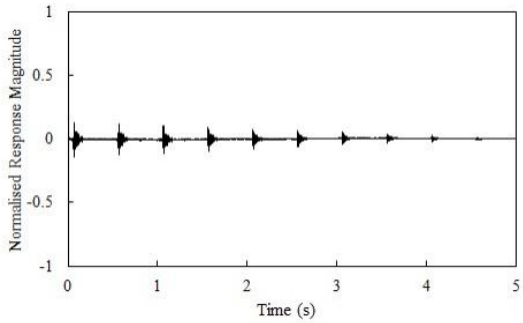

(e)

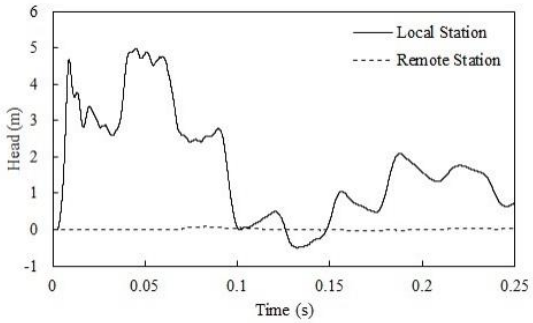

(f)

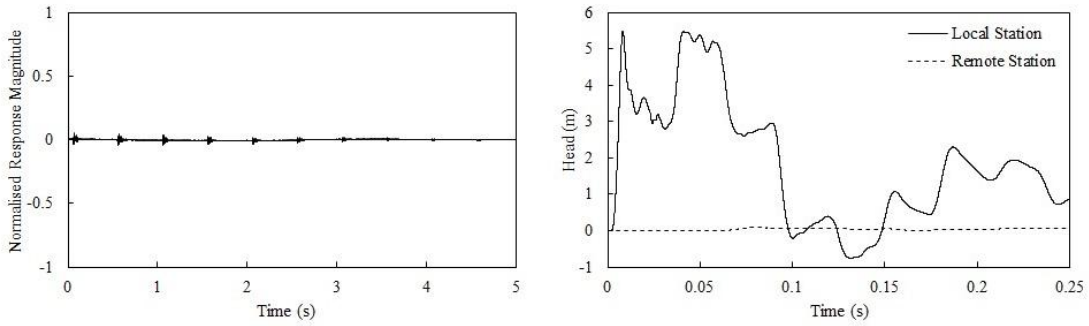

(g) (h)

Figure 4-20: Processed response at the remote station for the (a) open valve (τ* = 1), (c) τ* = 0.1, (e) τ* = 0.05, (g) closed valve (τ* = 0). Measured response for a step wave signal at local and remote stations for an (b) open valve (τ* = 1), (d) τ* = 0.1, (f) τ* = 0.05, (h) closed valve (τ* = 0).

4.4.3.3 Example of poorly-conditioned isolation valve (Site D2)

Site D2 consisted of a 100 mm AC pipeline with an isolation valve located between two hydrants. This section of pipeline was installed in 1963 and its condition was unknown prior to testing. The distance between the hydrants is 77.5 m and the valve is located 64.6 m from the PIPE SONAR generator. Figure 4-21 (a, c) shows the impulse response for the fully open and fully closed isolation valves respectively. The transmission of the signal has suffered only a 1% drop in magnitude with the isolation valve fully closed compared with when the valve is fully open. Similar results for signals created through the rapid closure of a 25 mm ball valve at the generator are shown in Figure 4-21 (b, d). Analysis of the signal transmission through the closed valve indicates a lumped loss coefficient of $C_v\tau$ = 1.2E-4 $m^{5/2}/s$ and based on steady flow considerations a leakage of 0.369 L/s could be expected under a pressure head of 10 m. This indicates that significant hydraulic transmission is occurring through the closed valve and that the valve is in poor condition. The local water asset operations team conducted further section isolation testing of the valve and found the closed valve to be passing water. The valve was subsequently excavated and photos of the valve are shown in Figure 4-22. The valve assembly contains significant tuberculation and the valve was in very poor condition, in line with the assessment found using the Pipe SONAR system.

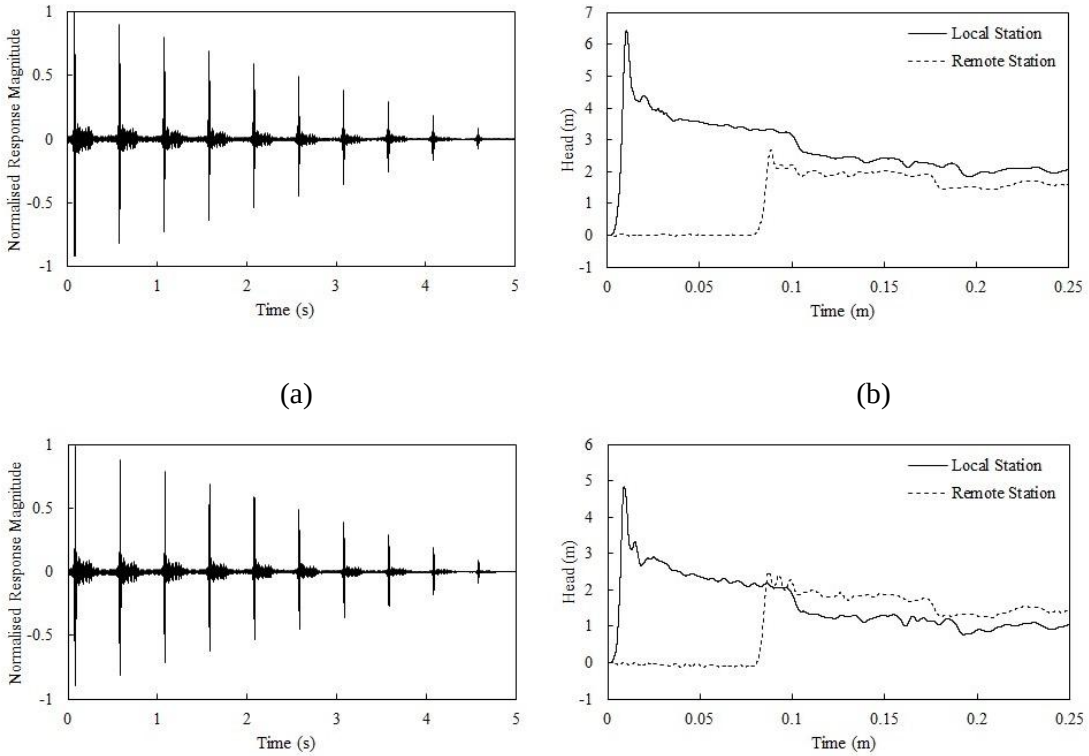

Figure 4-21: Site F2 – (a) Pipe SONAR impulse response function a fully open isolation valve, (b) measured response for a valve closure signal for a fully open isolation valve, (c) Pipe SONAR impulse response function a fully closed isolation valve, (d) measured response for a valve closure signal for a fully closed isolation valve.

Figure 4-22: Internal (a) and external (b) views of the excavated isolation valve at Site D2.

4.5 Assessment of pipeline condition

As a pipeline ages the pipe wall can undergo subtle changes in its material properties. For example, the physical thickness of the pipe wall can change through lining failure and corrosion in steel, CIP and DCIP pipes, while wall material can soften in the case of AC pipes (Bracken and Johnston 2013), or alternatively become increasingly brittle with age in plastic pipes. These physical changes will lead to observable changes in the system wave speed. Where accurate measurements of the wave speed can be determine for a section of pipeline the condition of the pipe can be estimated using theoretical relationships or empirical evidence. Determining pipe wall condition through wave speed analysis is a well-researched field including laboratory and field based studies (Bhimanadhuni 2014, Bracken and Johnston 2013, Carlson *et al*. 2013, Gong *et al*. 2013, Hachem and Schleiss 2012, Liu *et al*. 2012, Nestleroth *et al*. 2012, 2013, Stephens *et al*. 2008, 2013, Tuck and Lee 2013). There are also existing commercial techniques that utilise changes in wave speed for pipeline diagnosis include Echologics' LeakFinderRT™, ePulse™ and SmartBall® PWA systems.

This section investigates the viability of the Pipe SONAR system to be used in wave speed analysis by comparing results with established valve closure methods. Additionally, results are analysed to determine pipeline condition and demonstrate the usefulness of the technology.

4.5.1 Pipeline condition assessment theory

The wave speed within a pipeline is a function of the physical properties of the pipeline and can be an indicator of pipe condition. Equation (4-22) is the equation for wave speed (a) in a pipeline (Parmakian 1955, Wylie and Streeter 1993), which is a function of the pipe effective wall thickness (e), nominal diameter (D), Young's modulus (E), and the fluid bulk modulus (K) and density (ρ). The restraint conditions on the pipe are accounted for by the factor c_1 which is calculated as $c_1 = 1 - \mu^2$ for a fully restrained pipeline, where μ is Poisson's ratio.

$$a = \sqrt{\frac{K/\rho}{1 + [(K/E)(D/e)]c_1}} \tag{4-22}$$

Chapter 3 of this thesis focussed on identifying specific sections of a pipeline that are degraded. The focus in this chapter has shifted to consider the mean conditions along the pipeline assuming that pipe deterioration is evenly distributed between the measurement locations. Where the mean wave speed of a pipe length is known and the original pipe properties are known, remaining wall thickness or reduced materials' moduli can be determined.

4.5.2 Field testing results

Using the Pipe SONAR system the mean wave speed can be determined from the travel time (dt) between the signal generation station and the remote measurement station for a known length of pipe (L).

$$a = \frac{L}{dt} \tag{4-23}$$

The reduction in the pipeline properties can then be determined considering the difference between the measured wave speed and the original wave speed as calculated by Equation (4-22).

The operation of the Pipe SONAR system for wave speed measurement is illustrated in Figure 4-23 using the tests from an 84.5 m stretch of 100 mm diameter asbestos cement pipe and another from a 114.1 m stretch of 300 mm diameter ductile cast iron pipe.

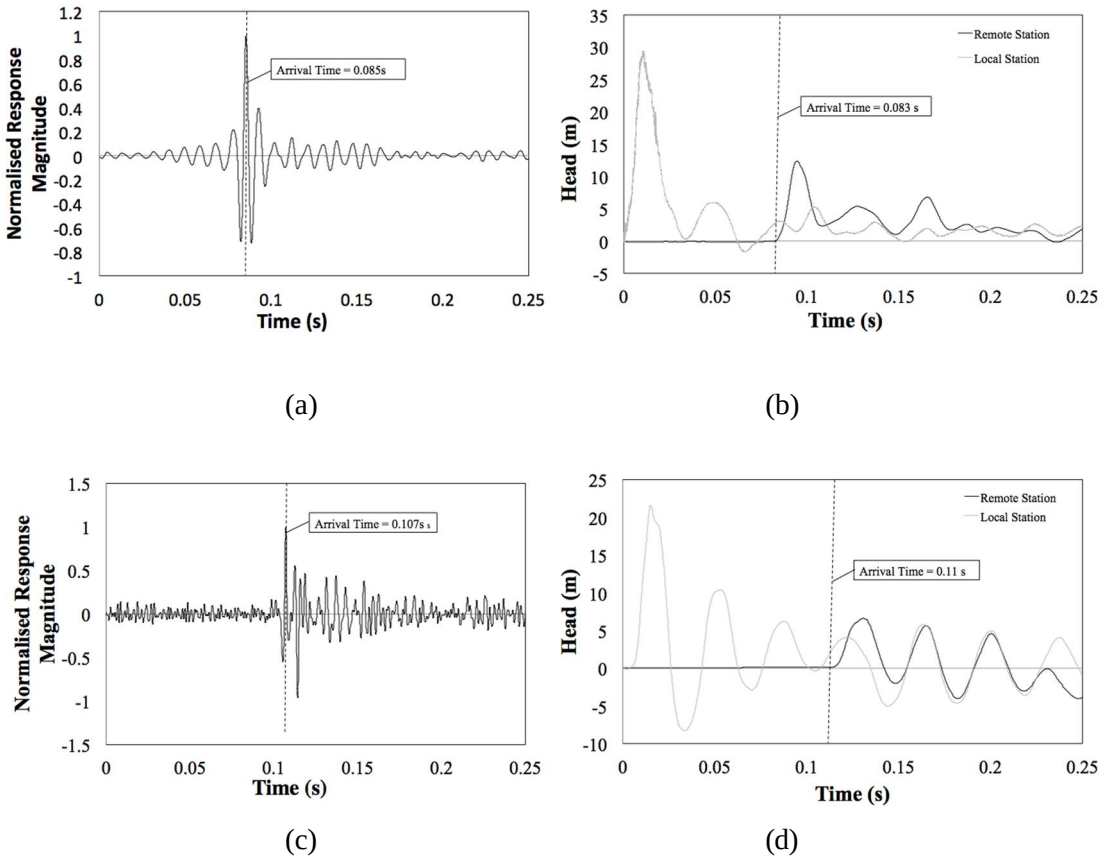

Figure 4-23: Arrival time analyses for an 84.5 m length of 100 mm asbestos cement pipe for (a) Pipe SONAR (b) valve closure methods and arrival time analysis for a 114.1 m length of 300 ductile cast iron pipe using (c) Pipe SONAR and (d) valve closure methods.

Figure 4-23 (a) and (c) show the estimated impulse response functions for the pipelines using the Pipe SONAR system. The cross-correlated response functions are calculated using Equation (4-1) and the measured pressure signals at each station. The y-axis is the dimensionless magnitude of the response function, normalised by the maximum response. Note that the actual value of the response function is not relevant for the applications shown in this paper and the normalising process allows the impulse responses of different pipelines to be directly compared. The Pipe SONAR signal begins transmitting at $t = 0$ and the occurrence time of the signal within the response functions in Figure 4-23 (a) and (c) is the time taken to travel between the local and remote stations. The first impulse in the response function appears with oscillations on either side of the main spike, and is an intrinsic numerical artefact created by the oscillatory chirp signals used in this study. The largest positive spike within the oscillation train is the time of actual transmission of the signal and these are identified as 0.085 s and 0.0107 s for the 100 mm and 300 mm pipes respectively.

To confirm the Pipe SONAR wave speed measurement, a low frequency transient signal was sent from the local station through the manual closure of a 25 mm ball valve and the results are shown in Figure 4-23 (b) and (d). The pressure signals at both the local and the remote stations are shown. The results show a signal transmission time (measured as the time for the remote station to detect a signal) of 0.083 s and 0.011 s for the 100 mm and 300 mm pipes respectively. These transmission times are within 0.3% of the Pipe SONAR measurement and this result confirms the applicability of the Pipe SONAR system for wave speed measurement.

The results of the same wave speed analyses carried out over 25 different sites are summarised in Table 4-3, with the results showing that the Pipe SONAR system produced very similar results to the valve closure tests. The average difference between the Pipe SONAR and manual valve measured wave speed is 0.56%. Each Pipe SONAR result in the table is the measured wave speed at each site repeated over 60 individual tests, with a total of over 1,600 transient tests across the field testing program. It is important to note that the Pipe SONAR system uses a signal that is approximately 0.1 m in pressure head compared to the valve signal, which ranges up to 30 m. The Pipe SONAR system is able to achieve the same outcome as the traditional valve closures but using a signal that is approximately 1% of the valve closure signal magnitude. In addition to this, the tests were conducted without any loss of water, under peak background noise conditions and with no necessary system alterations or pipe isolation.

The condition of each pipe in Table 4-3 is assessed by comparing the measured wave speed with the expected wave speeds for the pipes when they are in perfect condition. This analysis assumes wall thicknesses and diameters that correspond to the manufacturing specifications and the range of expected elastic moduli for the assumed pipe classes. The values for Young's modulus and Poisson's ratio of

each pipe wall material used in this study are presented in Table 4-4. These values use average values measured for various pipe samples taken by the commercial operator of the water networks as well as published ranges in cases where in situ test records are not available. The pipeline condition assessment considers the pipe has deteriorated (represented by a cross in Table 4-3) in cases where the measured wave speed is lower than the expected theoretical range. One of the pipes identified as being of poor condition (pipe "P") was excavated and a material test was conducted at the Veolia material laboratory in Changzhou, China. The results showed extensive and obvious corrosion of the pipe exterior with pitting depth of up to 1.0 mm, confirming the assessment through the Pipe SONAR system (see Figure 4-24). A more detailed approach can be undertaken, in which the effective wall thickness is determined from the measured wave speed using Equation (4-22). The remaining life of the pipe can then be determined through assuming linear deterioration rates from its install date and comparing this with published critical wall thickness values, such as those given by NZWWA (2001) for AC pipe. These methods are common practice in the field of pipeline condition assessment so are not illustrated here.

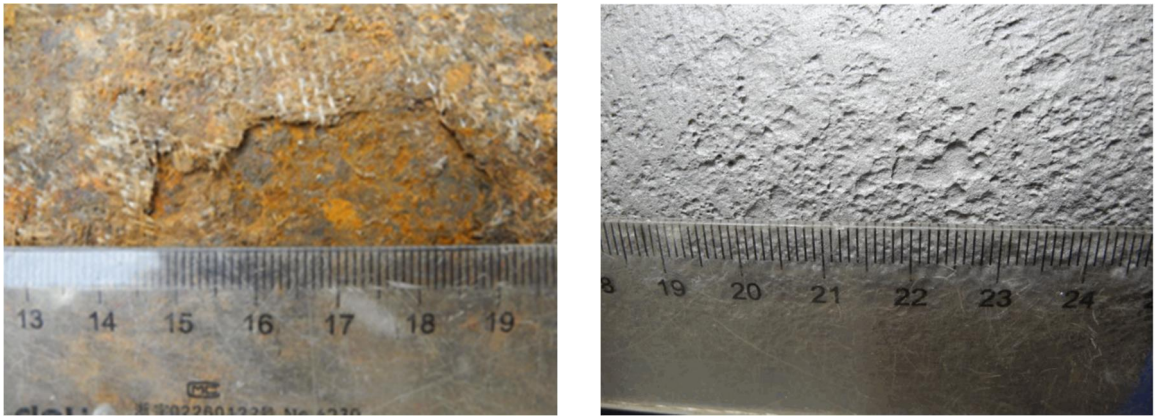

(a) (b)

Figure 4-24: Exterior surface of excavated pipe "P" assessed through Pipe SONAR to be of poor condition (a) exterior coating condition (b) exterior pipe wall condition.

Table 4-3: Wave speed comparisons between signal generation methods and theoretical range.

Site Ref.	Material	Diameter (mm)	Install Date	Length (m)	Wave Speed, Valve (ms^{-1})	Wave Speed, Pipe SONAR (ms^{-1})	Theoretical Wave Speed Range (ms^{-1})	Assessed Condition
A1	PVC	100	2008	39.7	371	375	387 - 460	û
B	AC	100	1971	72.1	1037	1022	1059 - 1070	û
C	AC	100	1981	84.5	1042	1019	1059 - 1070	û
D1	AC	100	1963	128.0	1061	1055	1059 - 1070	û
D2	AC	100	1963	77.5	1001	1002	1059 - 1070	û
E1	AC	150	1960	114.0	1008	997	967 - 978	ü
F1	AC	300	1991	91.2	1074	1073	972 - 984	ü
F2	AC	300	1991	88.7	1054	1044	972 - 984	ü
F3	AC	300	1991	267.1	1054	1055	972 - 984	ü
G	CIP	100	1956	68.3	1102	1079	1311 - 1395	û
H	CIP	100	1956	60.4	1128	1098	1311 - 1395	û
I	CIP	225	1956	201.1	1111	1107	1199 - 1329	û
J	DCIP	100	1992	37.78	1206	1194	1301 - 1349	û
K	DCIP	200	2009	68.71	1233	1231	1188 - 1263	ü
L1	DCIP	300	2013	114.11	1211	1202	1134 - 1215	ü
L2	DCIP	300	2013	118.4	1216	1227	1134 - 1215	ü
L3	DCIP	300	2013	116.34	1227	1224	1134 - 1215	ü
M1	DCIP	500	1999	107.97	1081	1080	1073 - 1155	ü
M2	DCIP	500	1999	110.88	1113	1098	1073 - 1155	ü
N	DCIP	500	1995	56.43	982	978	1073 - 1155	û
O1	DCIP	300	1993	79.21	1194	1204	1134 - 1215	ü
O2	DCIP	300	1993	179.67	1143	1156	1134 - 1215	ü
P	S	100	2009	108.88	1152	1140	1301 - 1323	û
Q	RCP	600	2004	101.59	1183	1147	1148 - 1210	ü
R	S	400	2000	128.53	1248	1264	1181 - 1213	ü
S	S	600	1995	122.12	1183	1181	1112 - 1149	ü

*Sites designated by the same letter indicate adjacent test sections on the same pipeline.

Table 4-4: Pipe material properties.

Material		Young's Modulus (GPa)	Poisson's Ratio
Asbestos Cement	AC	23 – 24	0.3
Cast Iron	CIP	78 – 143	0.22 - 0.3
Ductile Cast Iron	DCIP	160 – 180	0.275
Polyvinyl Chloride	PVC	2.4 – 3.5	0.24
Reinforced Concrete	RCP	30 – 40	0.2
Steel	S	200 – 210	0.3

4.6 Summary

A novel transient signal generation system for pipeline condition assessment has been tested in a detailed field based program. The signal generation system, named Pipe SONAR (PCT/EP2015/059540), offers advantages over existing methods as it has the ability to produce complex signal forms across bandwidths which provided significant tolerance to ambient noise. This enables the system to be used on water distribution networks while they remain fully operational. Implementing complex, long duration signals enables the use of low signal magnitude which significantly reduces the chance of damaging a system during testing, while improving signal repeatability and consistency of results. Further to these advantages the Pipe SONAR system does not require undesirable water discharge during testing. The system was tested in New Zealand and China at 31 sites in four cities, in a field testing program of over 1,600 individual runs. In all tests, the pipeline network was under full operational status and was often applied on main roads close to very heavy traffic. It was confirmed that the Pipe SONAR system does not require any system isolation or traffic diversion and there are no system base flow, topology or pressure requirements. The system easily attaches onto existing hydrants without any physical alteration to the system and is portable.

The Pipe SONAR system was implemented in two pipeline condition assessment methods and comparisons were made with the established valve closure method for transient signal generation. The first is a method to assess valve condition through analysis of signal transmission. Validation of the system and assessment methods was carried out in the laboratory and the field. In the laboratory, the two signal generation and corresponding analysis methods were found to represent the numerical model with similar accuracy. Small discrepancies were observed between experimentally and numerically determined transmission curves, indicating a lumped loss coefficient can be determined within an order of magnitude of that expected by the numerical model, thus suggesting the method is useful for determining valve condition and expected discharge rates. Further investigation would be valuable to look at incorporating models that better account for unsteady flow behaviour through the high loss elements and better quantify the errors. The condition assessment approach is applied to investigate valves in operational water distribution systems at 13 different sites. The assessment method was found to be successful by verification from water system operators and one valve assessed to be in poor condition was excavated and replaced following confirmation of the results.

The second application of the Pipe SONAR system was to identify pipe wall condition through an established method of wave speed analysis. During the field trials 25 pipelines were tested ranging in size from 100 mm to 600 mm and including seven different materials. Comparisons were made between

results from the Pipe SONAR system and conventional valve closure methods and they were found to be comparable. Moreover, the proposed system produced more consistent results while maintaining the advantages outlined previously.

5 CONCLUDING REMARKS

5.1 Overview

The aim of this research was to improve the understanding of fluid transient behaviour in pipelines and apply knowledge for practical use in the field. To achieve this the research was divided into two main components:

1. Laboratory and numerical investigations into the effect that extended faults have on transient behaviour.
2. Developing and testing a new transient generation system for use in the field and applying it for the analysis of in-line valves and pipeline condition through wave speed analysis.

5.1.1 Transient flow modelling for extended faults

Laboratory and numerical investigations demonstrated that the fundamental period of a system is altered when extended variations in the pipe diameter and wave speed occur, creating unique behaviour that can be used to identify and classify extended variations through direct and inverse transient analysis. Extended blockages are shown to impact maximum and minimum pressures observed in a system and combined with deterioration can increase a pipelines vulnerability to failure. Analysis of the experimental data has found that the rate of damping significantly increases in the higher frequency components of the pressure response and that this is under-predicted by numerical models. Consideration of this is important in applying fault detection methods in the field where this behaviour will be amplified due to increased irregularities.

Inverse transient analysis has been applied to detect and classify extended variations in laboratory data through accounting for reductions in wave speed and changes to the nominal diameter from deterioration. Consideration of periodic behaviour is shown to be beneficial in fault detection even when the time domain fit between numerical and experimental results degrades. The investigation showed that decreasing the closure duration of a valve and increasing the bandwidth of the input signal is advantageous for transient based fault detection. This was demonstrated through performing ITA on a pipeline with an extended blockage, with trends showing an improvement in the accuracy of four variables as closure durations decreased and is an important consideration in applying transient analysis in the field.

5.1.2 Development of Pipe SONAR signal generation equipment and application to the field

A new transient signal generation system has been developed and tested in a detailed field based program. The signal generation system is shown to offer advantages over existing methods enabling complex and continuous signals across selected bandwidths, as well as providing significant tolerance to ambient noise. The system has been used on water distribution networks while they remain fully operational, with low amplitude signals which reduce the chance of damaging a system during testing. The system is shown to be more accurate than other signal generation methods while also being desirable for regular application as it does not require undesirable water discharge during testing. The system was implemented for two pipeline condition assessment approaches and tested on 31 separate sites in an international testing program. The first condition assessment approach assessed valve condition through the analysis of signal transmission. Validation of the system and assessment methods was carried out in the laboratory to identify parameter estimation confidence in the field. The condition assessment approach is applied to investigate 13 different valves in operational water distribution systems. Confirmation of assessment results was given by water system operators. The second condition assessment approach was to identify pipe wall condition through an established method of wave speed analysis. Field trials on 25 pipelines ranging in size from 100 mm to 600 mm and including seven different materials were conducted. Comparisons were made between results from the Pipe SONAR system and conventional valve closure methods and they were found to be comparable. Moreover, the proposed system produced more consistent results while maintaining the advantages outlined previously. The results indicate that the technology has practical application and is suitable for use in the field.

5.2 Further research

In this thesis, the effect that extended blockages have on transient behaviour is investigated in the laboratory using an idealised smooth representation. It is recognised that in practice blockages typically contain high degrees of irregularity. Further investigations quantifying the effect that this has on the transient response from experiments on pipes with naturally developed blockages would be beneficial to future field application.

Improvements to the valve assessment approach could be made through incorporating steady state pressure measurements at the generation and measurement stations. This would enable the steady state head loss across the valve to be directly accounted for (as opposed to making a low flow assumption) in the transmission analysis, thus increasing assessment confidence. Note that in networks where multiple flow paths exist the head loss across the valve is not directly related to the flow through the valve, hence these measurements could not substitute the transmission analysis, only seek to improve it. The confidence of valve assessments could be improved with a greater understanding and implementation of energy loss models for unsteady flow through high loss elements. Additionally, assessing the potential for mechanical (non-hydraulic) signal transfer through a closed valve and how this may affect the transmission would be beneficial.

Further research that would benefit the application of the Pipe SONAR equipment for wave speed analysis includes: application of more advanced signal processing techniques for identifying transmitted signals to improve analysis range, and, optimising signal design for use with this system on specific pipe types and sizes.

REFERENCES

Adewumi, M. A., Eltohami, E. S. and Ahmed W. H. (2000). Pressure transients across constrictions. *J. Energy Resources Technology*. 122(1), 34-41.

Adewumi, M. A., Eltohami, E. S. and Solaja, A. (2003). Possible detection of multiple blockages using transients. *J. Energy Resources Technology*. 125(2), 154-159.

Akyildiz, I., Pompili, D. and Melodia, T. (2005). Underwater acoustic sensor networks: research challenges. *Ad Hoc Networks*. 3, 257-279.

AWWA – American Water Works Association (2012). *Buried no longer: confronting America's water infrastructure challenge.* Report.

Baral, M. P., Karney, B. W., Naser, G. and Colombo, A. (2006). An extended 1-D transient corrosion model including multi-component chemical species. *8th Annual Water Distribution Systems Analysis Symposium.* Cincinnati, Ohio USA, August 27-30, 2006. 1-17.

Beck, S. B. M., Williamson, N. J., Sims N. D. and Stanway, R. (2002). Pipeline system identification through cross-correlation analysis. *J. Process Mechanical Eng.* 216(3). 133-142.

Beck, S. B. M., Curren, M. D., Sims, N. D. and Stanway, R. (2005). Pipeline network features and leak detection by cross-correlation analysis of reflected waves. *J. Hydraulic Eng*. 131(8). 715-723.

Bergant, A. and Simpson, A. (1991). Quadratic-equation inaccuracy for water hammer. *J. Hydraulic. Eng.* 117-11, 1572-1574.

Bhimanadhuni, S. (2014). Pilot acoustic condition assessment of water distribution system, Washington Suburban Sanitary Commission (WSSC), Maryland. Case Study: Condition Assessment. Virginia Tech.

Bouchart, F. and Goulter, I. (1991). Reliability improvements in design of water distribution networks recognizing valve location. *Water Resouces. Res*. 27(12), 3029–3040.

Boulos, P. F., Karney, B. W., Wood, D. J. and Lingireddy, S. (2005). Hydrualic transient guidelines for protecting water distribution systems. *J. American Water Works Association.* 111-124.

Bracken, M. and Johnston, D. (2013). Listening for defects, acoustic technologies provide improved condition assessment of asbestos cement water mains. *Municipal Sewer and Water*. March 2013, 18-19.

Brunone, B., and Ferrante, M. (2001). Detecting leaks in pressurised pipes by means of transients. *J. Hydraulic Res*. 39(5), 539-547.

Brunone, B., Ferrante, M. and Meniconi, S. (2008a). Discussion of "Detection of partial blockage in single pipelines" by P. K. Mohapatra, M. H. Chaudhry, A. A. Kassem, and J. Moloo. *J. Hydraulic Eng*. 872-874.

Brunone, B., Ferrante, M. and Meniconi, S. (2008b). Portable pressure wave-maker for leak detection and pipe system characterization. *American Water Works Association.* 100(4), 108-116.

BS EN 805:2000 (2000). *Water Supply – requirements for systems and components outside buildings.*

Bullen, P. R., Cheeseman, D. J., Hussain, L. A. and Ruffell, A. E. (1987). The determination of pipe contraction pressure loss coefficients for incompressible turbulent flow. *Int J. Heat and Fluid Flow.* 8(2), 111-118.

Canadian Energy Pipeline Association (CEPA) (2016). *Pipeline Industry Performance Report*. Calgary, Alberta.

Carlson, M., Henke, J., Duppong, J. and Buonadonna, D. (2013). Drinking water pipeline condition assessment. *AWWA Conf. Spokane.* WA. 10th May.

Chen, L. C. (1995). Pipe network transient analysis – the forward and inverse problems. *PhD Dissertation.* Cornell University, USA.

Chopra, I. (2002). Review of state of art of smart structures and integrated systems. *AIAA Journal.* 40(11), 2145-2187.

Colombo, A.F., Lee, P.J. and Karney, B.W. (2009). A selective literature review of transient-based leak detection methods. *J. Hydro-Environment Res.* 2(4), 212-227.

Contractor, D. N. (1965). The reflection of waterhammer pressure waves from minor losses. *J. Basic Engineering.* 445-452.

Covas, D., Ramos, H., Brunone, B., and Young, A. (2004). Leak detection in water trunk mains using transient pressure signals: Field tests in Scottish water. *The practical application of surge analysis for design and operation. 9th Int. Conf. on Pressure Surges*, S. J. Murray, ed., Vol. I, BHR Group, Bedfordshire, U.K., 185–198.

Covas, D., Ramos, H. and Almeida, B. (2005). Standing wave difference method for leak detection in pipeline systems. *J. Hydraulic Eng.* 1106-1116.

Daily, J. W., Hankey, W. L. Olive, R. W. and Jordaan, J. M. (1956). Resistance coefficients for accelerated and decelerated flows through smooth tubes and orifices. *Trans. ASME,* 78, 1071-1077.

Davis, P., Magnus, M., Gould, S. and Burn, S. (2008). Failure prediction and optimal scheduling of replacements in asbestos cement water pipes. *J. of Water Supply: Research and Technology – AQUA.* 57(4), 239-252.

De Salis, M. H. F and Oldham, D. J. (2001). The development of a rapid single spectrum method for determining the blockage characteristics of a finite length duct. *J. Sound and Vibration.* 243(4), 625-640.

Duan, H. F., Lee, P. J., Ghidaoui, M. S. and Trung, Y. K. (2011a). Leak detection in complex series pipelines by using the system frequency response method. *J. Hydraulic Res.* 49(2), 213-221.

Duan, H. F., Lu, J. L., Kolyshkin, A. A. and Ghidaoui, M. S. (2011b). The effect of random inhomogeneities on wave propagation in pipes. *Proc. 34th IAHR Congress.* Brisbane, Australia, 26 June – 1 July 2011, 2273-2280.

Duan, H. F., Lee P. J., Ghidaoui M. S., and Tung Y. K. (2012a). Extended blockage detection in pipelines by using the system frequency response analysis. *J. Water Resour. Planning and Management.* 138(1), 55-62.

Duan, H., Lee, P., Ghidaoui, M. and Tung, Y. (2012b). System response function-based leak detection in viscoelastic pipelines. *J. Hydraulic Research.* 138(2), 143-153.

Duan, H. F., Ghidaoui, M. S., Lee, P. J. and Tung, Y. K. (2012c). Relevance of unsteady friction to pipe size and length in pipe fluid transients. *J. Hydraulic Eng*, 138-2, 154-166.

Duan, H., Lee, P., Kashima, A., Lu, J., Ghidaoui, M. and Tung, Y. (2013). Extended blockage detection in pipes using the system frequency response: Analytical analysis and experimental verification. *J. Hydraulic Eng.* 139(7), 763-771.

Echo Logics (2016). Retrieved from http://www.echologics.com/

Federation of Canadian Municipalities (FCM) (2003). Deterioration and inspection of water distribution systems. *A best practice by the national guide to sustainable municipal infrastructure.* April 2003, Issue No. 1.1.

Ferrante, M. and Brunone, B. (2003). Pipe system diagnosis and leak detection by unsteady-state tests-2, Wavelet analysis. *Adv. Water Res.* 26, 107-116.

Ferrante, M., Brunone, B., and Meniconi, S. (2009). Leak detection in branched pipe systems coupling wavelet analysis and a Lagrangian model. *J. Water Supply Res. Technol*. AQUA, 58(2), 95–106.

Fishler, E., Haimovich, A., Blum, R., Chizhik, D., Cimini, L. and Valenzuela, R. (2004). MIMO radar: an idea whose time has come. *Radar Conference, 2004. Proc. IEEE*. 26-29 April 2004, 71-78.

Forsythe, G. E. (1970). Pitfalls in computation, or why math book isn't enough. *Am. Math. Monthly.* 77-9, 931-956.

Gasmelseid, T.M. (2010). *Handbook of research on hydroinformatics: technologies, theories and applications.* Idea Group Inc, USA.

Genovese, M. (2016). Ultrasound Transducers. *Journal of Diagnostic Medical Sonography*. 32(1), 48-53.

Ghidaoui, M. S. and Karney, B. W. (1994). Equivalent differential equations in fixed-grid characteristics method. *J. Hydraulic Eng*. 120(10), 1159-1175.

Ghidaoui, M. S. and Karney, B. W. (1998). Energy estimates for discretization errors in water hammer problems. *J. Hydraulic Eng*. 124(4), 384-393.

Ghidaoui, M. S. and Mansour, S. (2002). Efficient treatment of the Vardy-Brown unsteady shear in pipe transients. *J. Hydraulic Eng.*, 128-1, 102-112.

Ghidaoui, M. S., Zhao, M., McInnis, D. A. and Axworthy, D. H. (2005). A review of water hammer theory and practice. *Applied Mechanics Reviews*. ASME. 58, 49-76.

Gong, J., Lambert, M. F., Simpson, A. R., Zecchin, A. C., Kim, Y. and Tijsseling, A. S. (2013). Detection of distributed deterioration in single pipes using transient reflections. *J. of Pipeline Syst. Eng. and Pract.* 4(1), 32-40.

Guo, W., Soibelman L. and Garrett J. H. Jr. (2009). Automated defect detection for sewer pipeline inspection and condition assessment. *Automation in Construction.* 18, 587–596.

Hachem, F. E. and Schleiss, A. J. (2012). Detection of local wall stiffness drop in steel-lines pressure tunnels and shafts of hydroelectric power plants using steep pressure wave excitation and wavelet decomposition. *J. Hydraulic Eng.* 138(1), 35-45.

Haqshenas, S. R. (2010). Leak detection in plastic water pipe using pulse-echo method. *Master's Thesis in Sound and Vibration.* Department of Civil and Environmental Engineering, Chalmers University of Technology, Goteborg, Sweden.

Heutschi, K. and Rosenheck, A. (1997). Outdoor sound propagation measurement using an MLS technique. *Applied Acoustics*. 51(1), 13-32.

Jiang, Y., Chen, H., and Li, J. (1996). Leakage and blockage detection in water network of district heating system. *ASHRAE Transactions.* 102(1), 291-196.

Jun, H., Loganathan, G., Deb, A., Grayman, W., and Snyder, J. (2007). Valve distribution and impact analysis in water distribution systems. *J. Environ. Eng*. 133(8), 790-799.

Jung, B. S. and Karney, B. W. (2004). Fluid transients and pipeline optimization using GA and PSO: the diameter connection. *Urban water Journal*. 1-2, 167-176.

Kagawa, T., Lee, I., Kitagawa, A. and Takenaka, T. (1983). High speed and accurate computing method of frequency-dependent friction in laminar pipe flow for characteristic methods. *Trans. Japanese Soc. Mech. Engineers*. 49-447, 2638-2644.

Kapelan, Z. S., Savic, D. A. and Walters, G. A. (2003). A hybrid inverse transient model for leakage detection and roughness calibration in pipe networks. *J. Hydraulic Research*. IAHR 41 (5), 481-492.

Kapelan, Z. S., Savic, D. A. and Walters, G. A. (2004). Incorporation of prior information on parameters in inverse transient analysis for leak detection and roughness calibration. *Urban Water Journal.* 129-143. 1-2 June.

Karney, B. W. and Ghidaoui, M. S. (1997). Flexible discretization algorithm for fixed-grid MOC in pipelines. *J. Hydraulic Eng.* 123(11), 1004-1011.

Karney, B. W., Tang, K., Papa, F., Eerkes, E., and Welker, R. (2007). Field application of inverse transient analysis to calibrate London's water distribution system model. *Joint Ontario Water Works Association (OWWA) and Ontario Municipal Water Association (OMWA) Conference.* Collingwood, Ontario, May 2007.

Karney, B. W., Parente, A., Eerkes, E., and White, C. (2008). Assessing the performance of a water transmission system using an inverse transient method. *Annual ASCE International Pipelines Conference.* Atlanta, Georgia, USA, July 2008.

Karney, B. W., and Radulj, D. (2009). Transient field monitoring as a key driver for decision making and design. *Proc. 33rd IAHR Congress: Water Engineering for a Sustainable Environment*, Vancouver, BC, Canada, August 2009.

Kashima, A., Lee, P. J., Ghidaoui, M. S., Davidson, M. (2013). Experimental verification of the kinetic differential pressure method for flow measurements. *J. Hydraulic Res*. 51(6) 634-644.

Katzir, S. (2012). Who knew piezoelectricity? Rutherford and Langevin on submarine detection and the invention of SONAR. *The Royal Society*. 66, 141-157.

Kilfoyle, D. and Baggeroer, A. (2000). The state of the art in underwater acoustic telemetry. *Journal of Oceanic Engineering.* 25(1), 4-27.

Kim, Y. I. (2008). Advanced numerical and experimental transient modelling of water and gas pipeline flows incorporating distributed and local effects. *Phd Dissertation.* University of Adelaide, Australia.

Klauder, J. R., Price, A. C., Darlington, S. and Albersheim, W. J. (1960). The theory and design of chirp radars. *Bell System Technical Journal*. 39(4), 745-808.

Kokossalakis, G. (2006). Acoustic data communications system for in-pipe wireless sensor networks. *PhD Thesis*. Civil and Environmental Engineering, Massachusetts Institute of Technology.

Lee, P. J. (2005). Using system response functions of liquid pipelines for leak and blockage detection. *PhD Thesis*. School of Civil and Environmental Engineering, University of Adelaide, Australia.

Lee, P. (2015). Flow rate determination method and apparatus. Patent No. 618705, New Zealand.

Lee, P., Vítkovský, J., Lambert, M., Simpson, A., and Liggett, J. (2004). Experimental validation of frequency response coding for the location of leaks in single pipeline systems. *The practical application of surge analysis for design and operation, 9th international conference on pressure surges*. BHR Group. Chester, UK, 24 – 26 March 2004, 239 – 253.

Lee, P. J., Vítkovský, J. P., Lambert, M. F., Simpson, A. R. and Liggett, J. A.. (2005). Leak location using the pattern of the frequency response diagram in pipelines: A numerical study. *Journal of Sound and Vibration.* Vol. 284. pp 1051-1073.

Lee P., Vítkovský J., Lambert M., Simpson A., Liggett, J. (2006). Experimental verification of leak detection in pipelines using linear transfer functions. *J. Hydraulic Res*. 44(5), 693-707.

Lee, P. J., Vítkovský, J. P., Lambert, M. F., Simpson, A. R., and Liggett, J. A. (2007). Leak location in pipelines using the impulse response function. *J. Hydraulic. Res*. 45(5), 643-652.

Lee, P. J., Vítkovský, J. P., Lambert, M. F., Simpson, A. R. and Liggett, J. A. (2008a). Discrete blockage detection in pipelines using the frequency response diagram: Numerical study. *J. Hydraulic Eng*. 134(5), 658-663.

Lee, P. J., Vítkovský, J. P., Lambert, M. F. and Simpson A. R. (2008b). Valve design for extracting response function from hydraulic systems using pseudorandom binary signals. *J. Hydraulic Eng*. 135(6). 858-864.

Lee, P. J., Duan, H. F., Tuck, J. and Ghidaoui, M. (2015). Numerical and experimental study on the effect of signal bandwidth on pipe assessment using fluid transients. *J. Hydraulic Eng*. 141(2), 04014074.

Liggett, J. A. and Chen, L-C. (1994). Inverse transient analysis in pipe networks. *J. Hydraulic Eng.* ASCE 120 (8), 934-955.

Liu, Henry. (2003). *Pipeline Engineering.* CRC Press LLC, Corporate Blvd, Boca Raton, Florida.

Liu, L., Zhou, S. and Cui, J. (2008). Prospects and problems of wireless communication for underwater sensor networks. *Wirel. Commun. Mob. Comput*. 8, 977-994.

Liu, Z., Kleiner, Y., Rajani, B., Wang, L. and Condit, W. (2012). Condition assessment technologies for water transmission and distribution systems. *Report Contract No. EP-C-05-057 Task Order No. 0062*, National Risk Management Research Laboratory Office of Research and Development, U.S. Environmental Protection Agency Cincinnati, OH 45268.

Manbachi, A. and Cobbold, R. (2011) Development and application of piezoelectric materials for ultrasound generation and detection. *Ultrasound*. 19-4, 187-196.

Marlow, D., Heart, S., Burn, S., Urquhart, A., Gould, S., Anderson, M., ... & Fitzgerald, A. (2007). Condition assessment strategies and protocols for water and wastewater utility assets. *Water Environment Research Foundation (WERF): Alexandria*. VA and IWA Publishing: London, United Kingdom.

Medwin, H. and Clay, C. (1998). *Fundamentals of Acoustical Oceanography*. Academic Press, London.

Meniconi, S., Brunone, B., Ferrante, M., and Massari, C. (2011a). Small amplitude sharp pressure waves to diagnose pipe systems. *Water Res. Management*. 25(1), 79-96.

Meniconi, S., Brunone, B., Ferrante, M. and Massari, Christian, M. (2011b). Potential of transient tests to diagnose real supply pipe systems: what can be done with a single extemporary test. *Water Resources Planning and Management*. 137-2, 238-241.

Meniconi, S., Brunone, B., and Ferrante, M. (2011c). In-line pipe device checking by short period analysis of transient tests. *J. Hydraulic Eng*. 137(7), 713-722.

Meniconi, S., Brunone, B., Ferrante, M., and Massari, C. (2012a). Transient hydrodynamics of in-line valves in viscoelastic pressurised pipes. Long period analysis. *Exp. Fluids*. 53(1), 265-275.

Meniconi, S., Brunone, B., and Ferrante, M. (2012b). Water hammer pressure waves at cross-section changes in series in viscoelastic pipes. *J. Fluids and Structures*. 33, 44-58.

Mermelstein, P. (1967). Determination of the vocal-tract shape from measured formant frequencies. *The J. the Acoustical Society of America*. 41(5), 1283-1294.

Misiunas, D., Simpson, A.R., Lambert, M.F. and Olsson, G. (2005). Hydraulic transients for diagnosis of inline valves in water transmission pipelines. *Conference on Computing and Control for the Water Industry (CCWI 2005)*. Exeter, UK, 5–7 September.

Mohapatra P. K., Chaudhry M. H., Kassem A. and Moloo J. (2006a). Detection of partial blockages in a branched piping system by the frequency response method. *J. Fluids Engineering*, Transactions of the ASME, 128(5), 1106-1114.

Mohapatra, P. K., Chaudhry, F., Kassem, A. A. and Moloo, J. (2006b). Detection of partial blockage in single pipelines. *J. Hydraulic Eng.* 200-206.

Nash, G. A. and Karney, B. W. (1999). Efficient inverse transient analysis in series pipe systems. *J. Hydraulic Eng.* 125-7, 761-764.

Nestleroth, B., Flamberg, S., Condit, W., Battelle J. M. and Wang L. (2012). Field demonstration of innovative condition assessment technologies for water mains: leak detection and location. *National Risk Management Research Laboratory Office of Research and Development.* U.S. Environmental Protection Agency Cincinnati, Ohio 45268.

Nestleroth, B., Flamberg, S., Lal, V., Condit, W., Battelle, J. M., Chen, A. and Wang, L. (2013). Field demonstration of innovative condition assessment technologies for water mains: acoustic pipe wall assessment, internal inspection, and external inspection. *National Risk Management Research Laboratory Office of Research and Development.* U.S. Environmental Protection Agency Cincinnati, Ohio 45268.

New Zealand Government (2010). *National Infrastructure Plan.* March 2010, Part 3 – Facts and Issues, Sectoral Analysis, Drinking Water (pp 115-118).

Niezrecki, C., Brei, D., Balakrishnan, S., and Moskalik, A. (2001). Piezoelectric actuation: State of the art. *Shock and Vibration Digest*. 33(4), 269-280.

NZS 4404:2010. *Land Development and Subdivision Infrastructure*. New Zealand Standard, Chapter 6 - Water Supply.

NZWWA - New Zealand Water and Wastes Association (2001). *New Zealand Asbestos Cement Watermain Manual*. Prepared by: Opus International Consultants, Aug 2001.

OHCHR. (2010). *(The) Right to Water. Fact Sheet No. 35*. United Nations, Office of the High Commissioner for Human Rights (OHCHR). United Nations Human Settlements Programme (UN-Habitat), World Health Organization (WHO).

Park, G., Sohn, H., Farrar, C. and Inman, D. (2003). Overview of piezoelectric impedance-based health monitoring and path forward. *The Shock and Vibration Digest*. 35(6), 451-463.

Parmakian, J. (1955). *Water-Hammer Analysis*. Prentice-Hall Englewood Cliffs.

Paulo, J. P., Martins, C. R. and Bento Coelho, J. L. (2009). A hybrid MLS technique for room impulse response estimation. *Applied Acoustics*. 70(4), 556-562.

Prenner, R. K. (2000). Calculation of the transient response of small in-line orifices in a straight pipe. *Proc. 4th Int. Conf. Hydrodynamics.* Yokohama, Japan, 405-410.

Proakis, J., Sozer, E., Rice, J. and Stojanovic, M. (2001). Shallow water acoustic networks. *IEEE Communications Magazine*. Nov., 114-119.

Pudar, R.S. and Liggett, J.A. (1992). Leaks in pipe networks. *J. Hydraulic Eng*. 118(7), 1031-1046.

Pure Technologies (2016). Retrieved from http://www.puretechltd.com/

Qunli, W. and Fricke, F. (1991). Determination of the size of an object and its location in a rectangular cavity by Eigen frequency shifts: first order approximation. *J. Sound and Vibration.* 144(1), 131-147.

Ranjani, B., Kleiner, Y., and Sadiq, R. (2006). Translation of pipe inspection results into condition ratings using the fuzzy synthetic evaluation technique. *J. Water Supply Res. and Tech.* 55-1, 11-24.

Richards, Mark A. PhD (2014). *Fundamentals of Radar Signal Processing, Second Edition*. McGraw-Hill Professional.

RIO+20 United Nations Conference on Sustainable Development (2012*). Agenda item 10, Outcome of the Conference. The Future We Want*. Rio de Janeiro, Brazil, 20-22 June 2012.

Rizzo, P. (2010). Water and wastewater pipe non-destructive evaluation and health monitoring: a review. *Advances in Civil Engineering*, 2010, 1-13. Doi:10.1155/2010/818597

Sattar, A. M., Chaudry, M. H. and Kassem, A. A. (2008). Partial blockage detection in pipelines by frequency response method. *J. Hydraulic Eng.* 134, 76-89.

Savic, D. A. and Walters, G. A. (1999). Hydroinformatics, data mining and maintenance of UK water networks. *Anti-Corrosion Methods and Materials*. 46-6, 415-425.

Schroeder, M. R. (1967). Determination of the geometry of the human vocal tract by acoustic measurements. *The J. the Acoustical Society of America.* 41(4-2), 1002-1010.

Scott, S. L., and Satterwhite, L. A. (1998). Evaluation of the back pressure technique for blockage detection in gas flowlines. *J. Energy Resources Technology.* ASME, 120, 27-31.

Sibertheros, I. A., Holley, E. R. and Branski, J. M. (1991). Spline Interpolations for Water Hammer Analysis. *J. Hydraulic Eng.* ASCE, 117(10), 1332-1351.

Silva, R. A., Buiatti, C. M. Cruz, S. L. and Pereira, J. (1996). Pressure wave behaviour and leak detection in pipelines. *6th European Symposium on Computer Aided Process Engineering*, Rhodes Greece. Part A, S491-S496.

Stephens, M. (2008). Transient response analysis for fault detection and pipeline wall condition assessment in field water transmission and distribution pipelines and networks. *PhD Thesis.* School of Civil and Environmental Engineering. The University of Adelaide. Australia.

Stephens, M. L., Simpson, A. R., Lambert, M. F., Vítkovský, J. P. and Nixon, J. B. (2002). The detection of pipeline blockages using transients in the field. *Australian Water Association SA Branch Regional Conf.* Adelaide Australia. 5th July, 1-8.

Stephens, M. L., Lambert, M. F., Simpson, A. R., Vítkovský, J. P. and Nixon, J. B. (2004a). Field tests for leakage, air pocket and discrete blockage detection using inverse transient analysis in water distribution pipes. *2004 World Water and Environmental Resources Congress.* EWRI, ASCE, 27 June-1 July, Salt Lake City, Utah, USA.

Stephens, M. L., Vítkovský, J.P., Lambert, M. F., Simpson, A. R., Karney, B. and Nixon, J. B. (2004b). Transient analysis to assess valve status and topology in pipe networks. *9th International Conference on Pressure Surges*. BHR Group, Chester, UK, 211-224.

Stephens, M. L., Lambert, M. F., Simpson, A. R., Vítkovský, J. P. and Nixon, J. B. (2005a). Using field measured transient responses in a water distribution system to assess valve status and network topology. *7th Annual Symposium on Water Distribution Systems Analysis.* ASCE, 15-19 May, Anchorage, Alaska, USA.

Stephens, M. L., Lambert, M. F., Simpson, A. R., Nixon, J. B. and Vítkovský, J. P. (2005b). Water pipeline condition assessment using transient response analysis. *Proc. 47th Conf. New Zealand Water and Wastes Association.* Auckland New Zealand, 1-21.

Stephens, M. L., Lambert, M. F., Simpson, A. R. and Vítkovský, J. P. (2005c). Field measurements of unsteady friction effects in a trunk transmission pipeline. *7th Annual Symposium on Water Distribution Systems Analysis*, ASCE, 15-19 May, Anchorage, Alaska, USA.

Stephens, M. L., Simpson, A. R. and Lambert, M. F. (2008). Internal wall condition assessment for water pipelines using inverse transient analysis. *Pro. 10th Annual Symp. On Water Distribution Systems Analysis*, ASCE, Reston, VA. 1-11.

Stephens, M., Lambert, M., and Simpson, A. (2013). Determining the internal wall condition of a water pipeline in the field using an inverse transient. *J. Hydraulic Eng*. 139(3), 310-324.

Stoianov, I., Dellow, D., Maksimovi, C. and Graham, N. (2003). Field validation of the application of hydraulic transients for leak detection in transmission pipelines. *Proceedings of the CCWI Advances in Water Supply Management Conference.* London, UK.

Tafuri, A. (2000). Locating leaks with acoustic technology. *Journal of AWWA*. 92(7), 57 – 66.

Trikha, A.K. (1975). An efficient method for simulating frequency-dependent friction in transient liquid flow. *ASME J. Fluids Eng.* 97-1, 91-105.

Tuck, J., Lee, P., Kashima, A., Davidson, M. and Ghidaoui, M. S. (2012). Transient analysis of extended blockages in pipeline systems. *11th Int. Conf. on Pressure Surges*, BHR Group, Lisbon, Portugal, 24-26 October, 2012, 101-112.

Tuck J. and Lee P. (2013). Inverse transient analysis for classification of wall thickness variations in pipelines. *Sensors.* 13(12), 17057-17066.

Tuck, J., Lee, P. L., Davidson, M. and Ghidaoui, M. S. (2013). Analysis of transient signals in simple pipeline systems with an extended blockage. *J. Hydraulic Research.* 51(6), 623-633.

Vardy, A. E. and Brown, J. M. B. (1997). Discussion on wall shear stress in accelerating and decelerating pipe flow. *J. Hydraulic Res.*, 35-1, 137-139.

Vardy, A. E. and Brown, J. M. B. (2003). Transient turbulent friction in smooth pipe flows. *J. Sound and Vibration.* 259(5), 1011-1036.

Vardy, A. E. and Brown, J. M. B. (2004). Transient turbulent friction in fully rough pipe flows. *J. Sound and Vibration*, 270, 233-257.

Vaseghi, S. V. (1996). *Advanced signal processing and digital noise reduction.* Wiley and Teubner, Chichester, West Sussex, England.

Vítkovský, J. P., Simpson, A. R. and Lambert, M.F. (2000). Leak detection and calibration using transients and genetic algorithms. *J. Water Res. Planning and Management*. 126-4, 262-265.

Vítkovský, J. P., Simpson, A. R. and Lambert, M. F. (2002). Minimization algorithms and experimental inverse transient leak detection. *1st Annual Enviromental & Water Resources Systems Analysis Symp. In conjunction with ASCE Eviromental & Water Resources Institute Annual Conference*. 19-22 May, Roanoke, Virginia, USA. 1-10.

Vítkovský, J. P., Lee, P. J., Stephens, M. L., Lambert, M. F., Simpson, A. R. and Liggett, J. A. (2003a). Leak and blockage detection in pipelines via an impulse response method. *Pumps, Electromechanical Devices and Systems Applied to Urban Water Management, Volume I, E*. Cabrera and E Cabrera Jr. (eds), 22-25 April, Valencia, Spain, 423-430.

Vítkovský, J. P., Liggett, J. A., Simpson, A. R. and Lambert, M. F. (2003b). Optimal measurement site locations for inverse transient analysis in pipe networks. *J. Water Res. Planning and Management.* 129-6, 480-492.

Vítkovský, J. P., Stephens, M. L., Bergant, A., Lambert, M. F., and Simpson, A. R. (2004). Efficient and accurate calculation of Zielke and Vardy-Brown unsteady friction in pipe transients. *9th Int. Conf. on Pressure Surges*, BHR Group, Chester, UK, 24-26 March, 2004, 405-419.

Vítkovský, J., Bergant, A., Simpson, A.R. and Lambert, A. (2006). Systematic evaluation of one-dimensional unsteady friction models in simple pipelines. *J. Hydraulic Eng.* 132-7, 696-708.

Walski, T. M. (1993). Water distribution valve topology for reliability analysis. *Reliability Engineering and System Safety*. 42, 21-27.

Wang, X. J. (2002). Leakage and blockage detection in pipelines and pipe network systems using fluid transients. *PhD Thesis*. School of Civil and Environmental Engineering. The University of Adelaide. Australia.

Wang, X. J., Lambert, M. F., Simpson, A. R., Liggett, J. A. and Vítkovský, J. P. (2002). Leak detection in pipelines using damping of fluid transients. *J. Hydraulic Eng.* 2002, 697-711.

Wang, X. J., Hayde, P., Ellis, D. and Crawley, P. (2005a). Pipe diameter reduction due to aging and biofilm developments: Implication to system design and operation. *Tonkin Consulting*, Paper Number o5155.

Wang, X. J., Lambert, M. F. and Simpson, A. R. (2005b). Detection and location of a partial blockage in a pipeline using damping of fluid transients. *J. Water Resources Planning and Management.* 2005, 244-249.

Washio, S., Konishi, T., Nishii, K. and Tanaka, A. (1982). Research on wave phenomena in hydraulic lines. 10th report, experimental discussion on unsteady nonlinearity of orifice flows, *Bulletin of the JSME.* 25(210-9), 1914-1920.

Washio, S., Takahashi, S., Yu, Y. and Yamaguchi, S. (1996). Study of unsteady orifice flow characteristics in hydraulic oil lines. *J. Fluids Eng.* 118, 743-748.

Wylie, E. B. and Streeter, V. L. (1993). *Fluid Transients in Systems.* Prentice Hall, Upper Saddle River, New Jersey, USA.

Zielke, W. (1968). Frequency-dependent friction in transient pipe flow. *Journal of Basic Engineering.* ASME, March 1968, 109-115.

APPENDIX A – SIGNAL TRANSMISSION CHARACTERISTICS THROUGH VALVES

Based on Equation (4-14) as the pressure differential across a valve is increased the transmission through the valve will decrease, and similarly Wylie and Streeter (1993) noted that larger amplitude waves will have a lower proportion of the wave transmitted for the same valve opening. For the application of valve assessment, it is important to consider what effect this behaviour may have when using signals of constantly varying magnitudes. Figures A-1 to A-3 show the variation in transmitted and reflected wave forms for a sinusoidal signal at transmission ratios of 5%, 50% and 90% respectively. The magnitudes of each of the waves has been normalised by the peak magnitude for that wave so that the wave forms can be directly compared. At low transmission ratios the smaller components of the wave form are transmitted with a relatively higher magnitude creating the wave form discrepancies seen in the figures. As the subsequent wave forms vary with the transmission ratio, the ratio of input signal energy to transmitted and reflected signal energy will not correlate linearly with the transmission ratio. This is an important consideration when using cross-correlation functions which consider signal energy as opposed to peak magnitude.

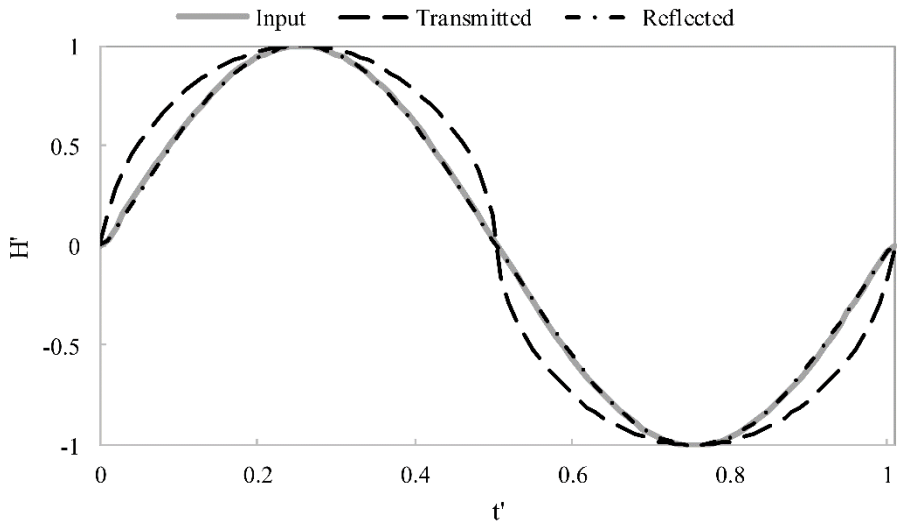

Figure A-1: Transmitted and reflected wave shape variations for a 5% transmission ratio.

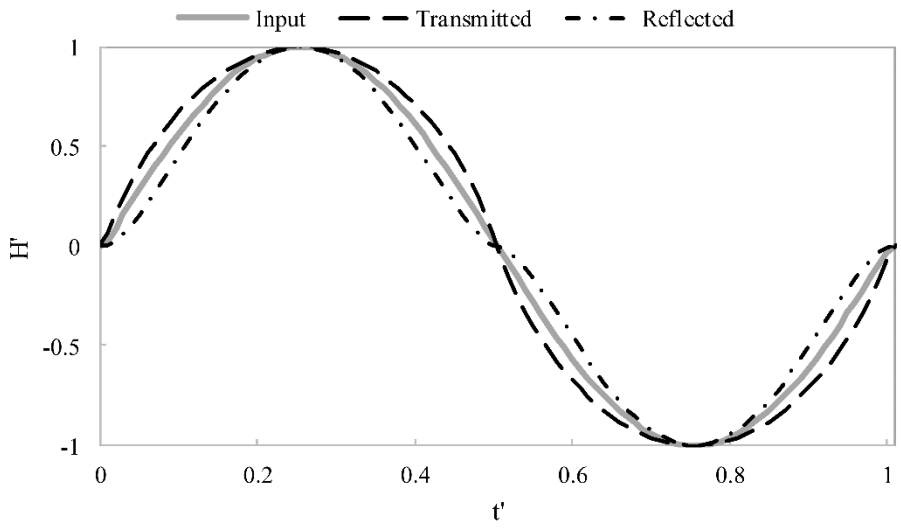

Figure A-2: Transmitted and reflected wave shape variations for a 50% transmission ratio.

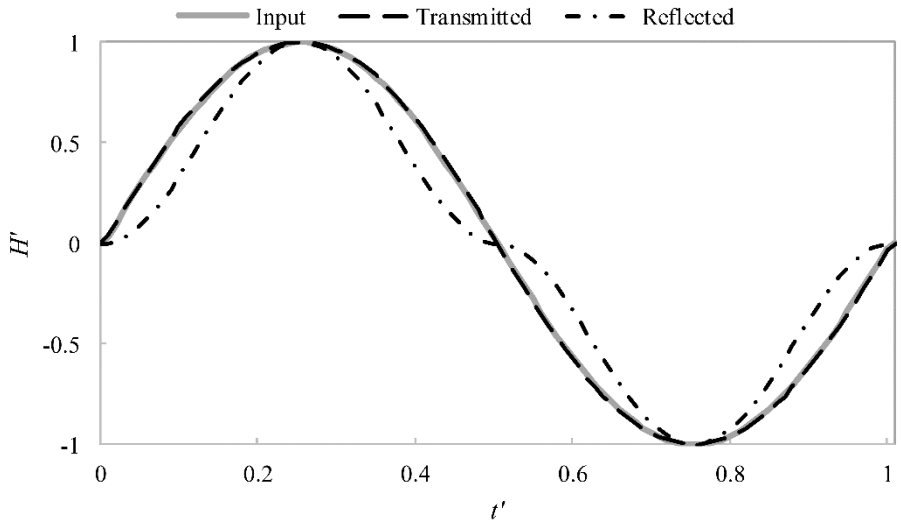

Figure A-3: Transmitted and reflected wave shape variations for a 95% transmission ratio.

APPENDIX B – FITTING THE LUMPED VALVE COEFFICIENT

So that comparisons can be made between unsteady hydraulic transmission and steady flow rates through a valve an empirical relationship between the lumped loss coefficient and valve position has been found. An 80 mm VAAS gate valve as shown in Figure B-1 has been used and modified with air bleed valves to remove all air from the valve during testing and fitted into a standard 200 mm pipeline test section with ports for pressure transducers in each flange. Figure B-2 shows the laboratory determined loss coefficients, $C_v\tau$ for a range of valve positions. The closed valve position is indicated by a 0 mm position. As the valve is opened the position is determined by measuring (with digital calipers) the distance from a set position on the fix valves frame (as indicated on Figure B-1) to the valves gate, then subtracting this from the distance for a fully closed valve. The loss coefficients are determined from Equation (3-6) where the head difference is determined from static pressure measurements each side of the valve and a flow metre was used to determine flow.

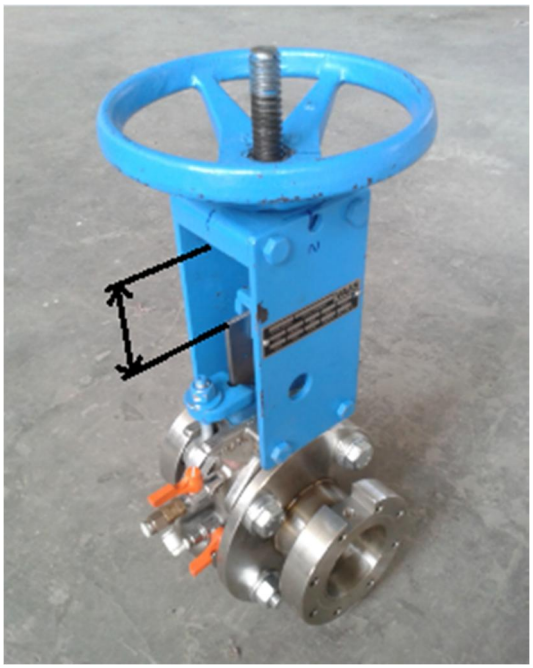

Figure B-1: VAAS 80 mm gate valve.

A two part polynomial equation (Equation (B-1)) has been fitted to the loss coefficients to provide an accurate fit. The factors to fit this equation are given in Table B-1 and the fitted curve is shown on Figure B-2. Due to limitations of the flow measurement equipment, the lowest experimentally determined loss coefficient is 3.6E-5 $m^{5/2}/s$ which equates to a flow rate of 1.1E-4 m^3/s. Below this value the results are extrapolated to account for no flow at a fully closed valve position.

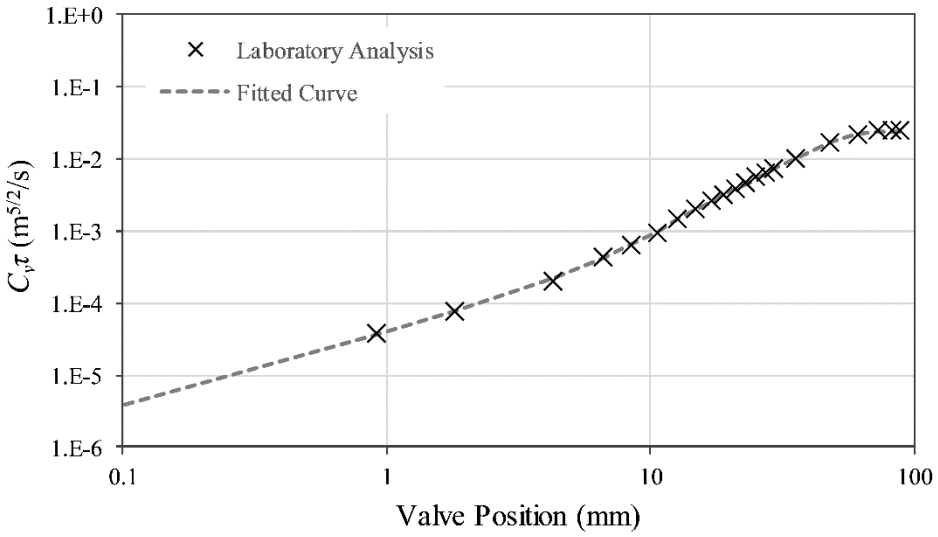

Figure B-2: Characterisation of the $C_v\tau$ curve for a gate valve from laboratory data.

$$C_v\tau = ax^6 + bx^5 + cx^4 + dx^2 + ex + f \quad \text{(B-1)}$$

Table B-1: Fitted factors for determining the lumped loss coefficient for a gate valve.

Coeff.	Valve Position ≤ 12.68 mm	Valve Position > 12.68 mm
a	3.4403E-11	0
b	-7.0645E-09	0
c	3.9734E-07	3.6484E-07
d	-1.9654E-06	1.0397E-06
e	1.2763E-04	3.8690E-05
f	-5.0768E-04	0